

The Thesis Entitled

**EFFECT OF DYNAMIC PROPERTIES OF CIRCUIT
BREAKER ON SHORT CIRCUIT CAPACITY**



Submitted to

**Dr. BABASAHEB AMBEDKAR MARATHWADA
UNVIERSITY, AURANGABAD**

*In partial fulfilment of the Requirement for the Award of the Degree of
DOCTOR OF PHILOSOPHY*

in

ELECTRICAL ENGINEERING

By

Mrs. Anita Arun Bhole

Under the Guidance of

Dr. W. Z. Gandhare

FACULTY OF ELECTRICAL ENGINEERING

**Dr. BABASAHEB AMBEDKAR MARATHWADA
UNVIERSITY, AURANGABAD-431 004 (MS), INDIA**

OCTOBER - 2017

***EFFECT OF DYNAMIC PROPERTIES OF CIRCUIT
BREAKER ON SHORT CIRCUIT CAPACITY***

Ph. D. Thesis

in Electrical Engineering

Author

Mrs. Anita A. Bhole

Research Scholar

Under the Guidance of

Dr. W. Z. Gandhare

Director, G. S. Moze College of Engineering, Pune

Research Guide in Electrical Engineering

Dr. Babasaheb Ambedkar Marathwada University

Aurangabad - 431 004 (MS) INDIA

OCTOBER 2017

EFFECT OF DYNAMIC PROPERTIES OF CIRCUIT BREAKER ON SHORT CIRCUIT CAPACITY



Submitted to
**Dr. BABASAHEB AMBEDKAR MARATHWADA
UNIVERSITY, AURANGABAD**

for the Degree of
Doctor of Philosophy
in
Electrical Engineering
By
Mrs. Anita Arun Bhole
Under the Guidance of
Dr. W. Z. Gandhare

FACULTY OF ELECTRICAL ENGINEERING
Dr. BABASAHEB AMBEDKAR MARATHWADA
UNIVERSITY, AURANGABAD-431 004 (MS), INDIA
OCTOBER - 2017

Dr. Babasaheb Ambedkar Marathwada University

Aurangabad (M. S.) - 431 004



CERTIFICATE

This is to certify that the thesis entitled "**Effect of Dynamic Properties of Circuit Breaker on Short Circuit Capacity**", which is being submitted herewith for the award of the '**Degree of Doctor of Philosophy**' in '**Electrical Engineering**' of **Dr. Babasaheb Ambedkar Marathwada University Aurangabad**. This is the result of the Original Research Work and Contribution by '**Mrs. Anita Arun Bhole**' under my supervision and guidance at Government College of Engineering, Aurangabad. The work embodied in this thesis has not formed earlier for the basis of the award of any degree or compatible certificate or similar title of this for any other diploma/examining body or university to the best of knowledge and belief.

Place: **Aurangabad**

Date : / /

Dr. W. Z. Gandhare

Research Guide

Electrical Engineering

Faculty of Engineering & Technology

Dr. Babasaheb Ambedkar Marathwada

University, Aurangabad

ABSTRACT

Modern high voltage circuit breaker (CB) consists of two contact sets of main and arcing contacts. The main contacts are made of copper with silver coating and carry the normal current continuously without heating whereas tungsten-copper arcing contacts opens followed by main contacts and are exposed to arcing. The arcing contacts have to sustain the arc current, arc energy and the high temperature around 10,000°K. Hence arcing contacts are liable to damage due to severe thermal stresses and Transient Recovery Voltage (TRV). Damaged main and arcing contacts reduce the short circuit capacity of circuit breaker. Therefore the condition assessment of circuit breakers contact is of prime importance. Static contact resistance measurement evaluates the condition of main contacts only. The lack of direct access to the arcing contacts and use of high pressure gas complicate the direct condition assessment of this part. Hence the Dynamic Contact Resistance Measurement (DCRM) test has been recently introduced as a condition assessment test for CB main and arcing contacts. Many parameters such as length of arcing contact, contact wipe and erosion of main and arcing contacts, contact misalignments, healthiness of linkage mechanism, main and arcing contact resistance, contact travel and speed *etc.* can be obtained from signature.

Switching under different fault condition and certain normal duty leads to severe TRVs across the contacts of the circuit breakers which may fail the circuit breaker to clear the fault and has the influence on the short circuit capacity of the circuit breaker. In this thesis study of TRV under different fault conditions for IEEE network is carried out and the short circuit capability of the CB is determined using computer simulations in EMTP-RV. DCRM tests and timing measurement tests are conducted on 400 kV and 245 kV SF₆ CBs at circuit breaker manufacturing industry, 400 kV substation Waluj, Aurangabad and 765 kV substation at Thapti

Tanda Aurangabad. Data of DCRM for healthy breakers as well as breakers with problems in condition of contact was collected from the largest utility company Power Grid Corporation of India Ltd. (PGCIL) as well as Maharashtra State Electricity Transmission Company Ltd. (MSETCL). DCRM signature obtained from the test is difficult to analyze as it needs the knowledge of circuit breaker design, operating mechanism, and interrupter assembly and also expertise to conclude the cause. Numbers of case studies are presented and the measured and collected DCRM data is analyzed and a new algorithm has been proposed to detect the contact anomaly. Computer program is developed to determine the health of CB.

Dr. Babasaheb Ambedkar Marathwada University
Aurangabad (M. S.) - 431 004



DECLARATION

I hereby declare that the work presented in the form of thesis entitled "**EFFECT OF DYNAMIC PROPERTIES OF CIRCUIT BREAKER ON SHORT CIRCUIT CAPACITY**" is an original research work carried out by me under the guidance of Dr. W. Z. Gandhare, Director, G. S. Moze College of Engineering Pune, and has not been previously submitted to this or any other University for the award of degree, diploma, associate-ship, or any other similar title.

Place: **Aurangabad**

Date : / /

Mrs. Anita Arun Bhole

Research Scholar

INTENT

List of Figures	i
List of Tables	v
Abbreviations	vi
1 INTRODUCTION	1
1.1 Introduction	1
1.1.1 Circuit Breaker Classification	4
1.2 Motivation	7
1.3 Objectives	8
1.4 Theme	9
1.5 Organization	11
2 LITERATURE SURVEY	12
2.1 The Electric Arc	12
2.1.1 Time-intervals in the interruption process of an electric arc .	13
2.2 Arc-Circuit Interaction	14
2.2.1 Thermal regime	15
2.2.2 Dielectric regime	16
2.3 Circuit Breaker Modeling during Opening Operations	18
2.4 Arc Modeling	18
2.4.1 Physical arc models (PAM)	20
2.4.2 Black box models (BBM)	20
2.4.2.1 Cassie model	21
2.4.2.2 Mayr model	22
2.4.2.3 Browne model	23

2.4.2.4	Avdonin model	24
2.4.2.5	Urbanek model	24
2.4.2.6	Kopplin model	25
2.4.3	Parameter models (PM)	26
2.5	Circuit Breaker Modeling During Closing	26
2.6	SF ₆ Circuit Breakers	27
2.6.1	Introduction	27
2.6.2	SF ₆ puffer circuit breakers	28
2.6.3	SF ₆ self-blast circuit breakers	32
2.7	Transient Recovery Voltage	32
2.7.1	Reactive equipment switching duty	33
2.7.1.1	First parallel oscillations	35
2.7.1.2	Second parallel oscillations	36
2.7.1.3	Main circuit oscillations	36
2.7.1.4	Source side oscillations	36
2.7.1.5	Load side oscillations	36
2.8	Time Definitions as per IEC	37
2.8.1	Contact resistance measurement	38
2.8.1.1	Static contact resistance measurement (SCRM) . .	38
2.8.1.2	Dynamic contact resistance measurement	41
2.9	Research Gap	45
3	SYSTEM DEVELOPMENT	46
3.1	Computational Models	46
3.1.1	Interruption of Three Phase to Ground fault	46
3.1.2	Interruption of Single Phase to Ground fault	47
3.2	Analytical Models	49
3.2.1	Transient Recovery Voltage types	49
3.2.1.1	Three phase terminal fault	49
3.2.1.2	Exponential (Overdamped) TRV	52
3.2.1.3	Single frequency recovery voltage	52
3.2.2	Traveling waves	53
3.2.3	Short Line Fault	53

3.3	Mathematical Model	57
3.3.1	Contact resistance measurement method	59
3.3.2	DCRM signature analysis	61
3.3.3	Case studies	61
3.4	New Algorithm for Contact Condition Detection of SF ₆ CB	77
4	PERFORMANCE ANALYSIS	84
4.1	Computational Analysis	84
4.1.1	Simulation results for case-I	84
4.1.2	Simulation results for case-II	85
4.1.3	Simulation results for case-III	85
4.1.4	Simulation results for arc interruption	86
4.2	Analytical Analysis	105
4.3	Comparison between Computational and Analytical Analysis	106
4.4	Validation of Algorithm	107
4.5	Justification for Difference	114
5	CONCLUSIONS	115
5.1	Conclusions	115
5.2	Future Scope	117
5.3	Applications	117

Contributions

References

Publications

Annexure A

Acknowledgement

List of Figures

1.1.1 Application of CBs	3
1.1.2 Maf-Rate per Drive Technology for Failures	4
1.1.3 Classification of CBs	6
1.4.1 Theme of the Research Work	10
1.4.2 Normal DCRM Signature	10
2.1.1 Potential Distribution Along an Arc Channel	13
2.1.2 Intervals and Failure Modes in the Interruption Process	14
2.2.1 Representation of the Network Connected to the Breaker Terminals	15
2.2.2 Curves of Short Circuit Current and Recovery Voltage	16
2.2.3 Current Shapes at Interruption	17
2.2.4 Dielectric Interruption Regime	17
2.5.1 Prestrike Phenomenon during Closing	26
2.6.1 Voltage Range of Application of Breaking Technologies	28
2.6.2 Main Components of the Puffer Interrupter	29
2.6.3 Function of a Puffer Interrupter	30
2.6.4 Pressure in the Puffer Cylinder at No-Load and during Interruption of an Asymmetrical Short-Circuit Current of 40 kA	31
2.7.1 Illustration of the Sources of TRV	33
2.7.2 IEC Two and Four Parameter Limiting TRV Curves	34
2.7.3 Shunt Reactor Equivalent Circuit	35
2.7.4 Oscillation Modes in Reactor Circuit	37
2.8.1 Time Definitions during Opening and Closing, As Per IEC	39
2.8.2 Time Definitions during Close-Open Cycle for CB without Switching Resistors	40

2.8.3	Flow Chart of DCRM	42
3.1.1	IEEE Network under Study	47
3.2.1	Circuit for Interruption of a Three-Phase-to-Ground Fault	51
3.2.2	Lattice Diagram to Evaluate the Characteristics of Travelling Wave	55
3.2.3	TRV across the Breaker during Short Line Fault	56
3.3.1	Schematic of Forces Exerted on the Fixed Contact by the Moving Finger Contacts	58
3.3.2	Schematic Diagram of Static Contact Resistance Measurement . . .	60
3.3.3	Schematic Diagram of DCRM	60
3.3.4	Test Set Up for DCR Measurement	62
3.3.5	Measurement Details from DCRM Signature	63
3.3.6	Enlarged View of Tripping Portion of DCRM Signature	64
3.3.7	Contact Bouncing after Closing Cycle on 400 kV SF ₆ Circuit Breaker	65
3.3.8	DCRM Signature Showing Fluctuations in Resistance Curve of B Phase Front Side Interrupter	66
3.3.9	Enlarged View of R-Pole DCRM in Closing Part	67
3.3.10	R-Pole DCRM in Tripping Zone	68
3.3.11	Y-Pole DCRM in Tripping Zone	68
3.3.12	Wrong Assembly of Arcing Contact	69
3.3.13	Closing Graph of 245 kV SF ₆ Circuit Breaker	70
3.3.14	Complete DCRM Signature of 245 kV SF ₆ Circuit Breaker	70
3.3.15	DCRM of 245 kV SF ₆ Circuit Breaker in Tripping Zone	71
3.3.16	Contact Bouncing in Closing Graph of 245 kV SF ₆ Circuit Breaker	71
3.3.17	Abnormal Variations in Resistance in no Action Zone of DCRM Signature for 220 kV Circuit Breaker	72
3.3.18	Loose Ring Connecting PTFE Nozzle of Main Contact	73
3.3.19	Problematic DCRM Signature	74
3.3.20	Increase in Resistance in Close Zone	74
3.3.21	Fix and Moving Contact Assembly	75
3.3.22	Deposition of Sulfide Powder on Contact Assembly	76
3.4.1	DCRM Signature Showing the Parameters used in Algorithm . . .	77
3.4.2	Flow Chart of Proposed Algorithm	83

4.1.1	TRV Waveform of the Three Phases for Multiple Line Switching at Terminal of Substation for Three Phase to Ground Fault	88
4.1.2	TRV Waveform of Phase A with Standard TRV and Delay Line for Multiple Line Switching at Terminal of Substation for Three Phase to Ground Fault	89
4.1.3	Standard TRV Envelope and Phase A TRV for Multiple Line Switching at Terminal of Substation for Three Phase to Ground Fault	90
4.1.4	Oscillatory TRV for Three Phase to Ground Terminal Fault for Transformer Switching	91
4.1.5	Three Phase Oscillatory TRV for Three Phase to Ground Terminal Fault for Transformer Switching	92
4.1.6	Phase A TRV, Standard TRV and Delay Line for Oscillatory TRV for Three Phase to Ground Terminal Fault for Transformer Switching .	93
4.1.7	Enlarged View of Phase A TRV and Standard TRV Envelope for Three Phase to Ground Terminal Fault for Transformer Switching .	94
4.1.8	TRV for Short Line Single Phase to Ground Fault for Constant Parameter Model of Lines	95
4.1.9	TRV for Short Line Single Phase to Ground Fault for Frequency Dependent Model of Lines	96
4.1.10	Comparative Waveform of TRV for Constant Parameter Model and Frequency Dependent Model of Line for Short Line Single Phase to Ground	97
4.1.11	TRV for Short Line Single Phase to Ground Fault at 1.2 km for Constant Parameter Model of Lines	98
4.1.12	TRV for Short Line Single Phase to Ground Fault at 2.2 km for Constant Parameter Model of Lines	99
4.1.13	TRV for Short Line Single Phase to Ground Fault at 3.2 km for Constant Parameter Model of Lines	100
4.1.14	TRV for Short Line Single Phase to Ground Fault at 5.2 km for Constant Parameter Model of Lines	101
4.1.15	TRV for Short Line Single Phase to Ground Fault at 6.2 km for Constant Parameter Model of Lines	102

4.1.16	Arc Interruption Waveforms for Three Phase to Ground Terminal Fault for Transformer Switching	103
4.1.17	Arc Interruption Waveforms for Three Phase to Ground Terminal Fault for Multiple Line Switching	104
4.2.1	Variation of RRRV with Fault Distance for Single Phase to Ground Short Line Fault	106
4.4.1	Fix and Moving Contacts with Different Worn Conditions	108
4.4.2	DCRM Signature in Trip Portion for Different Contact Configuration	109
4.4.3	Signatures of R-pole from Commissioning	111
4.4.4	Output of the Program	112
4.4.5	Signatures of Y-pole from Commissioning	113

List of Tables

1.1.1 Percentage of Maf Rate and Mif Rate per Failure Mode, Third Inquiry	5
2.3.1 Modeling Guidelines for Circuit Breakers	19
2.4.1 Arc Model Applications	25
4.1.1 TRV Rating for 30 kA Short Circuit Current Interruption	87
4.3.1 Comparison of Standard TRV and Simulated TRV	106
4.3.2 Simulation Results for TRV under Different Fault Conditions	107
4.4.1 Area below the DCRM Curve for Different Contact Configuration .	109
4.4.2 CB Parameters for the Healthy and Faulty Condition from DCRM Signature	110

Abbreviations

ANSI	American National Standards Association
CB	Circuit Breaker
CBY	Circuit Breaker Years
DCRM	Dynamic Contact Resistance Measurement
HVCB	High Voltage Circuit Breaker
IEC	International Electro Technical Commission
IEEE	Institute of Electrical and Electronics Engineers
MaF	Major Failure
Mif	Minor Failures
MSETCL	Maharashtra State Electricity Transmission Company Ltd.
PGCIL	Power Grid Corporation of India Ltd.
RRRV	Rate of Rise of Transient Recovery Voltage
SCRM	Static Contact Resistance Measurement
SF ₆	Sulpher Hexafluoride
TRV	Transient Recovery Voltage

Chapter 1

INTRODUCTION

1.1 Introduction

American National Standards Association (ANSI) defines the Circuit Breaker (CB) as, “A mechanical switching device, capable of making, carrying, and breaking currents under normal circuit conditions and also making, carrying for a specified time, and breaking currents under specified abnormal circuit conditions such as those of short circuit” [1]. CBs are required to fulfil following physical requirements apart from main functions [2].

- Should work as a good conductor when closed and a good insulator when opened
- Should quickly interrupt the short circuit current
- Should not generate over voltages during switching
- Should be highly reliable during operation

Components involved in basic functions of High Voltage Circuit Breakers (HVCBs) can be divided into five groups [3].

1. Contacts

Contacts are the main component which should be able to carry the rated current continuously without overheating and should carry large current without welding for a short period during short circuit condition. Hence

contacts are the key component in deciding the success or failure of the CB. Condition monitoring of contacts avoids the failure of this critical component.

2. Switching

CBs are subjected to electrical, thermal and mechanical stresses during switching. It is required that CBs should be able to perform its duty under normal and abnormal conditions without causing failure. The parameters like pole mismatch, contact travel, contact wear, operating time and arcing time are used to monitor the switching of CB.

3. Insulation

The insulating components must be so designed as to withstand the mechanical and electrical stresses. In HVCBs solid, liquid, vacuum and gaseous dielectric materials are used to provide electrical insulation.

4. Operating Mechanism

The function of the operating mechanism is to open and close the circuit breaker contacts within the specified limits. CBs remain in closed position for an extended period of time. But during fault condition, it has to open reliably. Hence the job of the operating mechanism is not simple. The percentage of failure of operating mechanism is large in the total failures of HVCBs.

5. Control and auxiliary functions

Control and auxiliary components are controlled by 110-220 V DC. According to reliability surveys, control and auxiliary components are exposed to failures relatively frequently. Delay in operation or failing to open or close on demand are some typical failures in these parts.

Renewable energy sources are being used to cater the power demand in the fast growing power systems. The reliable switching of CBs in controlling power flows and during critical contingency condition is important [4–6]. CBs gets deteriorated due to usage and ageing. Hence they need proper maintenance. Conventionally CBs have been maintained through time-based maintenance schedule [7–11].

In POWERGRID network failure survey was carried out. Since the CB operation

is not frequent for extra high voltage network, manufacturers recommend overhauling of CB after ten years of service or at a specific number of operations. It was observed that there had been damages in the components in the interrupting chambers much before ten years where as there were few CBs with 17-20 years of age in good condition with no abnormality [12]. Thus condition based maintenance has been reported as the most efficient to recognize the need for maintenance of CBs when necessary. It is the cost effective maintenance and ensures the reliability [13–17].

CIGRE has conducted three world wide surveys since 1970 on high voltage CBs reliability [18–21]. The reliability is expressed in failure per 100 CB years (CBY) or per 10,000 operating cycles for the relevant failure modes. Failures are classified as a major failure (MaF or MF) and minor failures (Mf or Mif). The third enquiry included CBs of all ages and the objective was the relationship between age and major failure rate. Figure 1.1.1 shows that 54% of the total population is for the overhead line.

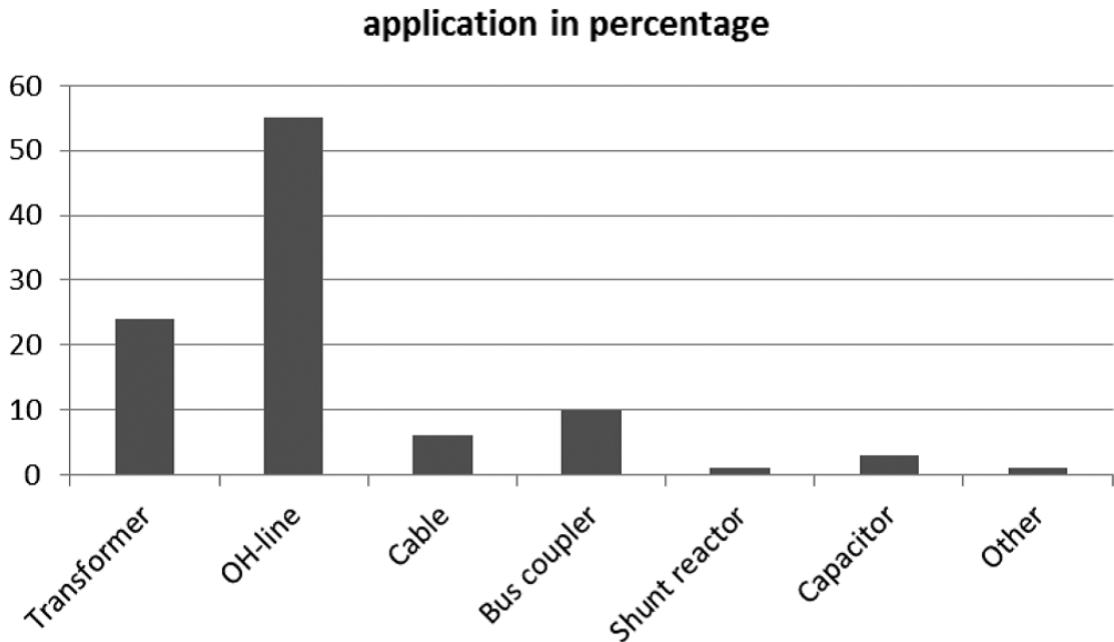


Figure 1.1.1: Application of CBs [18]

Shunt reactors and shunt capacitor bank percentage is very less, but they cover more than 20% of failure. The technology of operating mechanism is changing towards spring mechanism as seen in figure 1.1.2. Table 1.1.1 shows the percentage

of MaF and MiF rate per failure mode reported in the third enquiry.

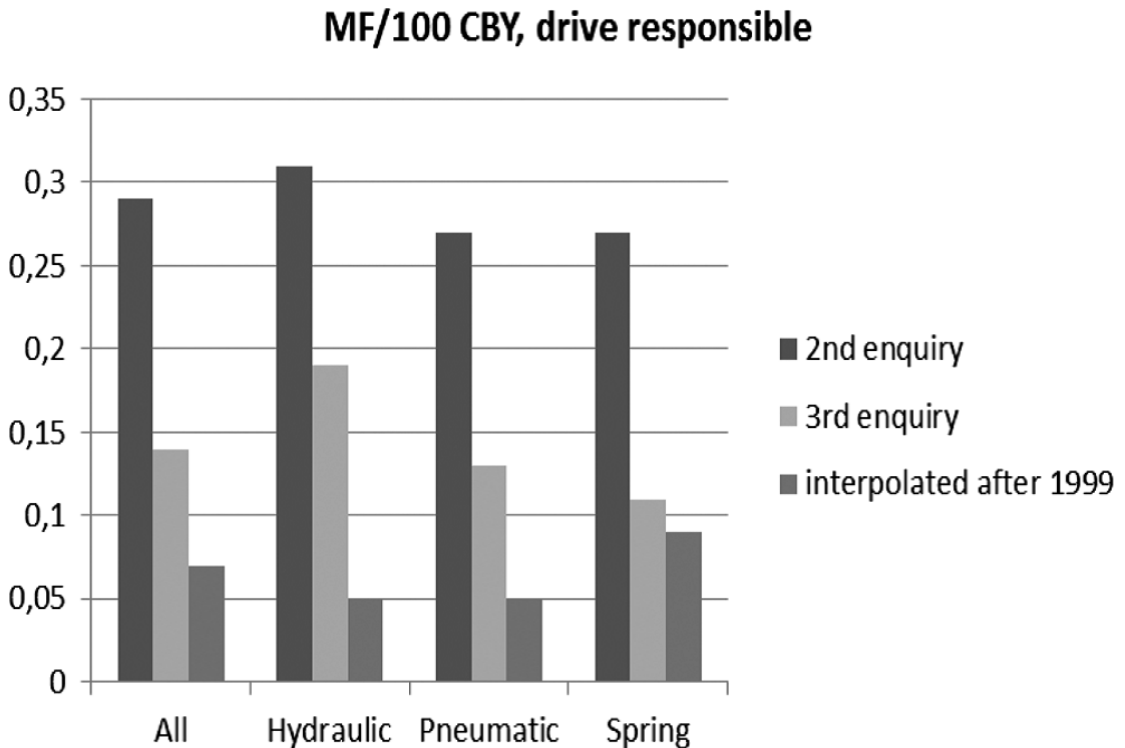


Figure 1.1.2: MaF-Rate per Drive Technology for Failures [18]

1.1.1 Circuit Breaker Classification

Figure 1.1.3 shows the complete classification of circuit breakers. However, CBs are classified mainly according to the dielectric medium used for arc extinguishing [22].

Table 1.1.1: Percentage of MaF Rate and MiF Rate per Failure Mode, Third Inquiry

MaF failure mode	MaF(%)	Comments
Does not close on command	28.2	Mainly with live tank circuit breakers
Does not open on command	16.4	
Closes without command	0.2	
Opens without command	5.4	
Fails to carry the current	1.3	
Dielectric breakdown	9.9	Breakdown to earth: 5%, Internal breakdown across open pole, during opening operation = does not break the current: 1.9%, Other across open pole: 1.8%, Breakdown between poles: 1.2%
Locked in open or closed position	25.1	Alarm has been triggered by the control system
Loss of mechanical integrity	8.1	Mechanical damage of parts
Other	5.2	
Total	100	
MiF failure mode	Mif(%)	Comments
Air or hydraulic oil leakage	20.3	In operating mechanism
Small SF ₆ gas leakage	35.6	Large leakage will give MF-mode “Locked”
Oil leakage in grading capacitors	1.0	
Change in functional characteristics	28.4	6.8% mechanical; 3.3% electrical 18.3% control and auxiliary systems
Other and no answer	14.6	
Total	100	

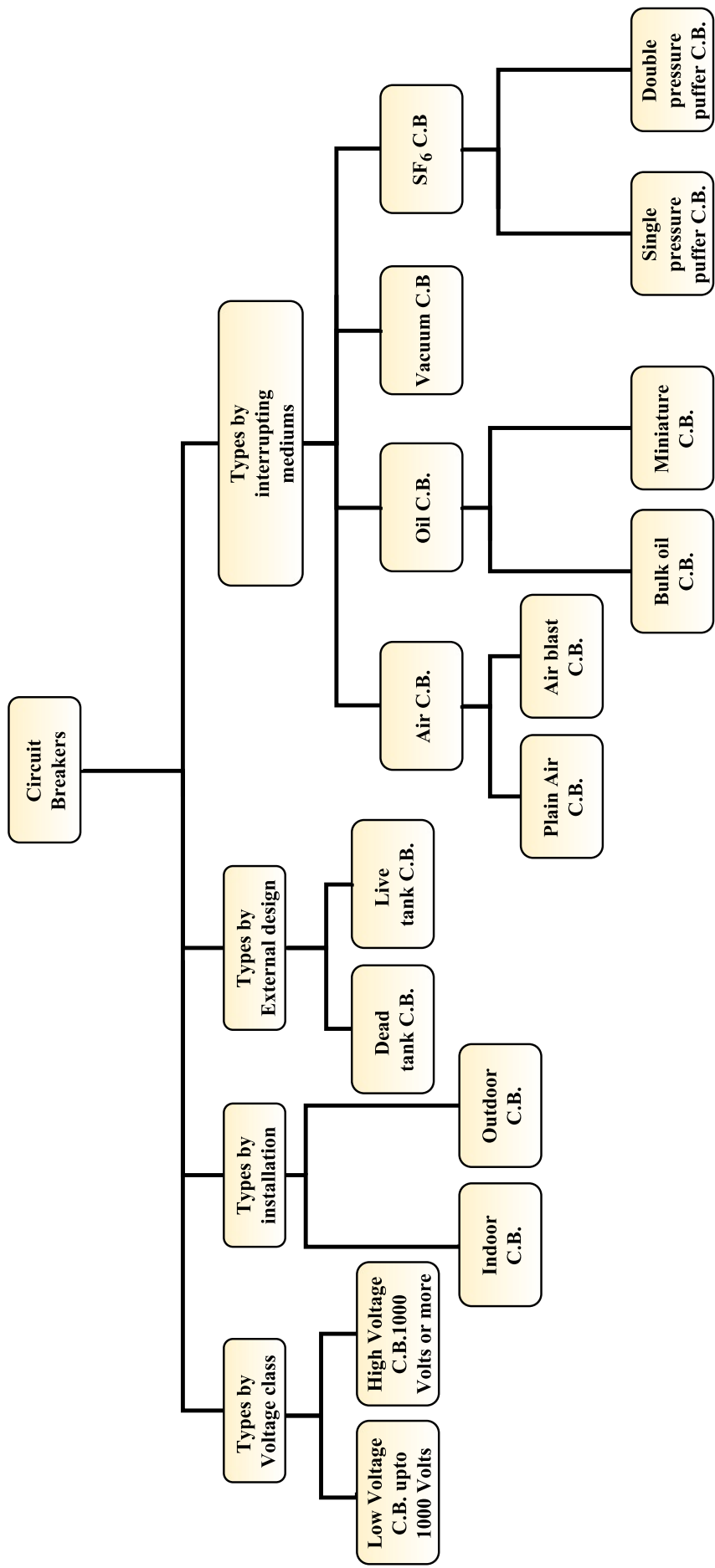


Figure 1.1.3: Classification of CBs

1.2 Motivation

The power system is growing at a faster pace. Increase in level of transmission voltage necessitates the use of HVCBs. The reliability of system depends on the CBs which has a crucial role in isolating the faults. Most of the population of circuit breakers in high voltage transmission is SF₆ circuit breakers. Modern high voltage puffer type SF₆ circuit breakers have two parallel contact sets. The low resistance silver plated main contacts carry the load current whereas the tungsten-copper arcing contacts, which opens after the main contact are exposed to arcing. Hence arcing contacts are liable to damage due to severe thermal stresses and Transient Recovery Voltage (TRV). Damaged main and arcing contacts reduce the short circuit capacity of the circuit breaker. Therefore the condition assessment of circuit breakers contact is of prime importance.

Study of CB failures survey by CIGRE working group observed that the failures are mainly due to malfunction of the operating mechanism and control circuit. The major contribution of the fault is from aging, wear and corrosion (50%) followed by the manufacturing faults, design faults and incorrect maintenance (15%) [18]. Failure survey motivated to study circuit breaker condition monitoring aspects.

1.3 Objectives

The objectives of the proposed research work are, to:

1. Study the interruption of current under three phase to ground terminal fault at the substation for multiple line switching and transformer switching and to measure the TRV and compare it with standard TRV to determine the short circuit capability of the CB
2. Study the interruption of single phase to ground short line fault and to measure the TRV and compare it with standard TRV to determine the short circuit capability of the CB
3. Measure and study the static contact resistance and dynamic contact resistance of 245 kV and 400 kV SF₆ CBs at the High Voltage circuit breaker manufacturing industry and in the field
4. Collect the data of DCRM for normal and abnormal cases from the PGCIL, MSETCL and High Voltage circuit breaker manufacturing industry
5. Analyze the DCRM data and develop an algorithm to determine the wearing of main and arcing contacts, contact wipe to determine the health of CB
6. Apply the Black Box Cassie - Mayer arc model for arc interruption studies

1.4 Theme

The interruption chamber of circuit breaker comprises of sets of the fixed and moving main and arcing contacts which are prone to erosion with time and usage. The lack of direct access to those and use of high-pressure gas complicate the direct condition assessment of this part. Circuit breakers need to perform various switching duties. Switching under the different fault condition and certain normal duty leads to severe TRVs across the contacts of the circuit breakers which may fail the circuit breaker to clear the fault and has the influence on the short circuit capacity of the circuit breaker. Hence the main theme of the proposed work has been to study the TRV under different fault conditions for IEEE network and determine the short circuit capability of the breaker using computer simulations in EMTP-RV. Also to measure the dynamic contact resistance of circuit breaker using the 4-wire method by injecting 100 A DC through the breaker. Measurements are recorded with a resolution of $100 \mu\text{s}$ with a sampling frequency of 100 kHz. Figure 1.4.1 shows the theme of the research work and Figure 1.4.2 indicates the DCRM signature. Measurements are done in the field and industry. Measured data and collected data from Power Grid Corporation of India Ltd. (PGCIL), Maharashtra State Electricity Transmission Company Ltd. (MSETCL) and High Voltage circuit breaker manufacturing industry have been analyzed in detail using HISAC Ultima test manager software. Results of analysis and simulations carried out are presented leading to conclusions and finally to new contributions. A new algorithm has been proposed to detect the contact anomaly. A computer program is developed in Java to determine the health of CB.

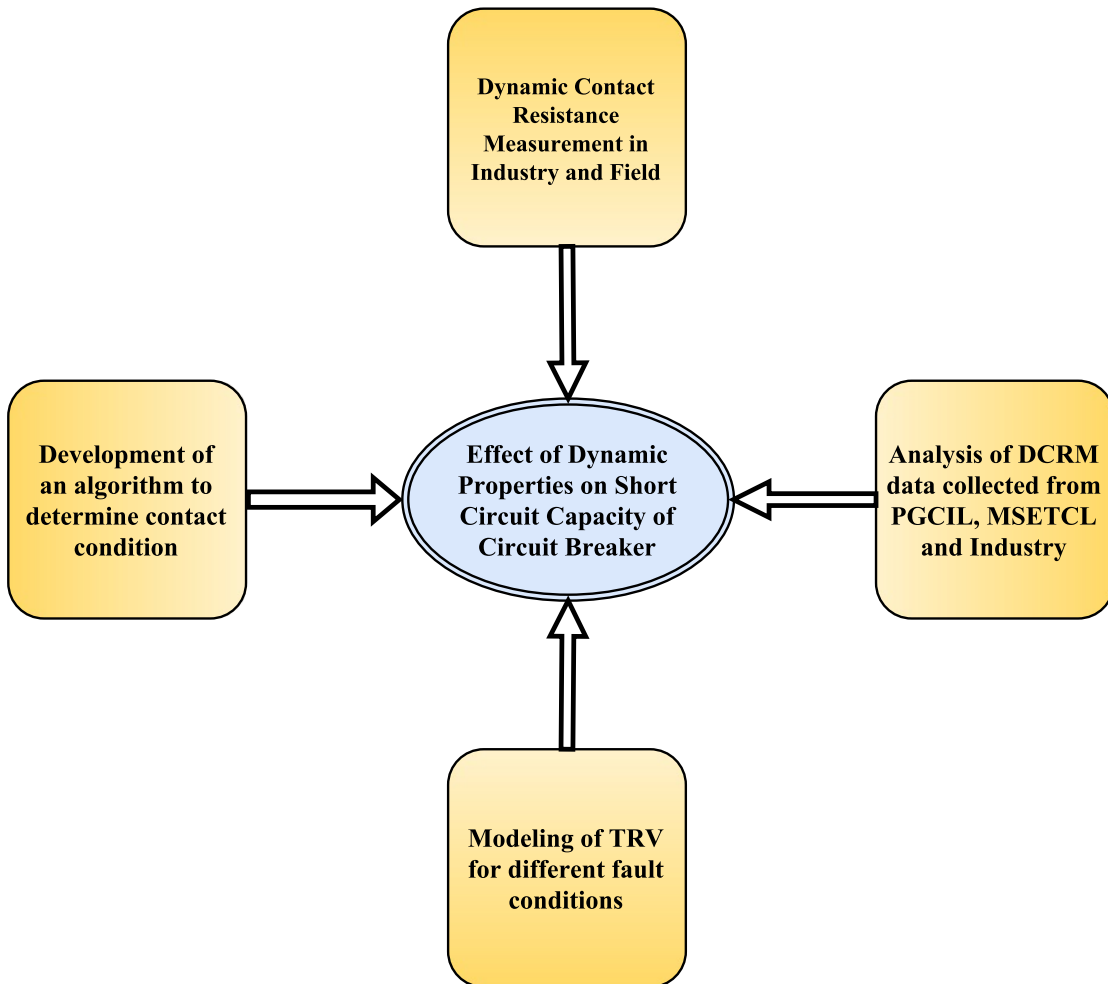


Figure 1.4.1: Theme of the Research Work

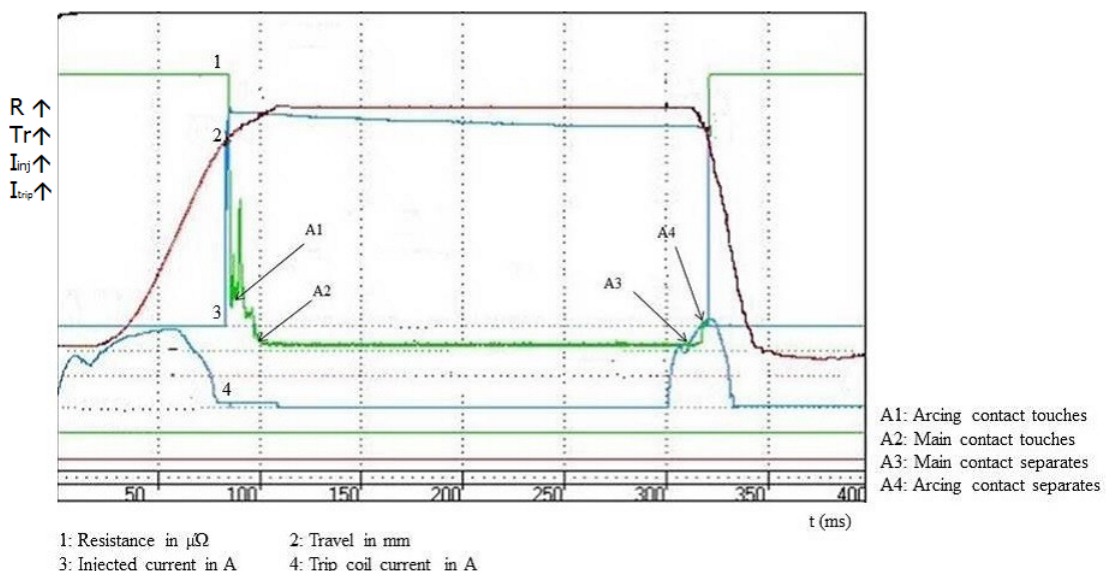


Figure 1.4.2: Normal DCRM Signature

1.5 Organization

The thesis is organized in following interdependent parts with a continuous theme as per abstract.

Chapter 1

Introduction - This chapter addresses the aspects containing introductory part. The necessity and the objectives of this research work are clearly mentioned. The overall theme of the complete research work is presented.

Chapter 2

Literature Survey - A summary of the exhaustive literature survey is represented. An overview of arc modeling, Transient Recovery Voltage, Dynamic Contact Resistance Measurement (DCRM), Standards related to circuit breaker timings are discussed in detail.

Chapter 3

System Development - Computational model of IEEE network for TRV study under different fault conditions is developed in EMTP-RV. Similarly analytical and mathematical models are developed. Dynamic contact resistance measurement is explained. Mathematical treatment is explained in detail with relevant references.

Chapter 4

Performance Analysis - Results of analytical and computational methods are presented. Justification for difference is given. Measured and collected data of DCRM from field is analyzed in detail using HISAC ULTIMA test manager software and new algorithm is proposed to detect the contact anomaly. Computer program in Java is developed to determine the health of circuit breaker.

Chapter 5

Conclusions - In this chapter conclusions of the research work, future work and applications are presented.

Chapter 2

LITERATURE SURVEY

2.1 The Electric Arc

The electric arc in a CB plays a major role in the interruption process which changes the status of breaker from conducting to a non-conducting state. An electric arc is the switching element of CB. Arc has nonlinear characteristics. The surface contact area is very small when the contacts are separated. As a result, the high current density increases the temperature that dissociates the molecules into atoms. Further increase in energy level, orbital electrons of the atoms dissociates into free moving electrons, leaving positive ions which lead to a plasma state. The Saha's equation gives the relation between the temperature T, the gas pressure P, and the fraction f of the atoms that are ionized

$$\frac{f^2}{1 - f^2} P = 3.16 \times 10^{-7} T^{5/2} e^{-eV_i/kT} \quad (2.1)$$

where

$e = 1.6 \times 10^{-19}$, the charge of an electron

V_i = ionization potential of the gaseous medium

$k = 1.38 \times 10^{23}$, Boltzmann's constant

As shown in the figure 2.1.1, the electric arc can be divided into three regions- the cathode region, the middle column, and the anode region. The figure also shows a potential distribution along the arc channel between the breaker contacts. The voltage drop near anode is around 5-10 volts whereas it is around 10-25 volts near the cathode region. Magnitude of arc current, length of column, types of gases

and gas pressure are the parameters on which the voltage drop in the arc column depends [23]

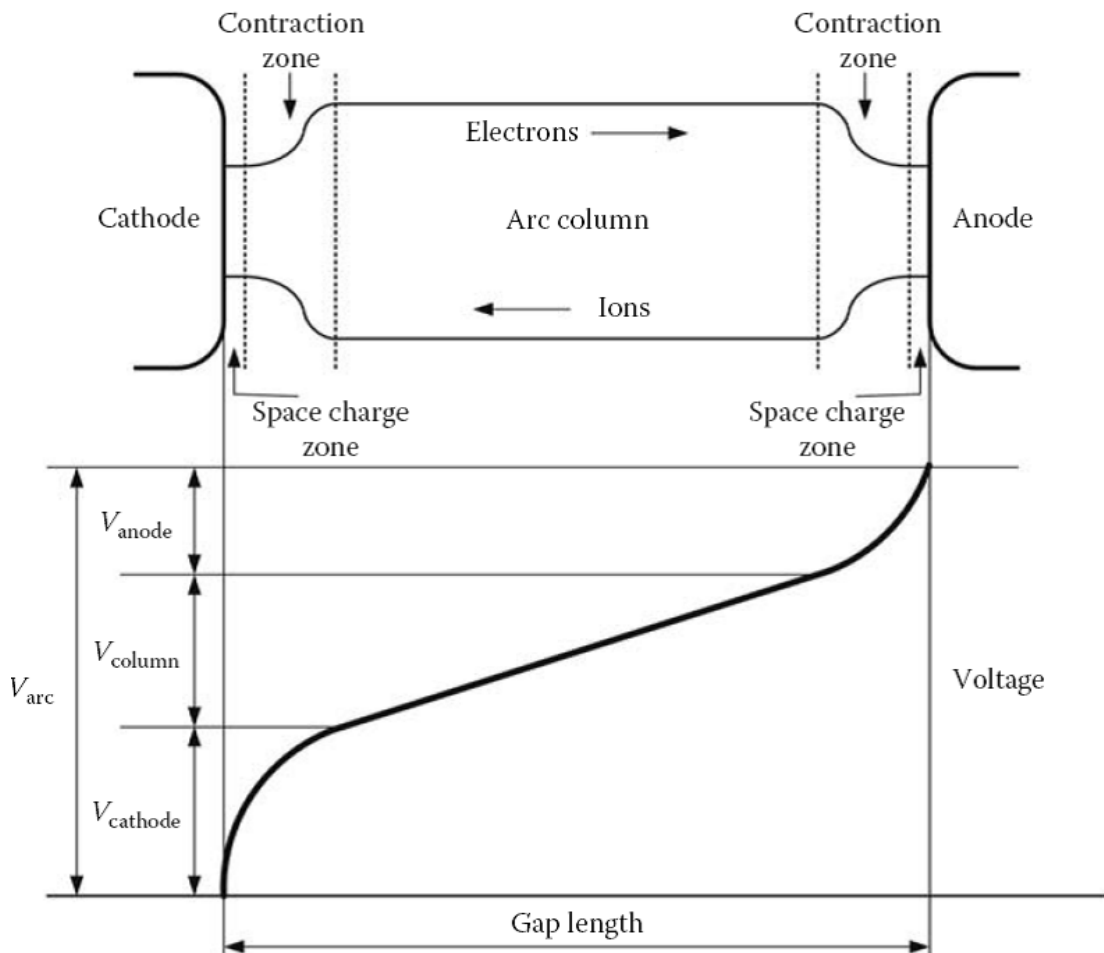


Figure 2.1.1: Potential Distribution Along an Arc Channel [2]

2.1.1 Time-intervals in the interruption process of an electric arc

CB is generally stressed in four intervals during fault current interruption:

- High current phase
- Interaction interval
- Dielectric recovery phase during TRV buildup
- Dielectric withstand phase during TRV peak and recovery voltage

The intervals of CB stresses are shown in figure 2.1.2.

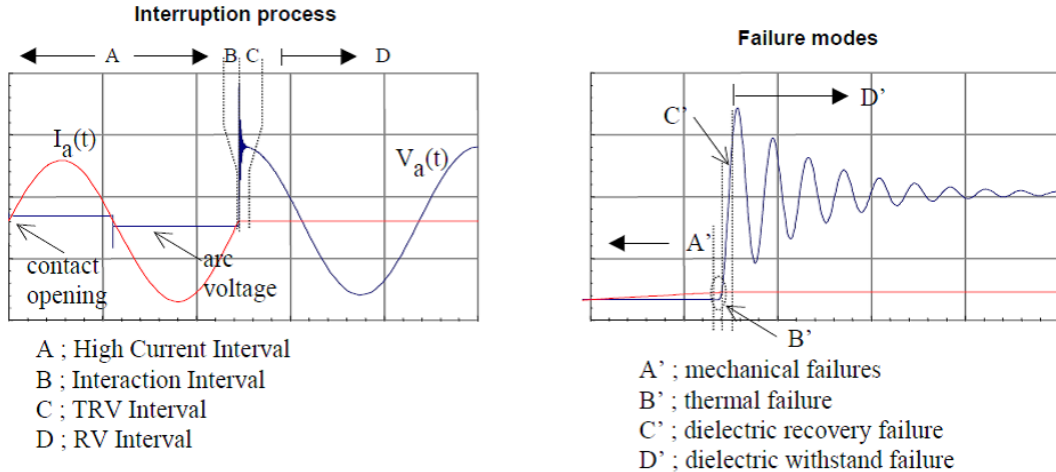


Figure 2.1.2: Intervals and Failure Modes in the Interruption Process [24]

Every interval during interruption stage has specific characteristics:

- high volume energy input during high current phase in the arc may cause the CB to overheat or result in mechanical damage
- possibility of reignition in interaction interval during thermal stress in arc circuit interaction
- dielectric stress which may cause a dielectric failure of the gap between the breaker contacts during the dielectric recovery and dielectric withstand period

2.2 Arc-Circuit Interaction

Interaction of several phenomena makes the current interruption process in a high-voltage circuit breaker a complex matter. At current zero arc diameter decreases with the cross section approximately proportional to the current. Current interruption of the CB occurs normally at current zero. During the current interruption process strong interaction exists between the physical process between the breaker contacts and the connected network.

Figure 2.2.1 shows the representation of the network connected to the breaker terminals.

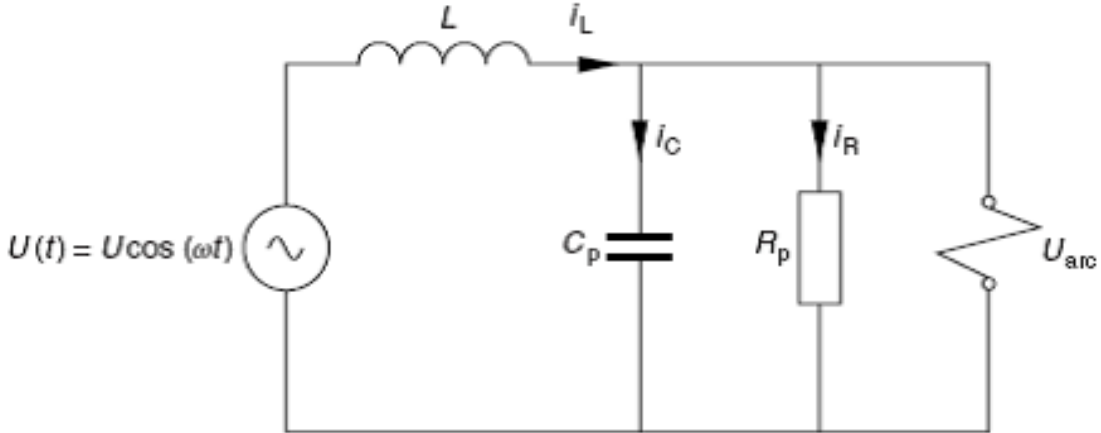


Figure 2.2.1: Representation of the Network Connected to the Breaker Terminals
 L - Total series inductance of the network; C_p - Total stray capacitance; R_p - Characteristic impedance of the connected overhead lines

During current interruption two physical requirements are involved:

- Thermal regime: The hot arc channel in the arcing region has to be cooled down so that the medium stops conducting
- Dielectric regime: The recovery voltage after the arc extinction contains high frequency transient component, Transient Recovery Voltage, which rapidly increases. The dielectric medium between the contacts must withstand this TRV for successful interruption

The current will flow for another half cycle till the next current zero if any of the above requirement is not met. Figure 2.2.2 shows the curves of short circuit current and recovery voltage and stresses on the extinction chamber at interruption.

2.2.1 Thermal regime

The thermal regime between the CB contacts during arc interruption depends upon the initial rate of rise of the transient recovery voltage (du/dt) immediately after current zero and the rate of decrease of the current to be interrupted (di/dt). Higher values of either of these two parameters make the interruption more severe. A high value of di/dt makes the interruption difficult due to a large amount of stored energy at current zero. High values of du/dt will result in an increase of

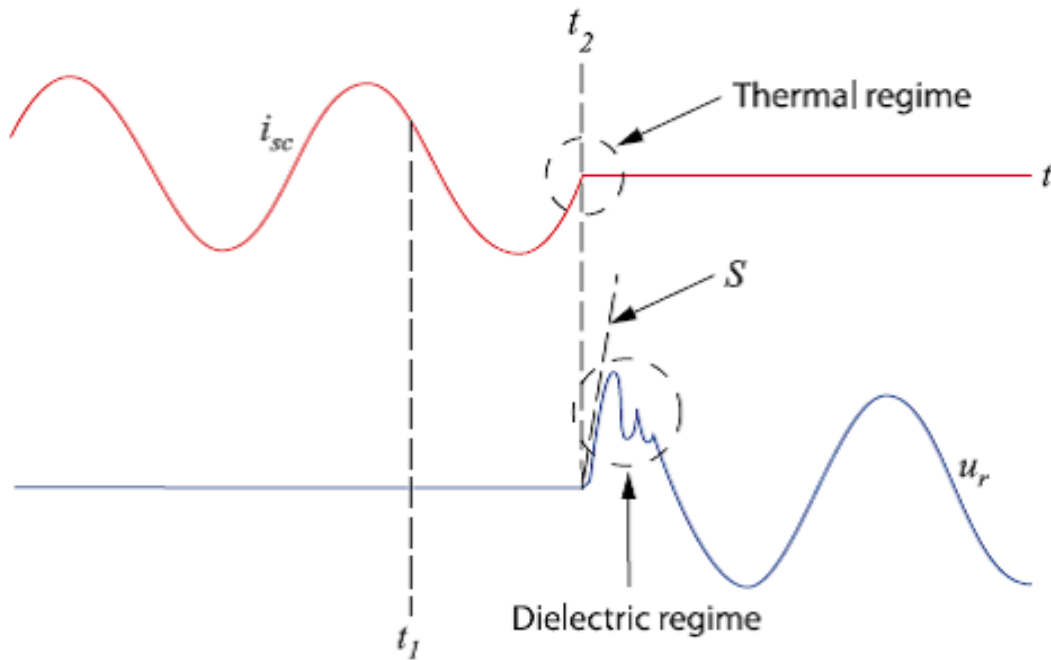


Figure 2.2.2: Curves of Short Circuit Current and Recovery Voltage [25]

t_1 - contact separation; t_2 - arc extinction; S - rate of rise of recovery voltage

the energy to the post-arc current. Post arc current up to few amperes flows after current zero due to electrical conductivity left in the arc path as shown in figure 2.2.3. The successful interruption depends on the race between the energy input in the arc path by the TRV and the cooling effect.

The thermal breakdown of CB will occur if the energy input is more.

2.2.2 Dielectric regime

In the dielectric regime, the temperature of the extinguishing medium is much higher than the ambient who reduce the voltage withstand capability of the contact gap. The stress on the CB depends on the Rate of Rise of Transient Recovery Voltage (RRRV). The interruption is successful if the rate of recovery of the contact gap at the instant of current zero is higher than RRRV otherwise dielectric failure will occur. Figure 2.2.4 shows the successful and failure interruption in dielectric interruption regime.

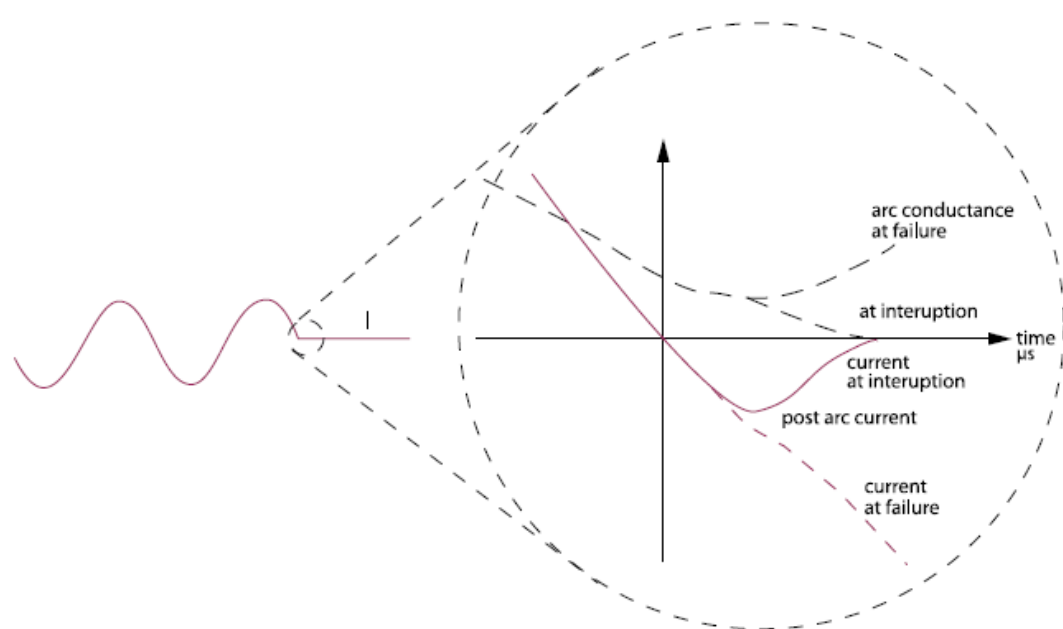


Figure 2.2.3: Current Shapes at Interruption [25]

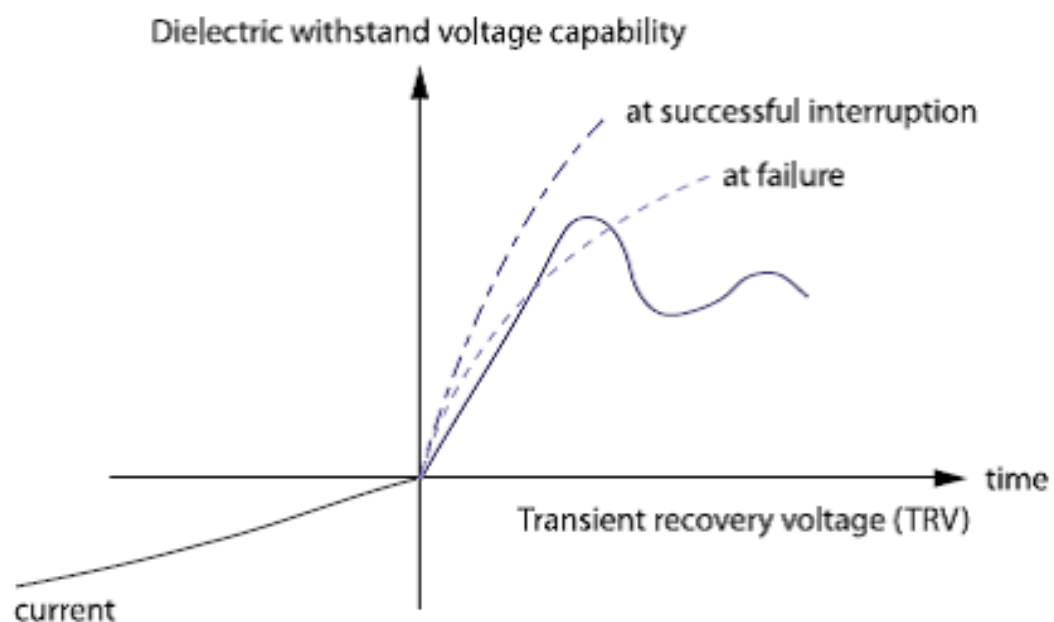


Figure 2.2.4: Dielectric Interruption Regime

2.3 Circuit Breaker Modeling during Opening Operations

CB models are needed to analyze both closing and opening operations. The separation of the contacts of the CB causes the formation of an electric arc. The main objectives of a circuit breaker model are [26]:

- to determine all voltages and currents that are produced in the system due to switching action of breaker
- to determine the reliability of CB operation under given set of conditions for the system

Modeling guidelines for CBs during closing and opening operations proposed by CIGRE WG 33-02 are shown in Table 2.3.1

2.4 Arc Modeling

The design of interrupting chamber of HVCBs plays an important role in the arc interruption. Arc models were used for the better understanding of current interruption process. However, the physical phenomena involved in the current interruption is very complex. Hence it is not possible to use the arc models for CB design. However, arc models can be used for arc circuit interaction. Arc models are able to simulate the nonlinear behavior of the CB arc. Correct numerical treatment of the arc circuit problem is important due to nonlinear behavior of the arc and small time constants.

To reproduce the arc interruption phenomenon in the testing, operation, and development of CBs several approaches can be used [28]. Arc models can be classified into three categories [2].

- Physical arc models
- Parameter models
- Black box arc models (P- τ models)

Table 2.3.1: Modeling Guidelines for Circuit Breakers [27]

Operation		Low-Frequency Transients	Slow Front Transients	Fast Front Transients	Very Fast Front Transients
Closing	Mechanical pole spread	Important	Very important	Negligible	Negligible
	Prestrikes	Negligible	Important	Important	Very important
Opening	High current interruption	Important for interruption capability studies only	Important for interruption capability studies only	Negligible	Negligible
	Current chopping	Negligible	Important for interruption capability studies only	Important for interruption capability studies only	Negligible
	Restrike characteristics	Negligible	Important for interruption capability studies only	Very important	Very important
	High-frequency current interruption	Negligible	Important for interruption capability studies only	Very important	Very important

2.4.1 Physical arc models (PAM)

In physical arc models, the physical process is considered in detail. The behavior of the arc is calculated from conservation laws, gas and plasma properties, and exchange mechanisms (radiation, heat conduction, turbulence). The design engineers use physical arc models for designing a new prototype. Equations 2.2 to 2.4 describe the physical arc model.

Conservation of mass:

$$\frac{\partial \rho}{\partial t} + \operatorname{div}(\rho u) = 0 \quad (2.2)$$

Conservation of momentum:

$$\rho \frac{\partial u}{\partial t} + \rho(u \cdot \operatorname{grad})u = -\operatorname{grad}(p) \quad (2.3)$$

Conservation of energy:

$$\underbrace{\rho \frac{\partial b}{\partial t}}_{\substack{\text{change} \\ \text{of energy} \\ \text{in unit} \\ \text{volume}}} + \underbrace{u \cdot \operatorname{grad}(\rho b)}_{\substack{\text{energy} \\ \text{input by} \\ \text{mass flow} \\ \text{convection}}} - \underbrace{\sigma E^2}_{\substack{\text{Joule} \\ \text{heating}}} = \underbrace{\operatorname{div}(\rho u)}_{\substack{\text{work} \\ \text{performed} \\ \text{by flow}}} + \underbrace{\operatorname{div}[K \cdot \operatorname{grad}(T)]}_{\substack{\text{thermal} \\ \text{conduction} \\ \text{loss}}} - \underbrace{R[T, \rho]}_{\substack{\text{radiation} \\ \text{loss}}} \quad (2.4)$$

p - pressure

σ - electrical conductivity

ρ - gas density

K - thermal conductivity

u - gas flow velocity

T - gas temperature

h - enthalpy of gas

R - radiation loss

E - electric field strength

r - arc radius

2.4.2 Black box models (BBM)

In black box models, the arc is described by a simple mathematical equation and gives the relation between the arc conductance, arc voltage, and arc current. For arc circuit interaction in network studies, the black box models are very useful for simulation. They are based on physical considerations. The electrical behavior of the arc is important than the internal processes. In transient programs, black box models are most suitable representations [28, 29].

The aim of a black box model is to describe the interaction of the switching device and the corresponding electrical circuit during an interruption process. The aim

of the Black box models is to obtain quantitatively correct performance of the CB [26]:

- In the simplest model the breaker is represented as an ideal switch that opens at first current-zero crossing after the tripping signal is given. This model can be used to obtain the voltage across the breaker which can be compared with a pre-specified TRV withstand capability for the breaker. This model cannot reproduce any interaction between the arc and the system
- Arc as a time-varying resistance or conductance is used in the elaborated model. Knowledge of the initial interrupting current and breaker characteristics is used to determine the time variation. This model requires advanced knowledge of the effect of the system on the arc however the model can represent the effect of the arc on the system. Precomputed TRV curves are required to determine the adequacy of the breaker
- In advanced model breaker is represented as a dynamically varying resistance or conductance. The value of conductance depends on the past history of arc voltage and current. Precomputed TRV curves are not required. Generally, these models are developed to determine initial arc quenching. Some advanced models are used in determining the arc reignition in CB which occurs due to insufficient dielectric withstand capability between the breaker contacts. The effect of the arc on the system and vice versa is possible in this model

Models for representation of SF₆ CBs during thermal and dielectric periods were discussed and used [30, 31]. Models proposed in last decades are available [32–47].

2.4.2.1 Cassie model

A. M. Cassie assumed that the shape of the arc channel is a cylinder filled with an ionized gas with a constant temperature T, but with a variable diameter. It is the convection losses that govern the high current arc during the high current time interval. As the current changes, the cross section of the arc changes but the temperature inside the arc column remains constant [32]. For the high current region, data collected from experimental results is in good agreement with the

model. However, around the current zero region, agreement is good only for high rates of current decay. Theoretically and practically, at current zero the arc diameter never decays to zero to result in arc interruption. At current zero there is a small filament of an arc remaining with a diameter of only a fraction of a millimeter. This filament is still high temperature plasma that can be easily transformed into an arc by the reappearance of a sufficiently high supply voltage. The Cassie model, in many cases, is referred to as the high current region model of an arc. This model has proved to be a valuable tool for describing the current interruption phenomena, especially when it is used in conjunction with the Mayr model.

The Cassie model is well suited for studying the behavior of the arc conductance in the high-current time interval when the plasma temperature is 8000°K or more. The Cassie model is given by equation 2.5.

$$\frac{1}{g} \frac{dg_c}{dt} = \frac{1}{\tau_c} \left[\left(\frac{v}{v_0} \right)^2 - 1 \right] = \frac{1}{\tau_c} \left[\left(\frac{i}{v_0 g_c} \right)^2 - 1 \right] \quad (2.5)$$

2.4.2.2 Mayr model

Mayr assumed that the power losses are caused by thermal conduction at small currents, which means that the conductance is strongly temperature dependent but is independent of the cross section area of the arc. Mayr considered the arc channel to be cylindrical with a constant diameter. The model describes the arc conductance around current zero. The removal of energy from arc column is through thermal conduction. The Mayr model is suited for modeling of the arc in the vicinity of current zero when the temperature of the plasma is below 8000°K. The Mayr model is given by equation 2.6

$$\frac{1}{g_m} \frac{dg_m}{dt} = \frac{1}{\tau_m} \left(\frac{v_i}{P_0} - 1 \right) = \frac{1}{\tau_m} \left(\frac{i^2}{P_0 g_m} - 1 \right) \quad (2.6)$$

In these equations

g - arc conductance

v - arc voltage

i - arc current

τ - arc time constant

P_0 - steady-state power loss

v_0 - constant part of the arc voltage

g_c is in the region of $1 \mu s$ and g_m is between 0.1 and $0.5 \mu s$ for SF₆ CB.

2.4.2.3 Browne model

Mayr assumed that the arc temperature is generally above 6000°K and is likely to be in excess of 20000°K. The high temperatures lead to a linear increase of gas conductivity instead of exponential relationship. In order to take the consideration of high temperature and dynamic response representation, Mayr model must closely follow the Cassie's equation during current controlled regime. T. E. Browne recognized this need and in 1948 he developed a composite model using an equation similar to Cassie's to define the current controlled arc regime, and then converting it to a Mayr-like equation for the temperature controlled regime, and in the event that interruption did not occur at the intended current zero, he reverted again to the Cassie model. In 1958 Browne extended the application of his combined model to cover the analysis of thermal re-ignitions that occur during the first few microseconds following the critical, post current zero energy balance period. Starting with the Cassie and the Mayr equations, and assuming that before current zero the current is defined by the driving circuit, and that after current zero, the voltage applied across the gap is determined strictly by the arc circuit, Browne assumed that the Cassie equation was applicable to the high current region prior to current zero and also shortly after current zero following a thermal re-ignition. The Mayr equation was used as a bridge between the regions where the Cassie concept was applied. This model was a valuable tool that has practical applications. It has been used extensively in the design and evaluation of circuit breakers. Browne's model is given by equation 2.7.

$$\frac{1}{g} = \frac{1}{g_c} + \frac{1}{g_m} \quad (2.7)$$

2.4.2.4 Avdonin model

Avdonin proposed a model for air-blast and SF₆ breakers [33]. The arc resistance of this model is expressed by equation 2.8

$$\frac{dr_a}{dt} = \frac{r_a^{1-\alpha}}{A} - v_a r_a \frac{r_a^{1-\alpha-\beta}}{AB} \quad (2.8)$$

which is derived from the modified Mayr equation 2.9

$$\frac{dr_a}{dt} = \frac{r_a}{\tau} \left(1 - \frac{v_a r_a}{P_0} \right) \quad (2.9)$$

with

$$\tau = Ar_a^\alpha \quad P_0 = Br_a^\beta \quad (2.10)$$

where

r - arc resistance

v_a - arc voltage

i_a - arc current

τ - arc time constant

P_0 - breaker cooling power

The thermal failure near current interruption and post-arc region conductivity studies are possible in this model.

2.4.2.5 Urbanek model

The Urbanek developed a model which can represent arc interruption and thermal as well as the dielectric failure [34]. Current chopping and reignition both are represented. The arc conductance is characterized by the equation 2.11.

$$\frac{1}{g} \frac{dg}{dt} = \frac{1}{\tau} \left\{ \frac{v_i}{e^2 g} - 1 - \frac{P_0}{e^2 g} \left[1 - \left(\frac{v}{v_d} \right)^2 - 2 \frac{\tau}{v_d^2} v \frac{dv}{dt} \right] \right\} \quad (2.11)$$

where

e - arc voltage for high currents

P_0 - minimum power to maintain the arc

v_d - dielectric breakdown voltage for cold arc channel

2.4.2.6 Kopplin model

Kopplin model is used for simulation of thermal breakdown. This model is used to represent generator circuit breakers [35]. For the arc conductance it is characterized by a Mayr-type equation 2.12

$$\frac{1}{g} \frac{dg}{dt} = \frac{1}{\tau} \left(\frac{v_i}{p_0} - 1 \right) \quad (2.12)$$

with

$$\tau = K_I \cdot (g + 0.0005)^{0.25} \quad (2.13)$$

$$P_0 = K_P \cdot (g + 0.0005)^{0.6} \quad (2.14)$$

where K_p and K_I are model parameters.

Table 2.4.1 gives the summary of applications of arc models used in the testing, development, and operation of CBs.

Table 2.4.1: Arc Model Applications [28]

Type of Problem	Development	Testing	Operation
Design optimization	PAM		-
Mechanical system dimensioning of flow and pressure build up studies	PAM, PM	PAM, PM	-
Dielectric recovery description	PAM, PM	PM	PM
Influence of arc asymmetry and delayed current zeros	PAM, BBM, PM	BBM, PM	PM
Interruption of small inductive currents	PAM, BBM, PM	BBM, PM	BBM, PM
Short-line fault with TRV	PAM, BBM, PM	BBM, PM	BBM, PM
Design and verification of test circuits	PM	BBM	-

2.4.3 Parameter models (PM)

Parameter models are basically black box models with more complex functions and tables which are derived from physical arc models and black box models.

2.5 Circuit Breaker Modeling During Closing

When the contacts of a breaker close and the gap between them get smaller, the breakdown will occur if the voltage across the gap exceeds its dielectric strength. Prestrike phenomenon during closing is shown in figure 2.5.1 [48].

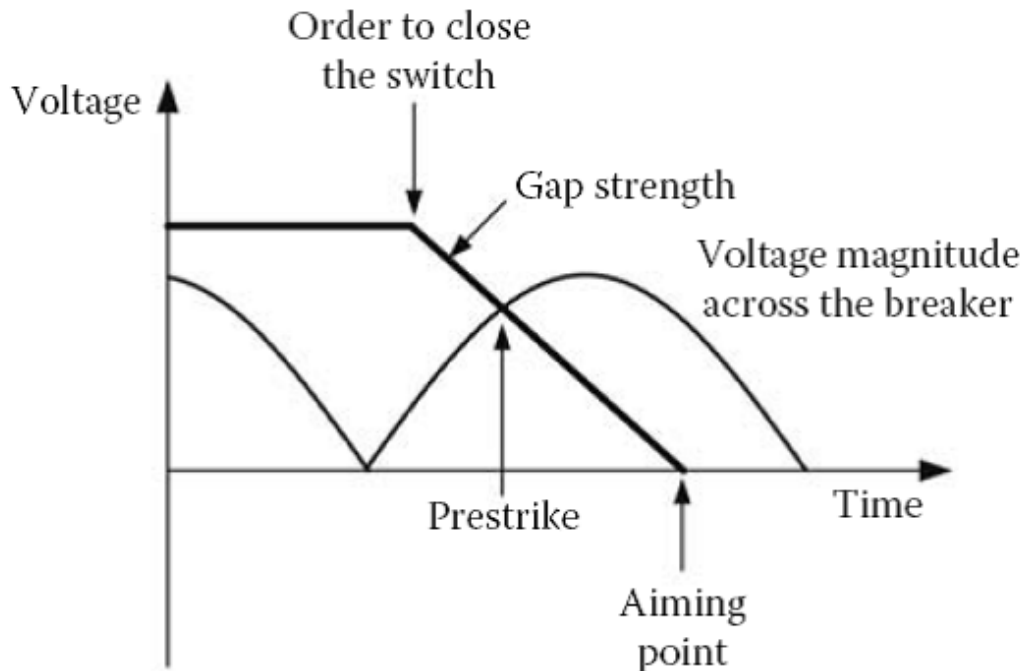


Figure 2.5.1: Prestrike Phenomenon during Closing

Breaker poles closing in a multiphase breaker is random in a cycle. Hence it is difficult to determine the probability of distribution of closing time. The network on the source side or the charge trapped on transmission lines in a reclosing operation determines the peak of the transient voltages during the closing operation of CB. Instant of closing influences the maximum peak which can be different for every pole of the breaker. Many models are available to represent a CB in closing operations [49]:

- In the simplest model breaker is assumed to behave as an ideal switch whose impedance changes from infinity to zero value when CB switches from open to the closing condition. The switching overvoltage across breaker depends on the closing time of breaker. For three phase system first pole to clear factor is added since all the poles do not close simultaneously. Closing instant is randomly determined in the improved approach of this model
- In advanced approach it is assumed that there is a closing time from the instant the contacts start to close to the instant they are closed finally. Arc will strike before the contacts are completely closed if the dielectric strength of the medium is less than the withstand voltage because the withstand voltage decreases as the distance between the contacts decreases. In [50], pre-strike effect and its influence on the switching overvoltage during line energization is analyzed
- In the third approach, pre-strike dynamic arc conductance is included in the study of opening operations

2.6 SF₆ Circuit Breakers

2.6.1 Introduction

Figure 2.6.1 shows the voltage ranges in which different breaking medium is used [51]. The figure shows that SF₆ CBs are used in the applications for the system voltages in the range between 72.5 to 800 kV. Recently 1200 kV SF₆ CB is installed at Bina substation of PGCIL in Madhya Pradesh, India. Excellent dielectric strength, electron affinity or electro negativity, rapid recovery of the dielectric strength around arc region, chemically stable, non-flammable, non-corrosive, non-poisonous properties made the SF₆ gas superior over the other mediums used in CBs.

Earlier SF₆ CBs were of double pressure type in which the extinguishing chamber was divided into two separate parts and were working on the principle that of air blast CBs. Nowadays puffer or self-blast principle is used for arc extinction in all high voltage SF₆ CBs.

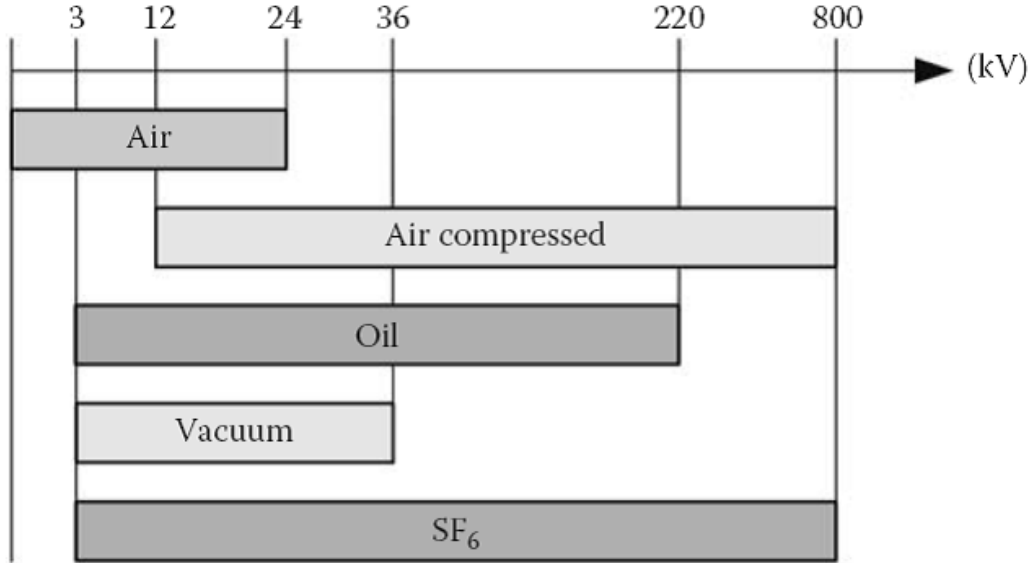


Figure 2.6.1: Voltage Range of Application of Breaking Technologies

2.6.2 SF₆ puffer circuit breakers

In the SF₆ puffer CBs during the opening stroke, the gas pressure for the cooling blast is created in a compression chamber. The compression of the gas will start at the same instant when the contacts start their motion during opening operation. When the arcing contacts leave the throat of the nozzle, the compressed gas is blown out along the axis of the arc. Figure 2.6.2 shows the main components of the puffer interrupter where as figure 2.6.3 shows its function. The current path through the closed interrupter is marked in red color.

The extinguishing pressure is current dependent in SF₆ puffer CBs. As seen in the no load curve figure 2.6.4, the maximum pressure in the puffer cylinder at no load operation is about twice the filling pressure. During a large current interruption, such as short circuit condition, gas flow through the nozzle is blocked by the arc. The arc diameter decreases during current zero which leaves more outlet area for the flow of the gas that gives maximum cooling when needed. A pressure is built up in the puffer cylinder due to blocking of the nozzle during the high current interval that may be many times the maximum no load pressure. The operating mechanism has to provide higher operating force to operate the CB due to high pressure in the puffer cylinder [25].

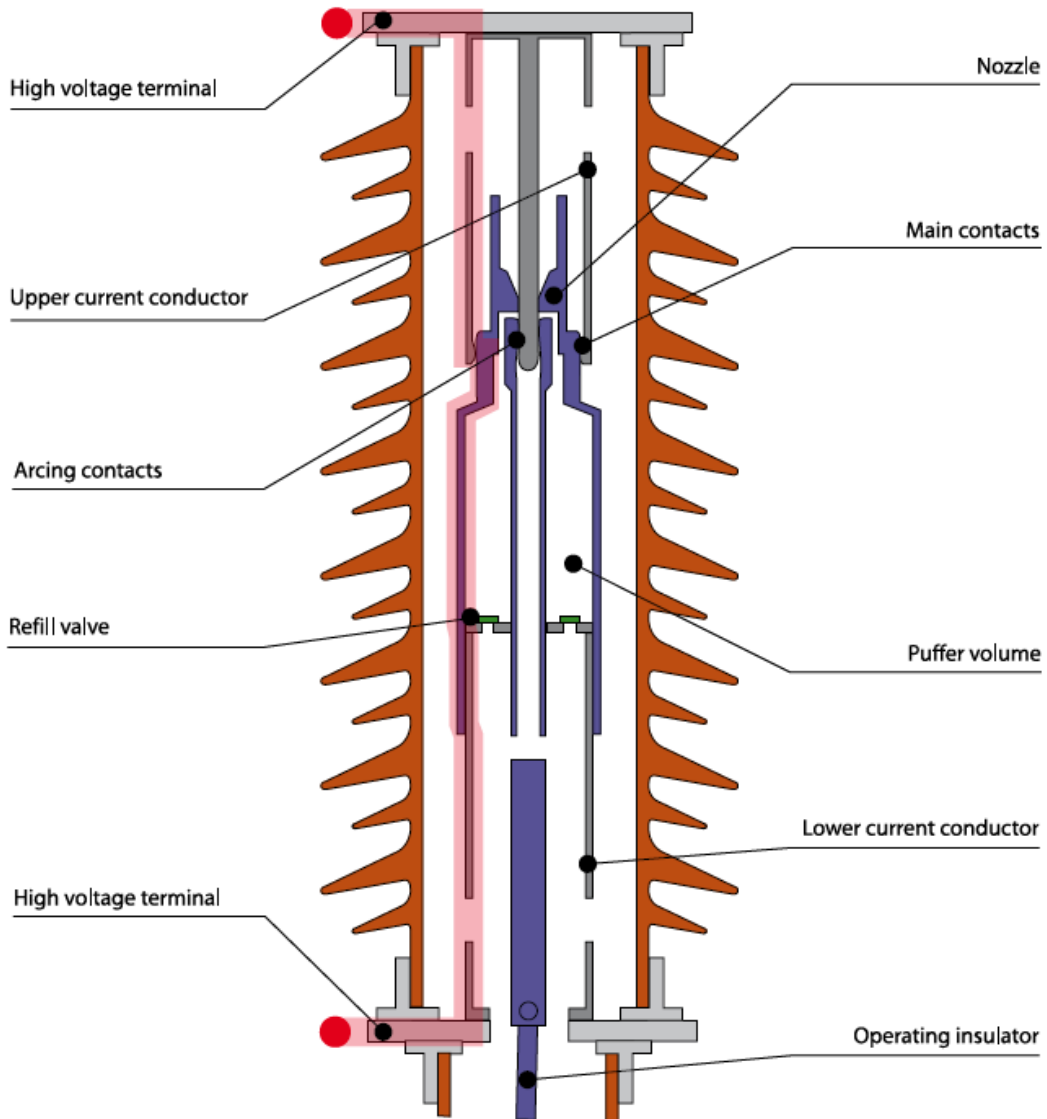


Figure 2.6.2: Main Components of the Puffer Interrupter

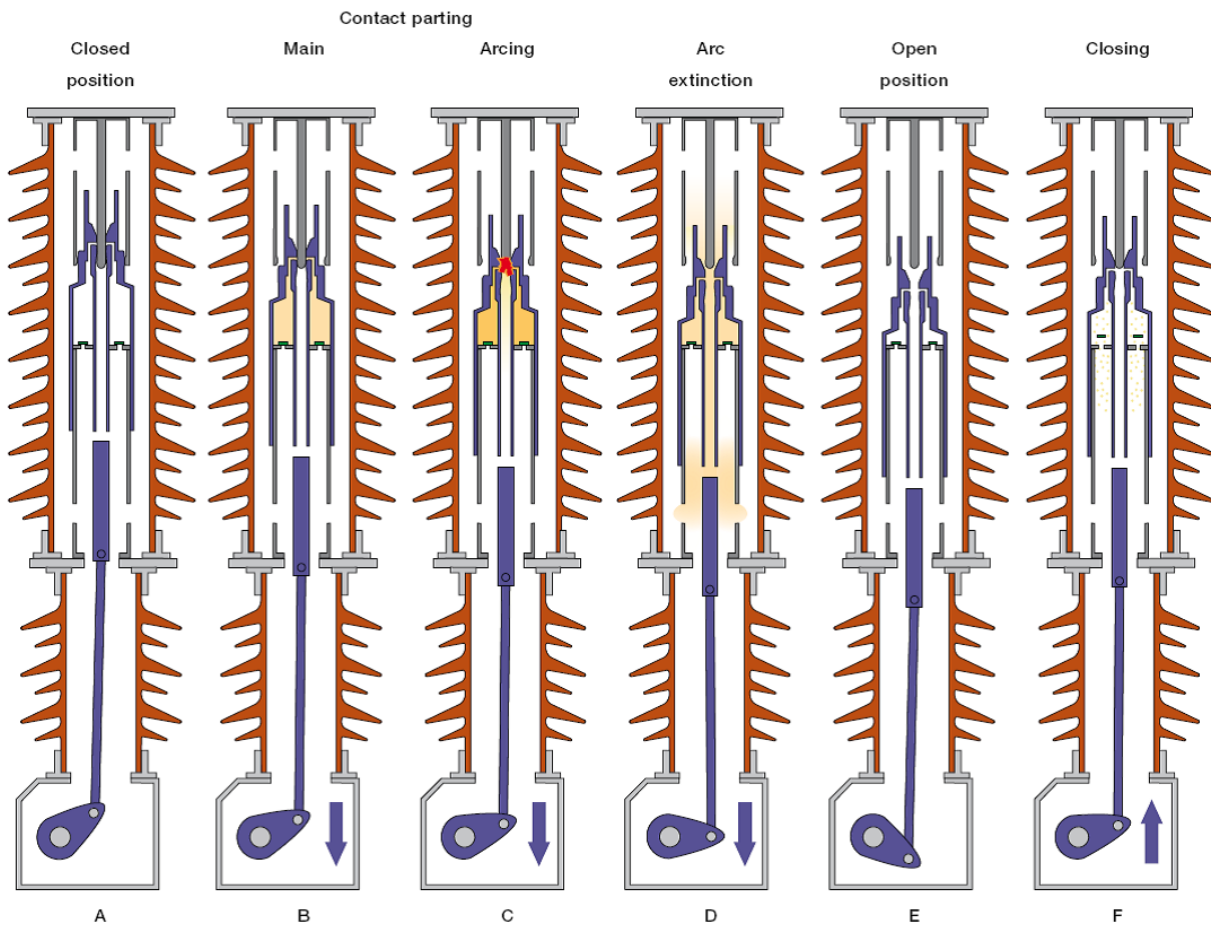


Figure 2.6.3: Function of a Puffer Interrupter

- A - Closed position. Current conduction through the main contacts.
- B. Main contacts separation. Starting of the moving contacts separated the main contacts commuting the current to the arcing contacts.
- C. Arc is established due to separation of arcing contacts. Pressure in the puffer cylinder starts to increase.
- D. Arc extinction. The cold gas from the puffer volume moves rapidly through the nozzle during current zero, cooling and extinguishing the arc.
- E. Contacts fully open.
- F. Closing operation. Puffer volume is filled with cold gas making the interrupter ready for the next operation.

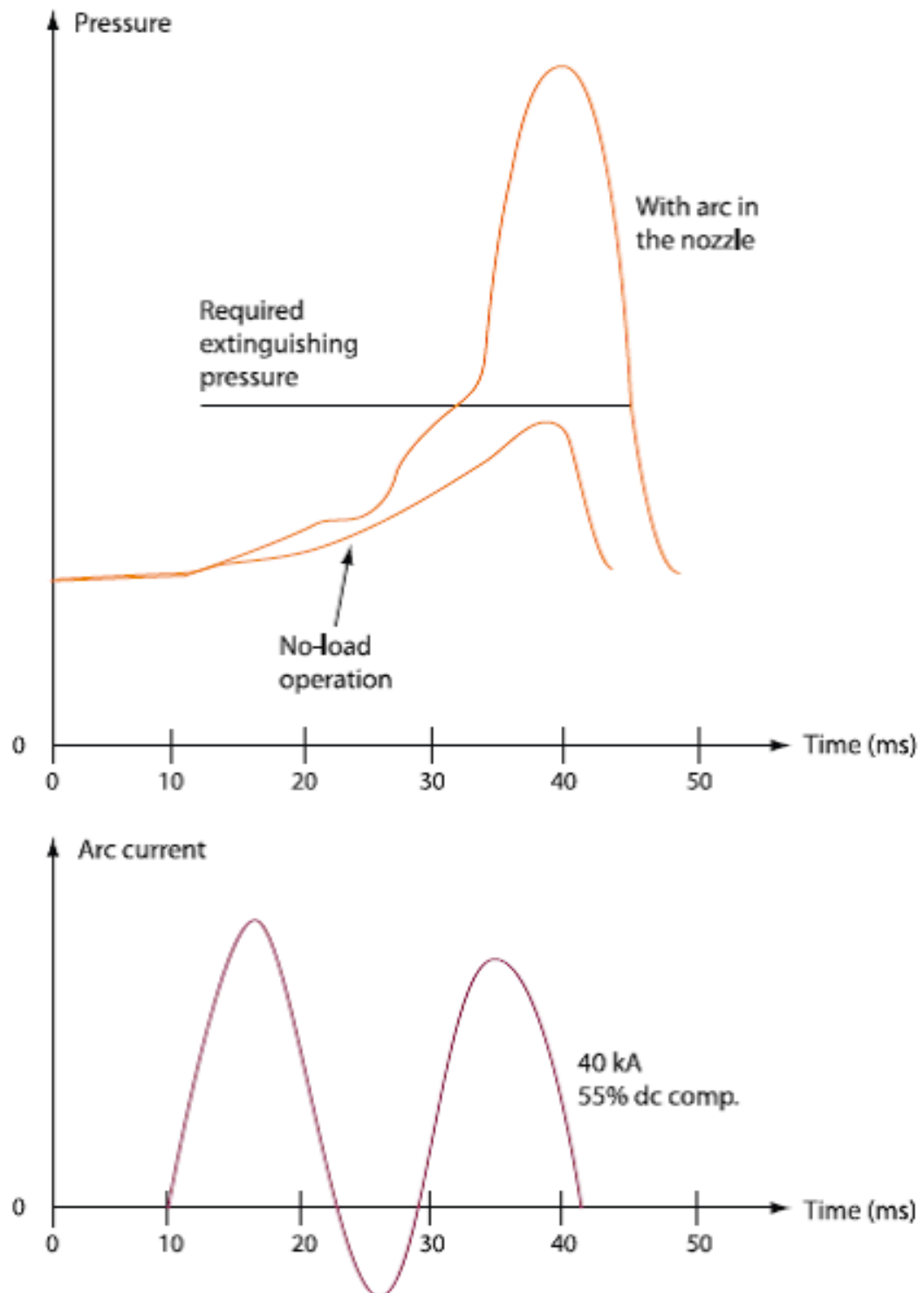


Figure 2.6.4: Pressure in the Puffer Cylinder at No-Load and during Interruption of an Asymmetrical Short-Circuit Current of 40 kA

2.6.3 SF₆ self-blast circuit breakers

Most of the CB failures are of mechanical nature [52]. Hence the reliability of the operating mechanism is of utmost important. In the normal puffer CB, energy from the operating mechanism is used to create the blast pressure. Self-blast principle reduced the operating energy. The arc extinction chamber in self-blast SF₆ CBs is divided into puffer volume and self-blast volume by the self-blast valve. During high fault current interruption, the pressure generated by the arc in the self-blast volume will be high. This high pressure closes the valve and prevents the gas from escaping into the puffer volume. The pressurized gas flows through the nozzle extinguishing the arc. But while interrupting no load current or small currents of few kA, the energy produced by the arc is insufficient to generate the pressure to close the valve. In this situation the interrupter than works as puffer interrupter.

2.7 Transient Recovery Voltage

The power system response to current interruption generates the TRV. TRV is the algebraic sum of the source side voltage and the load side voltage as shown in figure 2.7.1. The shape of the TRV depends on the circuit to interrupted, characteristics of the network connections and the type of fault.

IEEE and IEC both specify the standard TRV by the same approach.

- The two parameters representation is used for HVCBs with a rated voltage up to 100 kV, figure 2.7.2
- Four parameters representation is used for the CBs with rated voltage 100 kV and above, figure 2.7.2

The procedure and calculations necessary to apply TRV ratings for ac high-voltage circuit breakers rated above 1000 V are demonstrated in the IEEE Standard C37.011-2011 [53].

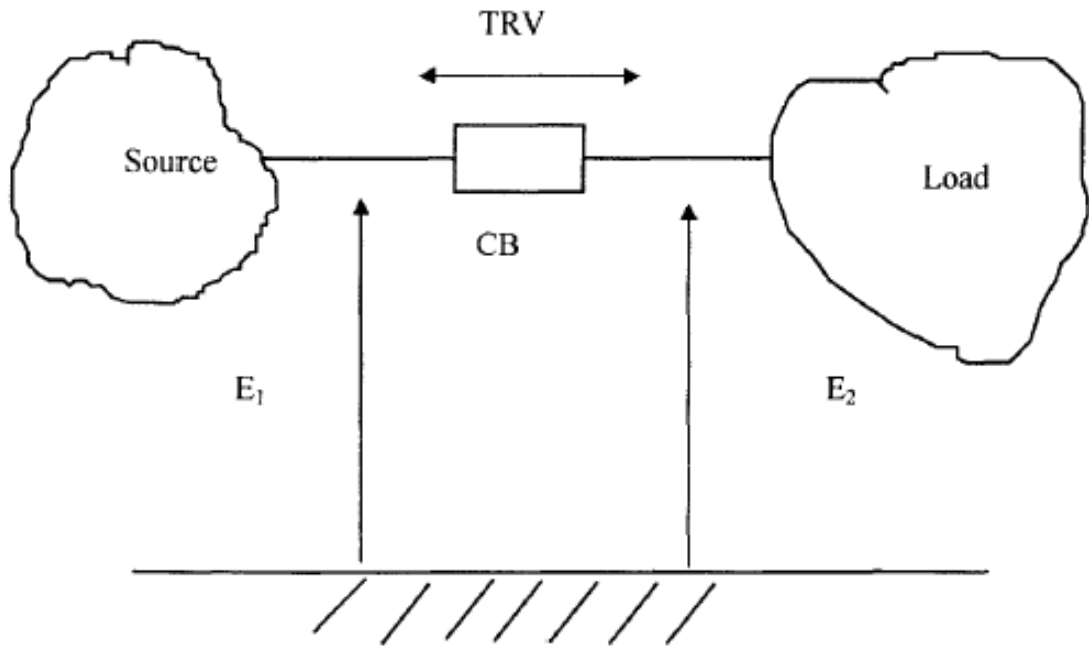


Figure 2.7.1: Illustration of the Sources of TRV [23]

2.7.1 Reactive equipment switching duty

Switching of reactive equipment such as capacitor bank and shunt reactor is supposed to be a severe duty for CB that causes a high rate of rise of TRV across the CB contacts [54]. The high percentage of failure of CB is recorded for reactor switching and capacitor switching [18]. The inrush current during switching of isolated capacitor bank as well as back to back capacitor switching is recognized in the standards [55]. Investigations and field experience of the failure of SF₆ CB in the switching of 420 kV shunt reactor is presented [56]. The switching transient of the shunt reactor is a high frequency response which is influenced by the surrounding circuit conditions. Figure 2.7.3 shows the shunt reactor equivalent circuit.

The CB is stressed by TRV after current interruption. Reignition will take place during interruption if the contact gap is small. The reignition leads to several modes of current oscillations. These oscillations are superimposed on the reestablishing of load current and may produce current zeros at which CB will attempt to interrupt. If new interruption takes place during the first, second or main oscillation modes, then the load side oscillation starts again. Due to

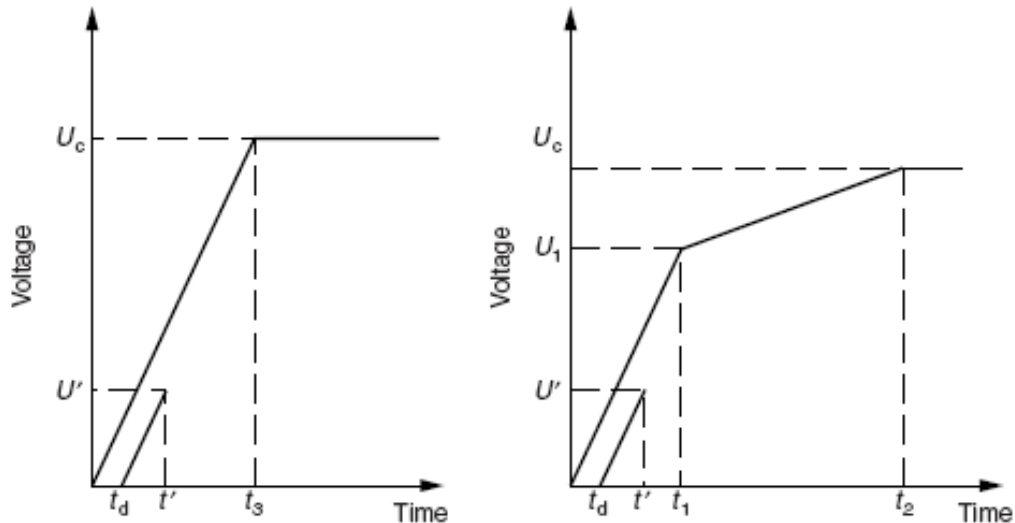


Figure 2.7.2: IEC Two and Four Parameter Limiting TRV Curves [53]

For two parameters method:

U_c - reference voltage, TRV peak value (kV)

t_3 - time to reach U_c (μs)

For four parameters method:

U_1 - first reference voltage (kV)

t_1 - time to reach U_1 (μs)

U_c - second reference voltage (TRV peak value) (kV)

t_2 - time to reach U_c (μs)

For delay line:

U' - reference voltage (kV)

t' - time to reach U' (μs)

t_d - time delay (μs)

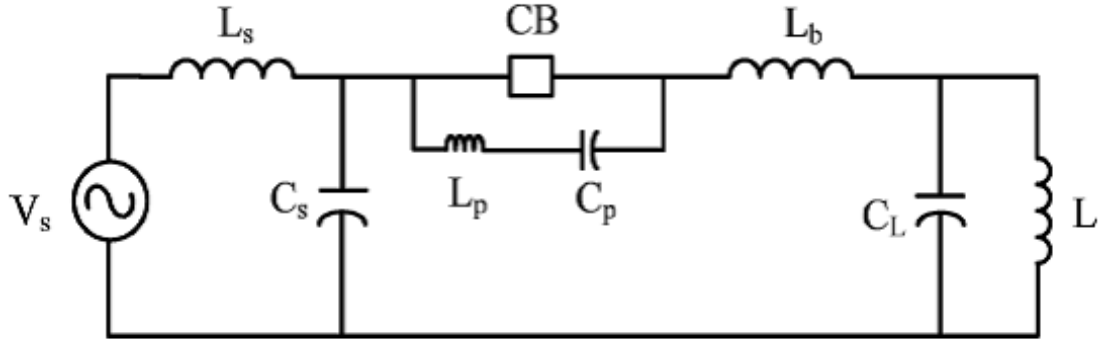


Figure 2.7.3: Shunt Reactor Equivalent Circuit

L_s - source side inductance; C_s - source side capacitance; L_p and C_p - stray inductance and capacitance between CB contacts; L_b - the connecting series inductance; C_L - load side capacitance; L - shunt reactor inductance

energy transfer between the source and load sides, the oscillating energy may change. A new reignition may occur close to the recovery peak, and if the energy has increased, the reignition voltage may be higher than at the first reignition. This procedure may be repeated several times giving multiple reignitions with an increase in voltage magnitude.

2.7.1.1 First parallel oscillations

Oscillations are occurring in the current through the circuit-breaker immediately after a reignition. Oscillation due to the energy source in the capacitances of direct vicinity of the circuit breaker is first parallel oscillation. These oscillations are in addition to oscillations caused by the parameters already connected in the system and parallel to them. These oscillations depend on the inherent “stray”capacitances of the circuit breaker pole and the few meters of conductors connected [57]. In first parallel oscillation electrostatic energy stored in C_p is dissipated through the CB with no exchange between the source and load sides. The frequency of this oscillation is given by equation 2.15 which is of the order of 1 to 10 MHz. The CB will not interrupt the current associated with the first parallel oscillation.

$$F_{P1} = \frac{1}{2\pi\sqrt{L_p C_p}} \quad (2.15)$$

2.7.1.2 Second parallel oscillations

The second parallel oscillation includes the elements CS, CL, and LP. The voltage across CS and CL are equalized, *i.e.* for an instant voltage across the CB is reduced to zero. The CB may interrupt the current associated with second parallel oscillation. The frequency of second oscillation, which is in the range of 50 to 1000 kHz, is given by equation 2.16

$$F_{P2} = \frac{1}{2\pi} \sqrt{\frac{C_L + C_S}{L_S C_L C_S}} \quad (2.16)$$

2.7.1.3 Main circuit oscillations

The components which relate to main circuit oscillation are: generator, capacitances and lumped inductances of the supply and load side network. Frequency is in the range of 5 to 20 kHz. During the main circuit oscillation, all circuit elements are involved, and the energy exchange is both electromagnetic and electrostatic.

2.7.1.4 Source side oscillations

If the CB does not interrupt the current in second parallel oscillation and if the TRV is higher than the strength of dielectric recovery voltage, the oscillation is extended to source side circuit and is termed as main circuit oscillation given by equation 2.17 frequency of which is in the range 1 to 20 kHz. This oscillation involves the total circuit and generally leads to a new loop of current.

$$F_m = \frac{1}{2\pi} \sqrt{\frac{L_S + L}{L_S L(C_S + C_L)}} \quad (2.17)$$

2.7.1.5 Load side oscillations

Load side oscillation with trapped energy oscillating between the inductance and capacitance of the load side circuit during successful interruption is given by the equation 2.18. The frequency is in the range of 1 to 5 kHz.

$$F_L = \frac{1}{2\pi\sqrt{LC_L}} \quad (2.18)$$

Figure 2.7.4 shows the oscillation modes occurring in the reactor circuit [58].

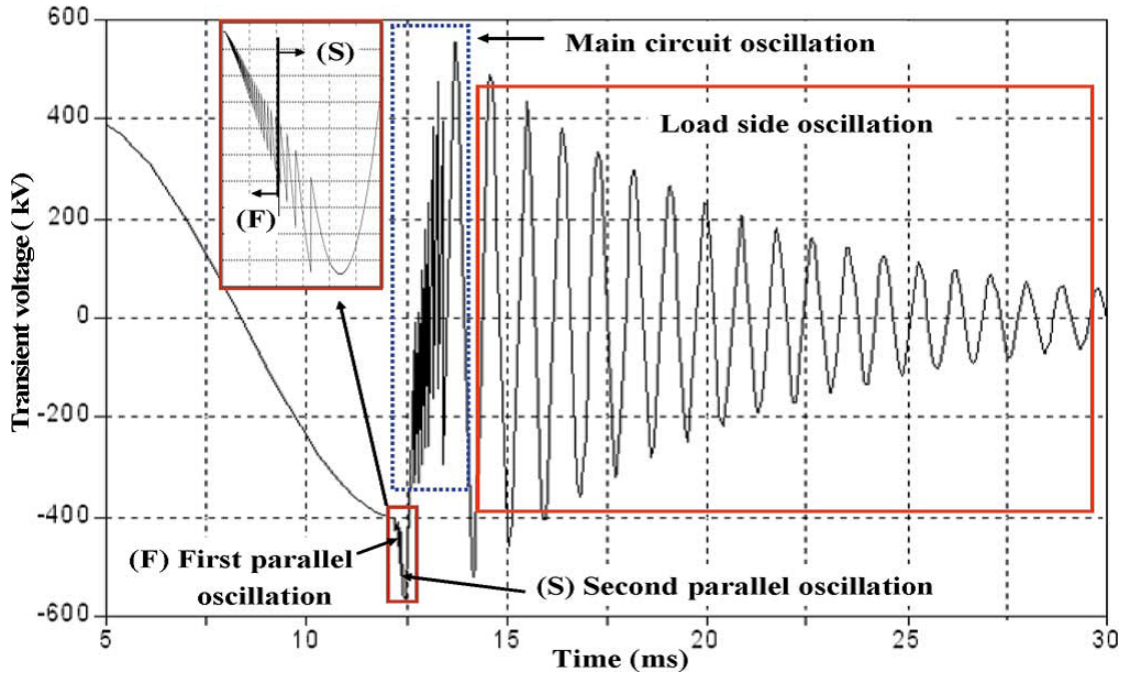


Figure 2.7.4: Oscillation modes in reactor circuit [58]

Circuit breaker interrupter failure is reported due to restrike which punctured right through the nozzle between the moving main contact and the fixed arcing contact of the interrupter [59].

2.8 Time Definitions as per IEC

The Standard IEC 62271-100 [52] covers the standard operating procedures for ac circuit breakers used for indoor or outdoor operation at 50 Hz and 60 Hz on the system having voltages above 1000 V. The most frequently used time definitions are -

opening time

opening time is the interval of time between the instant of energizing the opening release, and the instant when the arcing contacts have separated in all poles, the circuit-breaker being in the closed position

arching time

interval of time between the instant of the first initiation of an arc and the instant of final arc extinction in all poles

break time

interval of time between the beginning of the opening time of a mechanical switching device and the end of the arcing time

closing time

the circuit-breaker being in the open position, closing time is the interval of time between energizing the closing circuit and the instant when the contacts touch in all poles

make time

the circuit-breaker being in the open position, make time is the interval of time between energizing the closing circuit and the instant when the current begins to flow in the first pole

pre-arcng time

during a closing operation, pre-arcng time is the interval of time between the initiation of current flow in the first pole and the instant when the contacts touch in all poles for three-phase conditions and the instant when the contacts touch in the arcng pole for single-phase conditions

close-open time

interval of time between the instant when the contacts touch in the first pole during a closing operation and the instant when the arcng contacts have separated in all poles during the subsequent opening operation

Figures 2.8.1 to 2.8.2 show the time definitions during opening and closing and close-open cycle respectively.

2.8.1 Contact resistance measurement

2.8.1.1 Static contact resistance measurement (SCRM)

Condition monitoring of CB through coil current signature, operational timings, tank gas pressure and the temperature is found [60–65]. However, coil current analysis does not give any information about contact condition. Generally, static contact resistance measurement is done to assess the condition of contacts. CB

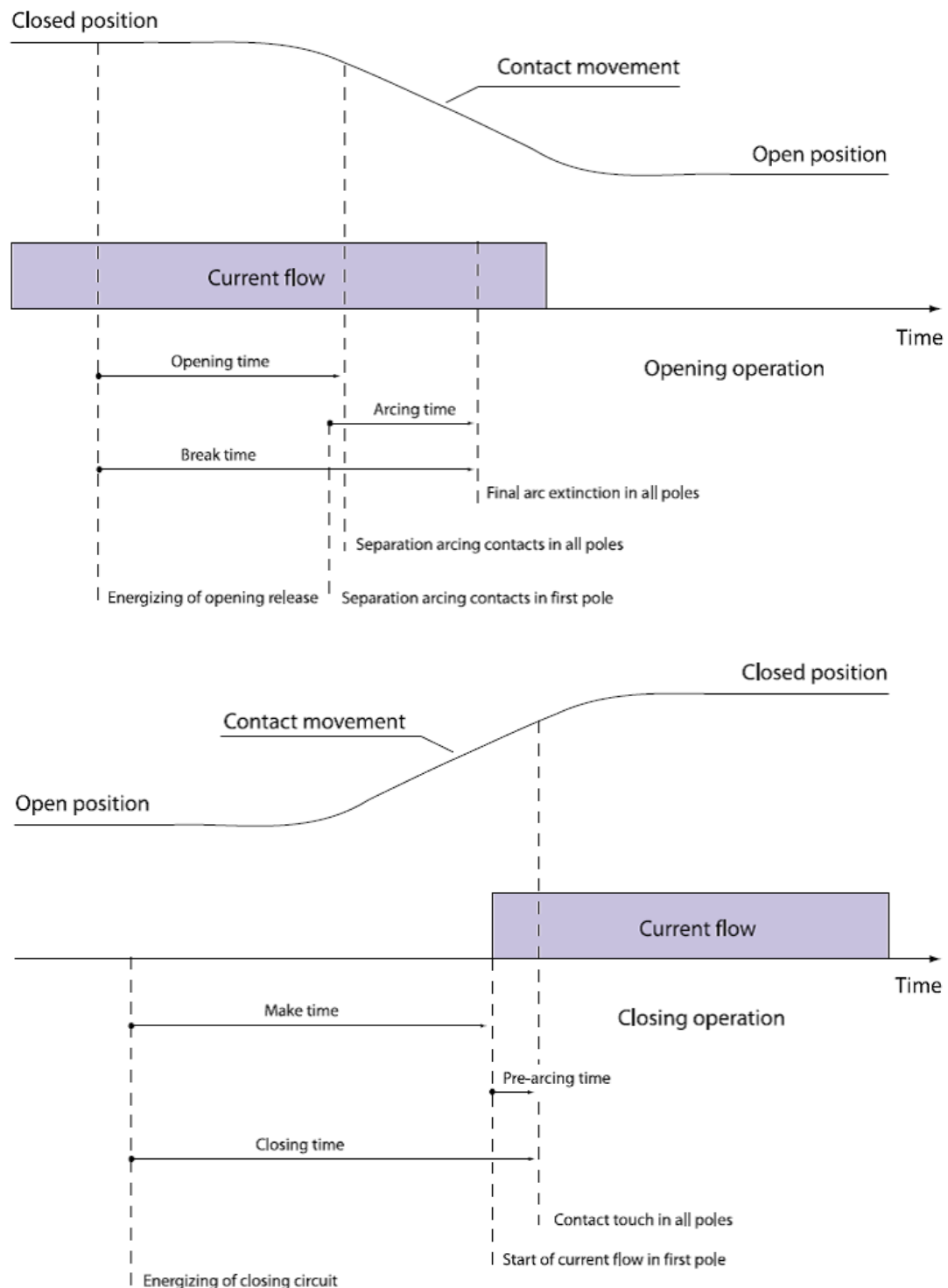


Figure 2.8.1: Time Definitions during Opening and Closing, As Per IEC

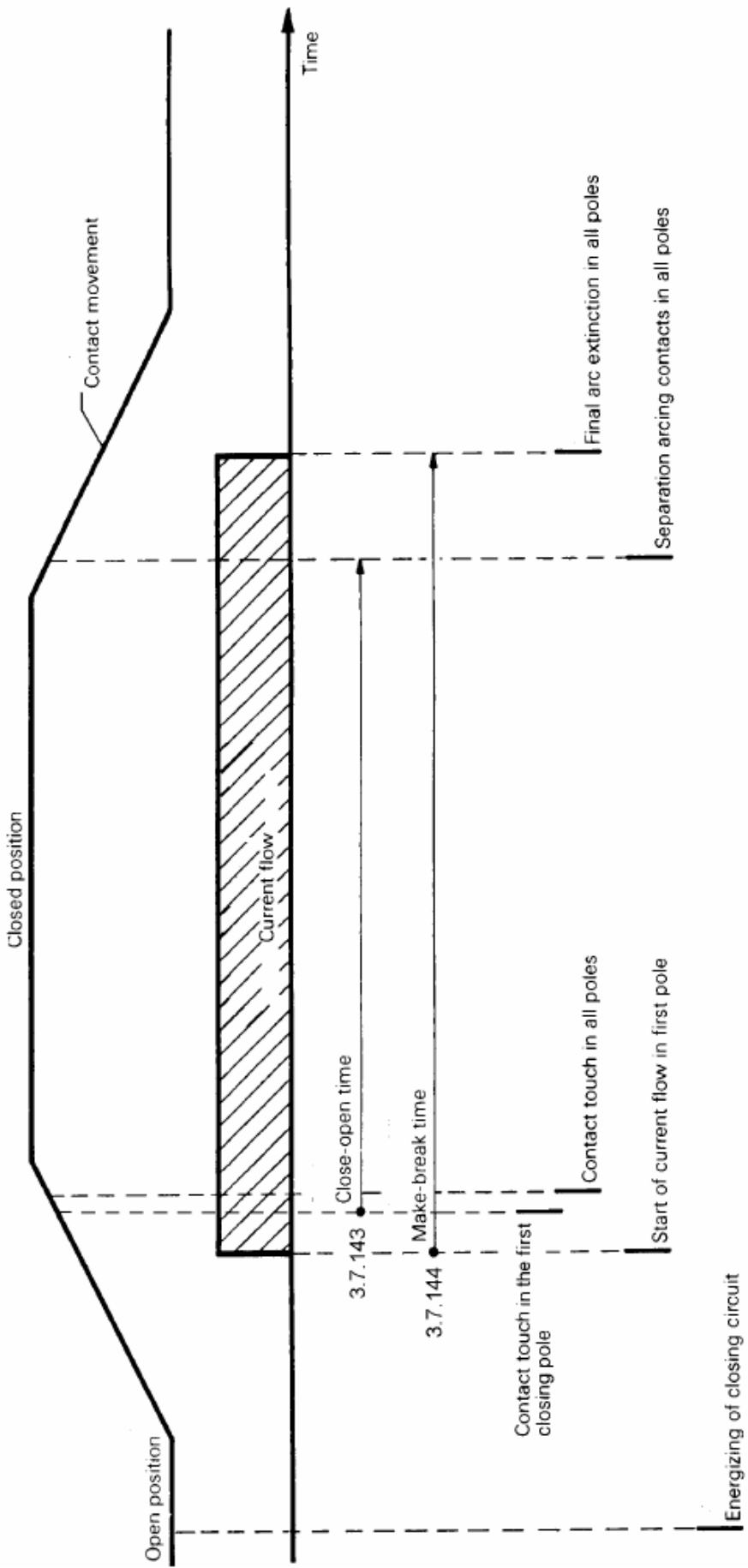


Figure 2.8.2: Time Definitions during Close-Open Cycle for CB without Switching Resistors

contacts are closed, and a DC current is passed through the contacts. IEC and ANSI recommend a value of 50A and 100A respectively. The voltage drop across the contacts is measured. The measured voltage drop, when divided by current, gives the resistance of main contacts. However, this method of resistance measurement evaluates the condition of main contacts only [66].

2.8.1.2 Dynamic contact resistance measurement

The condition of the arcing contacts is important from the point of short circuit current interruption capability of CB. It can be done by opening the CB interruption chamber. But this is time consuming and expensive due to high pressure SF₆ gas in the chamber. Also, reassembly of the unit may lead to new problems. DCRM is an indirect method of determining the condition of arcing contacts. It is quite similar to static contact resistance measurement with a difference that instead of a single value of resistance, a curve of resistance Vs time or distance is measured. Figure 2.8.3 gives the flow chart of DCRM. Close- open command is given to the CB and 100A DC current is injected. The instantaneous value of voltage and current is measured when CB opens. Resistance is calculated at each point. A curve of resistance Vs time is called as DCRM signature. DCRM signature along with the contact travel can be used to measure the main contact wipe, arcing contact wipe, average main contact and arcing contact resistance.

DCRMs during closing operations are not useful as the sudden change from infinity to the arcing contact resistance is difficult to measure. Also, undesired noise gets generated at the arcing contact touch [67]. Several spikes are observed in the DCRM curve due to partial contact separation for the CBs operated with a high speed of contact movement [68–70].

Measurement at low speed

M. Landry *et al.* [66] observed that the DCRM curves at rated speed are not comparable. The identification of main contact part was difficult. High contact speed was the reason anticipated for partial contact part. DCRMs at low speed were found identical. It was observed that the DCRM curves were smooth and the main contact parting was easy to identify. However, for some breaker mechanism,

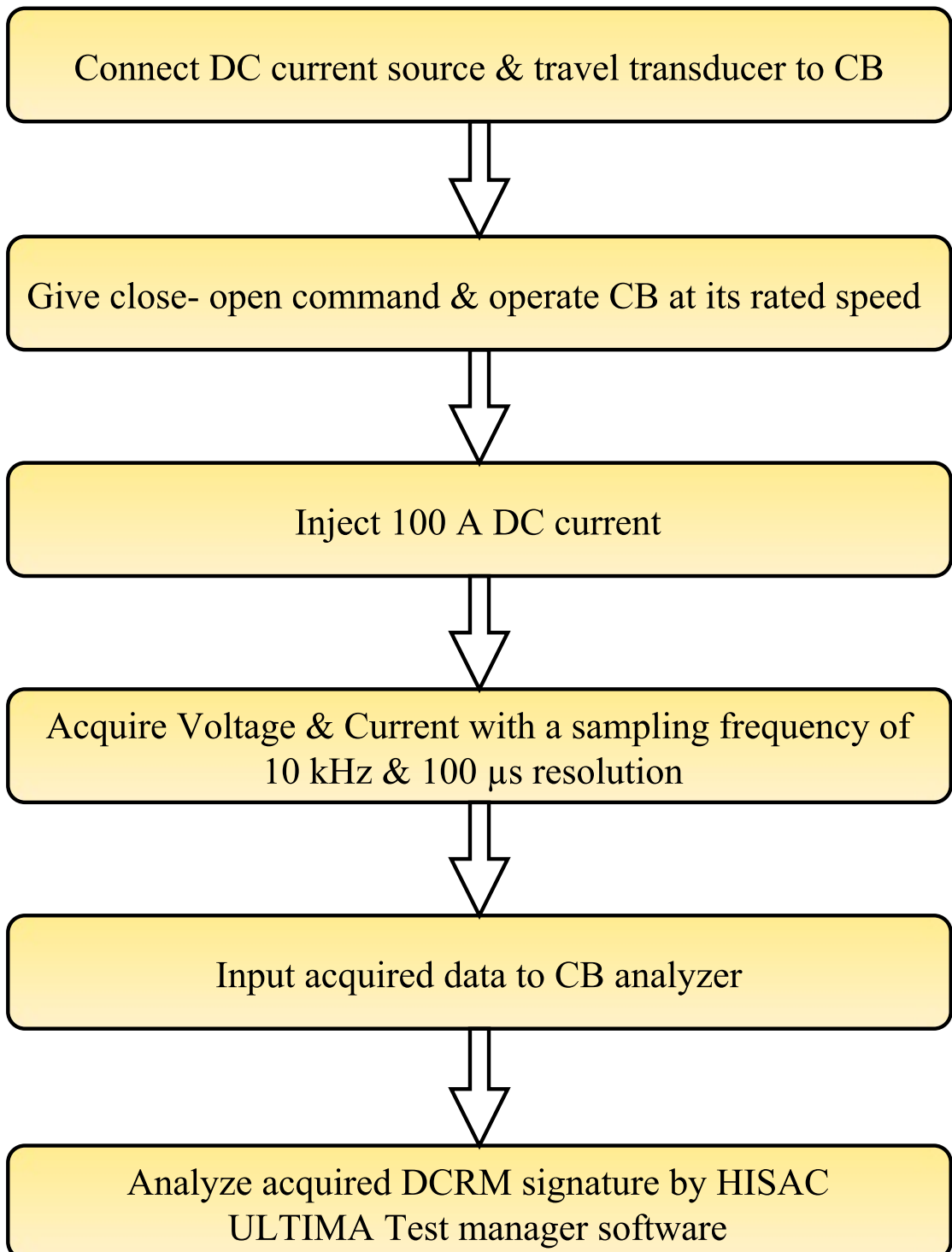


Figure 2.8.3: Flow Chart of DCRM

it is time-consuming to do the adjustments of a mechanism for low-speed operation. The CBs in the field are operated at rated speed. Hence the operation at low speed may not give the correct information of contacts.

DCRM in the presence of metallic fluorides

Due to arcing metallic fluorides are formed which get deposited on the CB contacts in the form of nonconductive dust powder. The effects of metallic fluorides on contact resistance have been dealt in [69]. High contact resistance was observed for the CB used for capacitor bank switching and which has performed a large number of operations. However, the deposition of metallic fluorides did not affect the short circuit capacity of CB. If the scraping or wiping action in the CB contact is not proper, then the high contact resistance will appear [66]. Conventional equipment was used to perform the static contact resistance measurement at 100 A DC current. A high value of the contact resistance of the order of 4500-6000 $\mu\Omega$ was measured which could be interpreted as defective contacts. Michel Landry *et al.* developed a method to determine the reason for high resistance which does not require the opening of CB interrupting chamber. Three current sources were connected in parallel to deliver 2800 A DC current. For carrying this high current from source to the breaker, six 4/0 copper cables were used. A measuring shunt of 51.32 Ω along with data acquisition system was used for recording the signals. Breaker contacts were kept in closed condition, and contacts were heated for different intervals in order to vaporize the metallic fluorides that were deposited on the CB contacts. DCRM were recorded for each phase at different currents. From this experimentation Michel Landry *et al.* observed that heating of contacts for 15 minutes at 2800 A current reduced the arcing contact resistance to the acceptable level [67].

Measurement at low speed

The conventional DCRM system needs heavy and long cables to connect the current source to the breaker. Ultra capacitors as a current source are discussed [71]. The ultra capacitors along with constant charger are light weight as compared to batteries and are capable of generating few hundred amperes. A low resistance meter based on a large value of capacitor with a very small value of internal

resistance, charger for the capacitor and control along with measurement circuitry for 250 A DC current was developed. The developed low resistance meter can be used for static as well as dynamic resistance measurements.

A DCRM system was developed using a stationary battery of 12V/220Ah [72]. DCRM parameters that are useful in contact diagnosis are discussed.

A power grid experience of DCRM of CBs from PGCIL is shared [12]. DCRM signatures of CBs from field with problems in contacts are described.

Erosion of arcing contact takes place during every operation of CB depending on the breaking current. The erosion of arcing contacts leads to the time difference between contact separations in successive operation. The contacts need the overhaul when the overlap time falls below a defined minimum value [73].

On line monitoring of contact electrical erosion of CBs based on the theory of accumulative effect and the statistical average is developed [74].

High frequency DC/DC converter as a power source for generating high DC current and measuring the dynamic contact resistance of the CB is presented [75].

Principal component analysis is used to get the information from dynamic resistance signal [76].

Scoring and weighting techniques and health index are applied to identify the healthy, needs maintenance and risky condition of CB [77].

Design and development process of control, acquisition, and analysis of the DCRM results for high voltage circuit breaker is presented [78].

Use of Arduino platform in measuring and processing the dynamic contact resistance curve is described [79]. However, it has the limitation of the sampling rate.

Testing of 400 kV CB in high induction environment is presented [80]. To overcome the induction voltage in recorded signal, grounding on both sides of HVCB is suggested.

All the work described in above papers focus on the measurement process of dynamic contact resistance. Methodology to detect the contact failure through DCRM is not discussed in the literature. Since the interrupter is sealed, it is not feasible to detect the contact condition. Intentional failure and then correlating the DCRM signature is not possible.

2.9 Research Gap

Literature survey reveals that condition based maintenance has been the most efficient maintenance strategy. Lot of work has been done on the coil current analysis. Coil current signature can be acquired during the switching operation, and various approaches are available to determine the real time health of control circuit. Another crucial part of the circuit breakers is the main and arcing contacts.

It is observed that papers on Dynamic Contact Resistance Measurement focus on the measurement process of dynamic contact resistance. Methodology to detect the contact failure through DCRM is not discussed in the literature. Since the interrupter is sealed, it is not feasible to detect the contact condition. Intentional failure and then correlating the DCRM signature is not possible.

The Dynamic Contact Resistance Measurement was developed around 20 years ago to assess the condition of arcing contacts without dismantling the breaker, and in India, the utility companies are using this test for condition monitoring from last ten years.

Arc formation and the TRV at the arc interruption of every CB connected to the same system configuration will be different. This is due to design aspect of CB. Hence every CB has a unique signature. Knowledge of CB design such as types of contacts, mechanism, the principle used in arc extinction, *etc.* is necessary. Hence the signatures obtained from Dynamic Contact Resistance Measurement (DCRM) are difficult to interpret and may lead to wrong decisions about the condition of contacts. Signature analysis of circuit breaker for dynamic resistance measurement is developing. It is an emerging area for research.

Chapter 3

SYSTEM DEVELOPMENT

Study of parameters affecting short circuit capacity of the circuit breaker is divided in:

1. Modeling of system for TRV studies under different fault conditions
2. Modeling of system under different fault conditions for arc interruption studies
3. Measurement of Dynamic Contact Resistance of CBs and analysis of collected DCRM signature data

3.1 Computational Models

3.1.1 Interruption of Three Phase to Ground fault

A model of IEEE network is developed in EMTP-RV. As shown in figure 3.1.1, the system consists of local sources and remote sources connected through transmission lines. Four transmission lines and two transformers supply the 145 kV station. Details are shown in figure 3.1.1. Stray capacitances of equipments are also considered. The system is studied for Three Phase to Ground fault at the terminal of station for multiple lines switching and transformer switching. Breaker rating of 30 kA maximum current interruption capacity is selected for the study. Current in the steady state through fault is found out. Accordingly standard TRV is built. TRV through simulation is compared with standard TRV provided by application guide. The ability of fault interruption capability of CB is found out.

3.1.2 Interruption of Single Phase to Ground fault

The network is further studied for Single Phase to Ground short line fault at 4.2 km from station for 16 km line. The lines are modeled in constant parameter mode as well as frequency dependent mode TRV through simulation is compared with standard TRV provided by application guide for both frequency dependent and constant parameter line model. The ability of fault interruption capability of CB is found out.

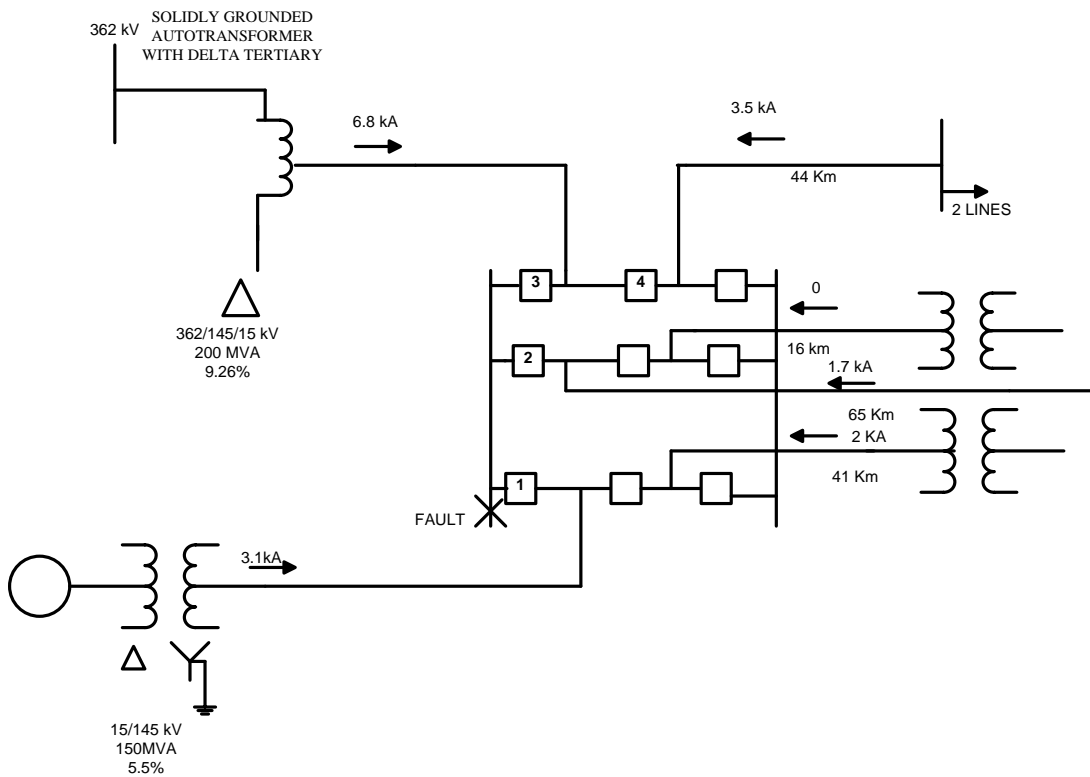


Figure 3.1.1: IEEE Network under Study [53]

Parameters of the model

1. Local Source 1

L-L RMS Voltage - 362 kV

Resistance - 0.16Ω

Inductive Reactance - 16.2Ω

2. Transformer

Nominal Rating - 200 MVA

L-L RMS Primary Voltage - 362 kV

L-L RMS Secondary Voltage - 145 kV

Connection type - Yg-Yg

Winding Resistance - 0.0009 pu

Winding Reactance - 0.0926 pu

3. Generator Transformer

Nominal Rating - 150 MVA

L-L RMS Primary Voltage - 15 kV

L-L RMS Secondary Voltage - 145 kV

Connection type - DYg+30°

Winding Resistance - 0.0005 pu

Winding Reactance - 0.055 pu

4. Local Source 2

L-L RMS Primary Voltage - 15 kV

Resistance - 0.002 Ω

Inductive Reactance - 0.209 Ω

5. Transmission Line

L-L RMS Voltage - 145 kV

Positive Sequence Resistance - 0.01Ω

Zero Sequence Resistance - 0.1 Ω

Positive Sequence Surge Impedance - 350 Ω

Zero Sequence Resistance - 560 Ω

Propagation Speed - 1.9×10^5 m/s

Length of lines - 44 km, 16 km, 65 km , 41 km

6. Parameters of lines for frequency dependent model

Phase	DC resistance Ω	Outside diameter (m)	Horizontal distance (m)	Vertical distance (m)	Vertical distance at mid span (m)
1	0.126	0.12	-8	20	20
2	0.126	0.12	0	20	20
3	0.126	0.12	8	20	20
0	3	0.08	-6	26	26
0	3	0.08	6	26	26

7. Arc parameters

$$\tau_m = 0.5 \text{ E-06}$$

$$P_0 = 10.0 \text{ E+04}$$

$$\tau_c = 1\text{E-06}$$

$$U_C = 2000$$

$$g_0 = 5\text{E+07}$$

$$t_{trip} = 20 \text{ E-03}$$

3.2 Analytical Models

3.2.1 Transient Recovery Voltage types

Three phase terminal fault is the most severe fault used to define the breaker rating. However, for the transmission voltages, the probability of occurrence of three phase terminal fault is very low. Hence the three phase to ground faults are the basis for rating the CB. Short line faults have lower crest magnitudes, but they have high RRRV.

3.2.1.1 Three phase terminal fault

The circuit showed in Figure 3.2.1 defines the electrical equivalent network for the first phase to clear during the interruption of a three-phase terminal fault.

The corresponding one-line diagram representation is shown in Figure 3.2.1a, while Figure 3.2.1b indicates the three-phase representation. The reduced simple parallel RLC circuit is shown in the equivalent circuit given by Figure 3.2.1c. The equivalent components are given by

Equivalent inductance

$$L_{eq} = \frac{3L_0L_1}{L_1 + 2L_0} \quad (3.1)$$

In effectively grounded systems, for three-phase-to-ground faults *i.e.*, with first pole-to-clear factor equal to 1.3; $L_{eq} = 1.3L_1$.

In ungrounded systems (L_0 infinite), for three-phase-to-ground faults *i.e.*, with first-pole-to-clear factor equal to 1.5; $L_{eq} = 1.5L_1$

Equivalent surge impedance

$$Z_{eq} = \frac{3}{n} \times \frac{Z_0Z_1}{Z_1 + 2Z_0} \quad (3.2)$$

where

$$Z_0 = 1.6Z_1$$

$$Z_{eq} = 1.14Z_1/n$$

Equivalent capacitance

$$C_{eq} = \frac{C_0 + 2C_1}{3} \quad (3.3)$$

where

Z_1 - positive-sequence surge impedance of the transmission lines

Z_0 - zero-sequence surge impedance of the transmission lines

n - number of lines

L_1 - positive-sequence inductance, of all other parallel sources terminating at the station

L_0 - zero-sequence inductance, of all other parallel sources terminating at the station

C_1 - positive-sequence capacitance

C_0 - zero-sequence capacitance

For three-phase ungrounded faults on effectively grounded systems:

$$L_{eq} = 1.5L_1; Z_{eq} = 1.5Z_1/n; C_{eq} = C_1/1.5$$

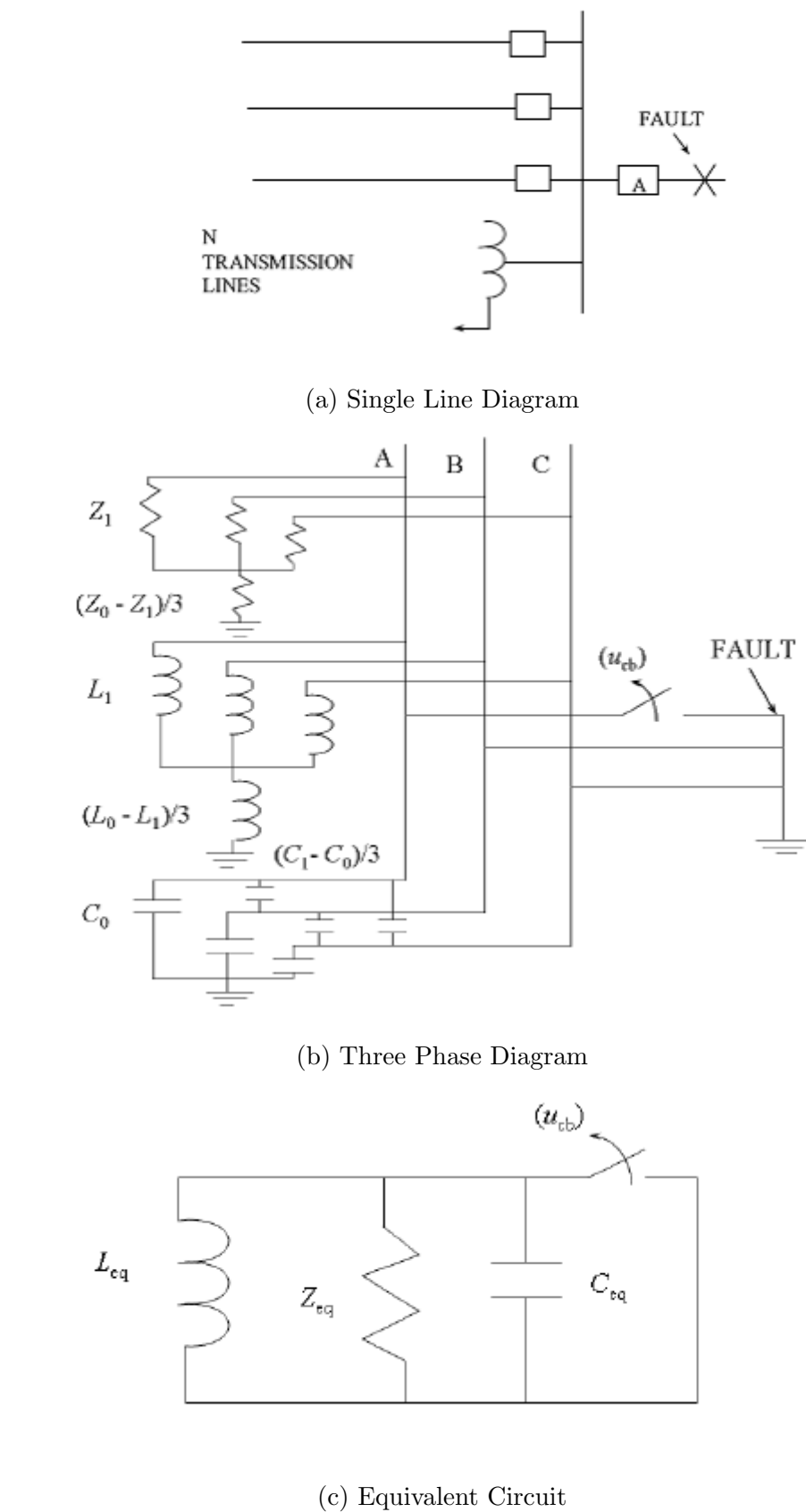


Figure 3.2.1: Circuit for Interruption of a Three-Phase-to-Ground Fault

3.2.1.2 Exponential (Overdamped) TRV

The TRV across the CB contacts can be found using current injection technique as the time span is short (microseconds). The current can be represented by a ramp. The solution for the parallel RLC network shown in Figure 3.2.1c is given by Equation (3.4):

$$u_{cb} = u_1 \left(1 - e^{\alpha t} \left(\cosh \beta t + \frac{\alpha}{\beta} \sinh \beta t \right) \right) kV \quad (3.4)$$

u_{cb} = voltage across the open circuit-breaker contacts

$$u_1 = \sqrt{2} I \omega L_{eq}, (kV)$$

$$\omega = 2\pi f, (rad/s)$$

$$I = \text{rms value short-circuit current, (kA)}$$

$$\alpha = \frac{1}{2Z_{eq}C_{eq}}$$

$$\beta = \sqrt{\alpha^2 - \frac{1}{(L_{eq}C_{eq})}}$$

Z_{eq} - equivalent impedance (Ω)

L_{eq} - equivalent inductance (H)

C_{eq} - equivalent capacitance (F)

In most of the applications, the parallel resistance of the line surge impedances of the lines is such that it effectively swamps the capacitance of the circuit. Hence it is a common practice to neglect the capacitance. The solution to the simple RL circuit is given by equation (3.5):

$$u_{cb} = u_1 \left(1 - e^{-t/\tau} \right) kV \quad (3.5)$$

where

$$\tau = \frac{L_{eq}}{Z_{eq}} s$$

3.2.1.3 Single frequency recovery voltage (Oscillatory underdamped TRV)

When the short circuit is fed by a transformer and numbers of lines remain connected to the bus, the resulting TRV is oscillatory single frequency TRV. Figure 3.2.1c shows the equivalent circuit with resistance removed. The circuit becomes

underdamped and the response is a typical 1-cosine waveform. Equation 3.6 is the approximate equation for the voltage across the open circuit breaker contacts of CB.

$$u_{cb} = u_1 \left[1 - \cos \left(\frac{t}{\sqrt{L_{eq}C_{eq}}} \right) \right] \quad (3.6)$$

3.2.2 Traveling waves

The transmission line can be represented as an inductive elements connected in series and capacitive elements distributed along the line in parallel. The voltage applied at one end travels as an electromagnetic wave with the speed of light. When the transmitted wave reaches discontinuity, the wave gets reflected and refracted depending on the discontinuity. The time for the wave to go out from the discontinuity and back is given by:

$$T = 6.68l\sqrt{\mu\epsilon} \text{ } \mu\text{s} \quad (3.7)$$

l - distance to the first discontinuity (km)

μ - magnetic permeability

ϵ - dielectric constant

The coefficients for the new voltage waves are

$$\text{Reflection, } K_R = \frac{Z_2 - Z_1}{Z_2 + Z_1} \quad (3.8)$$

$$\text{Refraction, } K_T = \frac{2Z_2}{Z_2 + Z_1} \quad (3.9)$$

Z_1 and Z_2 are the surge impedances on either side of the discontinuity.

3.2.3 Short Line Fault

The TRV across the CB contacts after the interruption of short line fault consists of the voltage generated by the supply network and of the voltage created by the line side oscillation. Due to distributed constants of the transmission line, the line side oscillations are in the form of traveling waves. The reflection of this traveling wave against the short circuit point and the open end at the breaker side cause a triangular shaped waveform.

The travel time of the electromagnetic waves in case of single line to ground fault at a distance ' l ' from the breaker to the fault location is given by

$$\tau_{Line} = \frac{l}{\vartheta}$$

Where ϑ is the wave velocity that depends on the transmission line parameters. The wave reflected by the short circuit point arrives at the open end near the breaker after twice the travel time. The lattice diagram shown in figure 3.2.2 is used to evaluate the characteristics of travelling wave for short line fault. The numerical value of the coefficients for the reflected and transmitted wave shows the amplitude multiplier for the voltage wave. Single phase circuit for short line fault with source (X_S) and the line reactance ($\lambda * X_L$) is shown in figure 3.2.3a. The fault current is given by equation 3.10.

$$I_L = \frac{u_{LG}}{\lambda \times X_L + X_s} \quad (3.10)$$

X_L - reactance of the line to the fault point per kilometer, given by $\frac{(2L_1\omega + L_0\omega)\omega}{3}$

L_1 - positive sequence power-frequency line inductance per kilometer

L_0 - zero sequence power-frequency line inductance per kilometer

u_{LG} - line to ground system voltage (kV)

λ - distance of CB to the fault (km)

I_L - terminal fault current (kA)

$$\frac{du_L}{dt} = \sqrt{2}\omega I_L Z_{eff} \quad (3.11)$$

The source side and line side TRV shapes during short line fault is shown in figure 3.2.3.

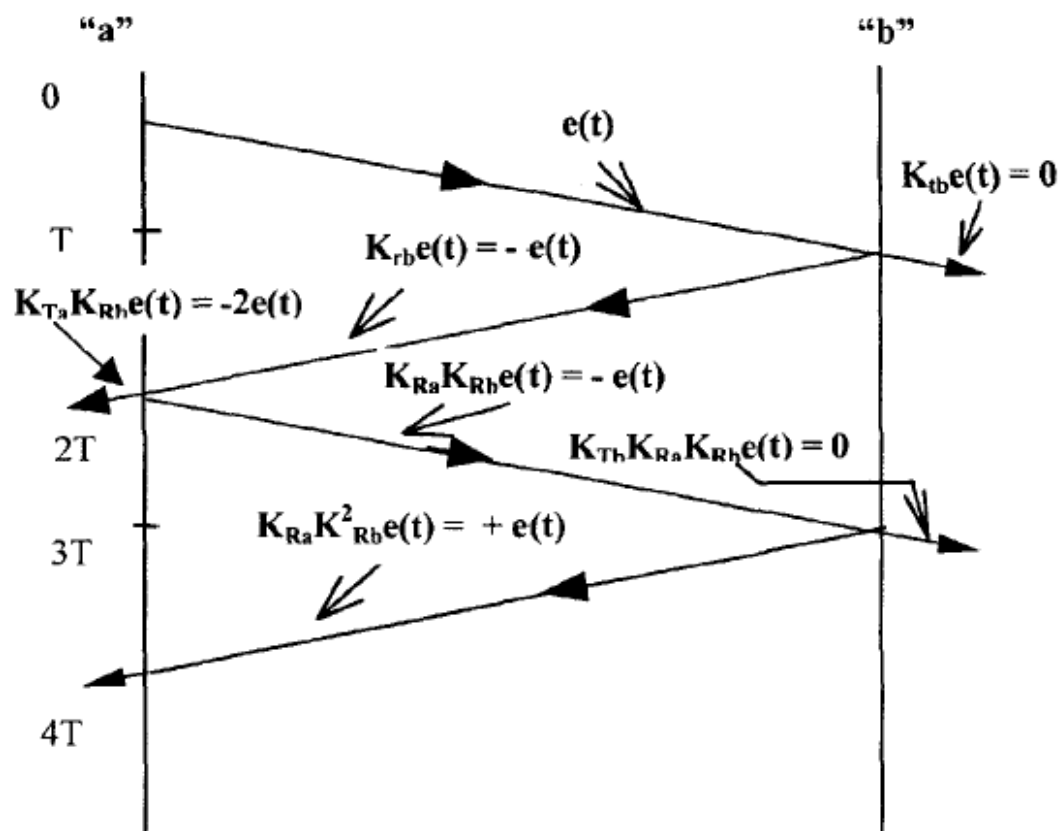
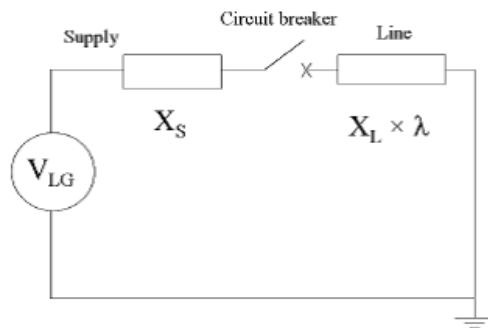
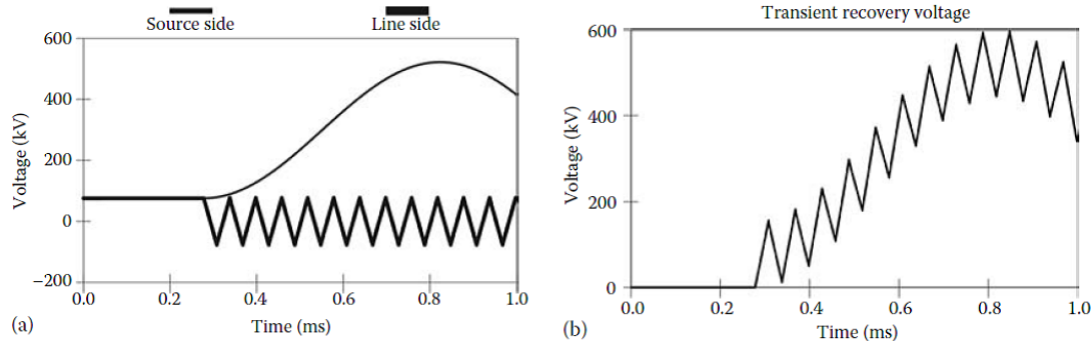


Figure 3.2.2: Lattice Diagram to Evaluate the Characteristics of Travelling Wave



(a) Single-Phase Circuit with Short-Line Fault



(b) Line Side and Source Side Voltages

(c) Transient Recovery Voltage

Figure 3.2.3: TRV across the Breaker during Short Line Fault

3.3 Mathematical Model

Configuration of contacts plays a crucial role in the performance of CB. Contact resistance depends on the contact forces and the actual contact area. The contact resistance is given by

$$R_T = \frac{\rho}{2} \sqrt{\frac{\pi K H}{F_T}} + R_F \quad (3.12)$$

Where:

H - Material hardness

K - Constant between 0.1 and 0.3

ρ - Resistivity of contact material

R_F - Film resistance

F_T - Total force acting on a contact. The current get constricted at the point of contact. This constriction of current is responsible for contact resistance and the heat generated at the contacts. It is also the source of electromagnetic force that acts upon contact structure.

For a circular cluster contacts, three forces act upon: the attractive force (F_A), repulsive force (F_R) and contact spring force (F_S). Thus the total force (F_T) acting on a contact is given by

$$F_T = F_S + F_R - F_A \quad (3.13)$$

The attraction force should be greater than the repulsive force for a CB contacts. When SF₆ CB contacts are subjected to arcing, a sulfide coat is formed. This sulfide coat increases the contact resistance if there is no scrapping or wiping motion between the contacts. The sulfide coat gets removed by slight friction and decomposed by heat. The force of attraction exists between two opposite fingers of a circular cluster contacts when current is flowing in the same direction. This force of attraction for contact having ' n ' fingers and distance ' d ' between fingers with a current of I/n through each finger is given by

$$F_A = 0.102(n-1) \left(\frac{I}{n}\right)^2 \left(\frac{l}{d}\right) \quad (3.14)$$

The attractive force pinches the moving contact fingers on the fixed contact which

reduces the contact resistance as shown in Fig 3.3.1. The wiping action on the contacts get improved which helps in removing the sulfide coat [4]. The CB contacts should be properly designed for wiping action so that the problem of metallic fluoride deposition is minimized [5].

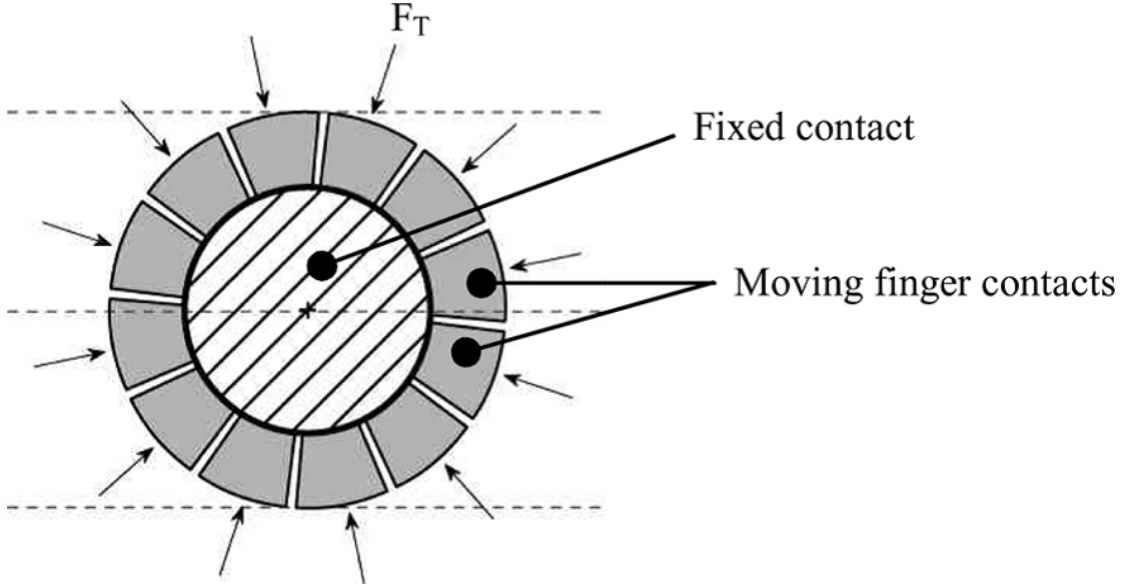


Figure 3.3.1: Schematic of Forces Exerted on the Fixed Contact by the Moving Finger Contacts

CB is an electromechanical device. Hence its model is governed by mechanical and electromagnetic equations. Mechanical equation of a CB is expressed by the Newton's second law, as shown in equation 3.15

$$\rho \left(\frac{\partial^2 u}{\partial t^2} \right) = \nabla \cdot FS + F_v \quad (3.15)$$

F_v - force per unit volume of deformed mass (N)

ρ - mass density (kg/m^3)

S - second order Piola-Kirchhoff stress

F - deformation gradient

U - mechanical displacement (m)

Electromagnetic equations of CB are expressed by (3.16)-(3.20)

$$J = \sigma E + J_e \quad (3.16)$$

$$E = -\nabla V \quad (3.17)$$

$$\nabla \cdot J = Q_j \quad (3.18)$$

$$\nabla \times (\mu \nabla \times A_z) = J \quad (3.19)$$

$$F = J \times B \quad (3.20)$$

σ - electrical conductivity (S/m)

J_e - applied current density (A/m^2)

J - current density (A/m^2)

V - voltage (V)

E - electric field (V/m)

Q_j - charge per unit volume (C/m^3)

μ - average permeability

A_z - magnetic vector potential

B - magnetic field in Tesla

F - magnetic force of the Lorentz law (N)

Passage of electricity produces heat, and this heat affects the resistance and electrical and mechanical properties of CB.

3.3.1 Contact resistance measurement method

Standard Timing test is performed on breaker followed by static contact resistance measurement. Figure 3.3.2 shows the arrangement for static contact resistance measurement. The value of test current should be as per the manufacturers specifications. IEC and ANSI recommend 50 A and 100 A respectively. Breaker is kept in closed position. 100 A DC current is passed through the contacts. Voltage drop is measured and contact resistance is calculated.

The schematic diagram of DCRM is shown in figure 3.3.3. The close-trip command is given to CB. 100A DC current is injected, and the CB is operated at rated speed. Depending on the breaker technology, linear or rotary contact travel transducer is used for recording contact movement. The instantaneous value of resistance is measured along with contact travel. The test kit of Scope Company with Hisac Ultima test manager software for analysis is used. Measuring system with a sampling frequency of 10 kHz and 100 μs resolution is used to record the resistance with precision as well as to record the transfer of current from

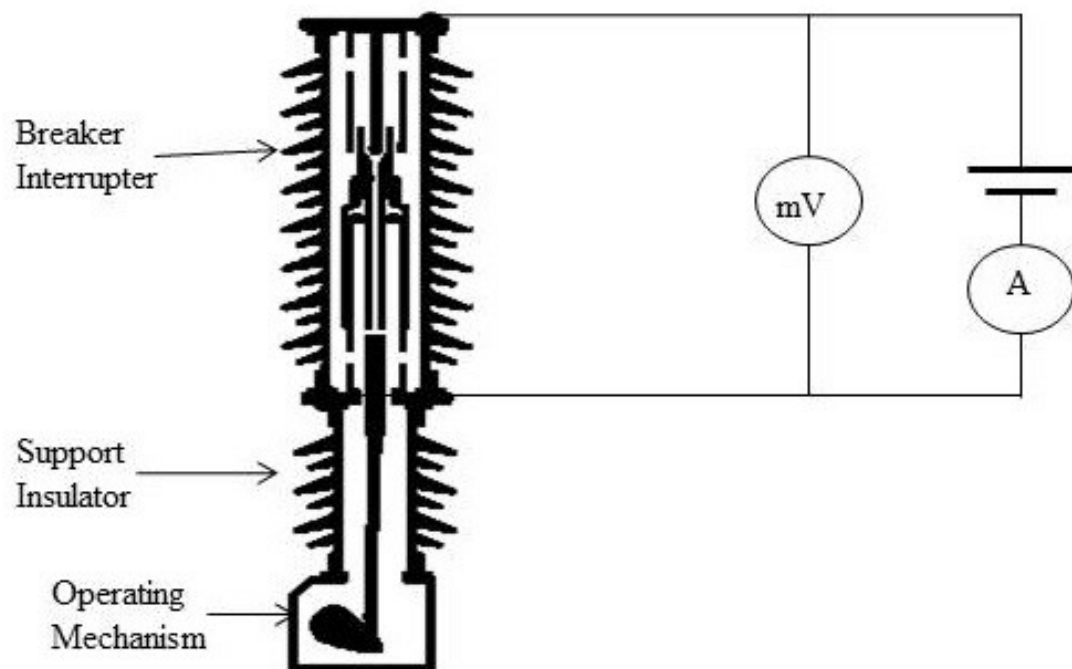


Figure 3.3.2: Schematic Diagram of Static Contact Resistance Measurement

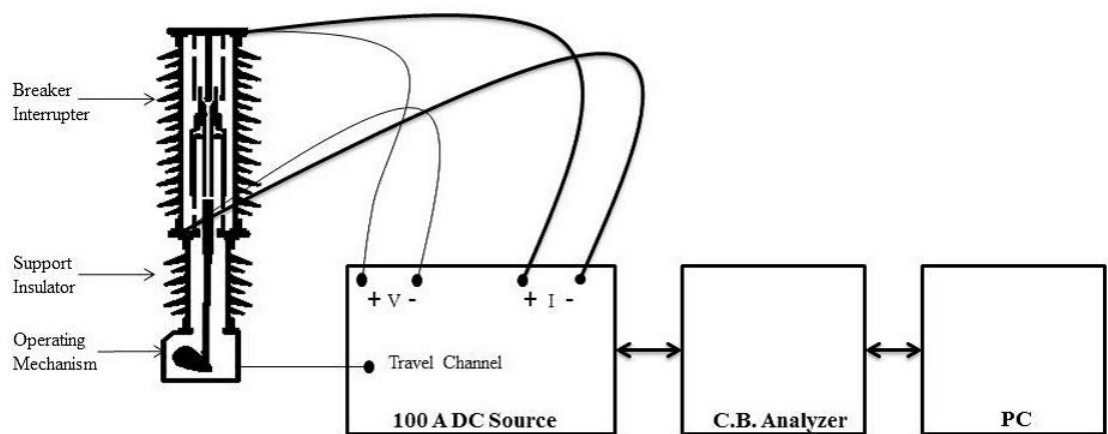


Figure 3.3.3: Schematic Diagram of DCRM

arching contact to the main contact and vice-versa. A time delay of 300 ms is kept between close-trip operations. The test set up is connected to a portable computer for calculation of instantaneous contact resistance, data analysis and interpretation using the software. The variations in the resistance over time are recorded as a finger print for the breaker contacts. This recorded signature can be used as a benchmark for comparison of the future measurement record of the same breaker. The DCRM signature provides information on the breaker contacts and the operating mechanism. Measuring system and test set up is shown in Figure 3.3.4.

3.3.2 DCRM signature analysis

Figure 3.3.5 shows the measurement details from DCRM signature. DCRM may be called as an ECG of the circuit breaker. The analysis software provided with a test kit can be used for analysis. However, analysis of signature needs the knowledge of CB design, interrupter design, operating mechanism and also expertise to detect the problem. Every CB has a different shape of DCRM signature which mainly depends on contact design, type of operating mechanism, contact wipe, contact speed, *etc.* The deviations in the signature can be found by superimposing earlier signature. Parameters such as length of arcing contact, erosion of contacts, mechanical problem, contact travel and speed, healthiness of mechanism, *etc.* can be obtained from the signature. An enlarged view of DCRM signature in the tripping zone is shown in figure 3.3.6.

3.3.3 Case studies

POWERGRID and many utility companies in India are using DCRM test for condition assessment of CBs. Case studies from the field are discussed in this section which signifies the use of DCRM signature in detecting the problems at an early stage in CBs.



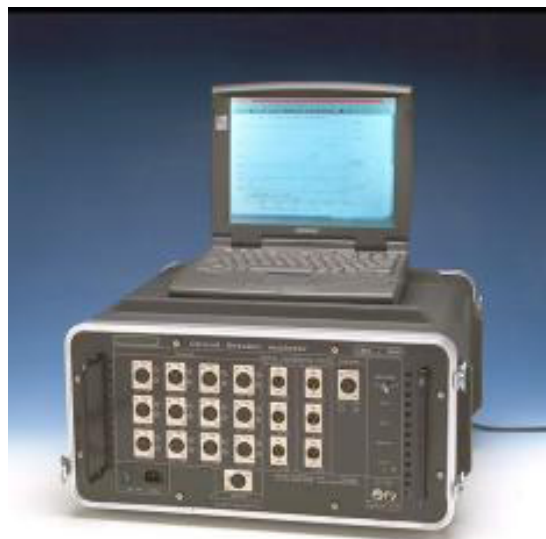
(a) Stable Current Source



(b) Data Acquisition System



(c) Voltage and Current Sensors



(d) Test Manager Software

Figure 3.3.4: Test Set Up for DCR Measurement

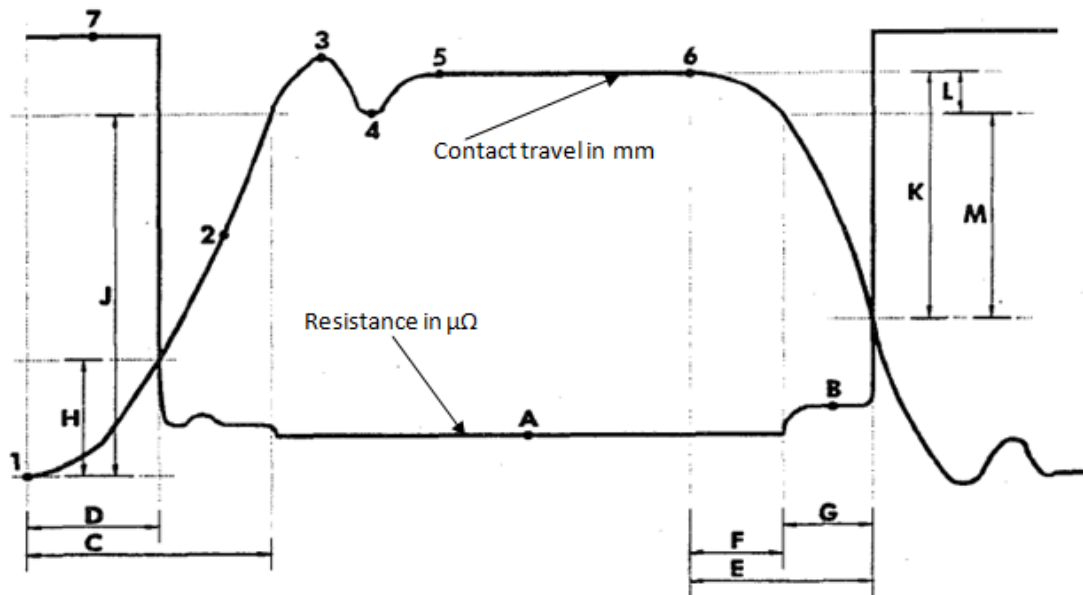


Figure 3.3.5: Measurement Details from DCRM Signature

- A: main contact resistance
- B: arcing contact resistance
- C: time for main contacts to make
- D: time for arcing contacts to make
- E: time for arcing contacts to break
- F: time for main contacts to break
- G: time arcing contact made
- H: distance for arcing contacts to make
- J: distance for main contacts to make
- K: distance for arcing contacts to break
- L: distance for main contacts to break (wipe of main contact)
- M: distance arcing contacts made (wipe of arcing contact)

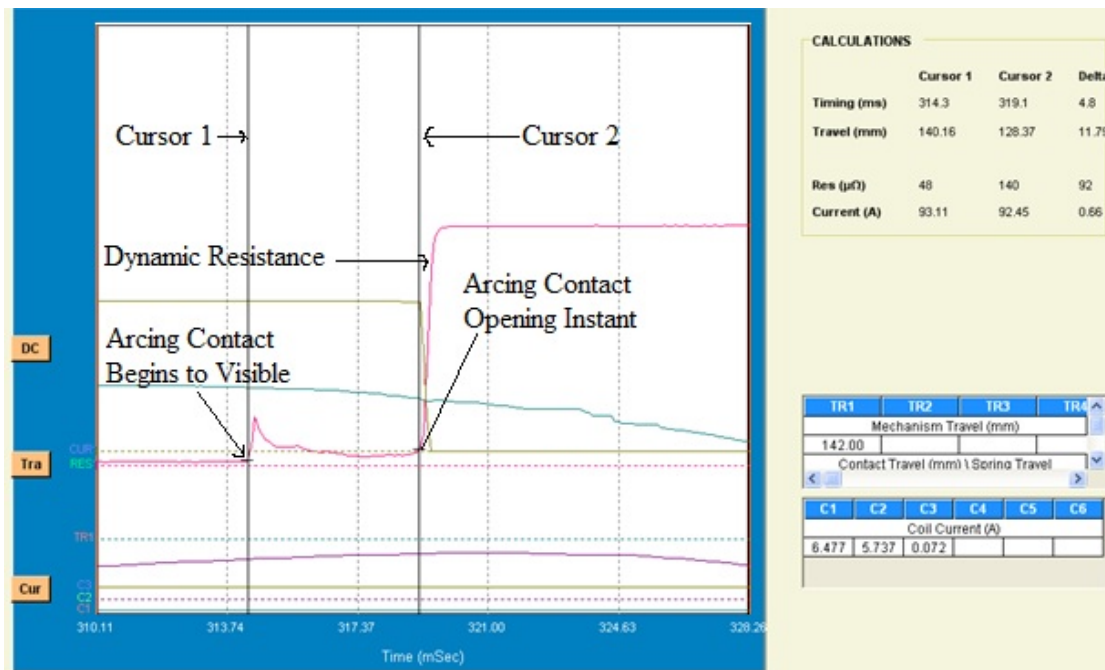


Figure 3.3.6: Enlarged View of Tripping Portion of DCRM Signature

Case no. 1

Contact bouncing for longer duration in no load closing characteristics at manufacturer works (Figures 3.3.7 to 3.3.8) was seen for a 400 kV SF₆ CB during closing operation. The bouncing was noticed after the completion of mechanical travel. Problem was analyzed in the following steps:

1. The external connections were verified and were found normal. The connections of the test leads connecting main contacts to analyzer were also checked and found correct. The test was repeated with a different analyzer to rule out the electrical signaling fault. But the same problem persisted. It was then confirmed that the problem is within the interrupter assembly
2. Static contact resistance was measured and found to be very high 120 to 160 k Ω
3. The bouncing in the no load closing characteristics is verified by conducting the DCRM test of a B-phase front side interrupter
4. Lot of fluctuations in the current and resistance curve in the no action zone was observed in the DCRM signature

5. Abnormal DCRM signature for the rear side of the same pole was obtained even though no abnormal contact bouncing was seen in no load closing operation
6. The investigations in subassemblies were done in steps and the cause of the problem was detected in moving contact assembly. The puffer cylinder and cylinder support joint was found loose. During assembly of the interrupter, tightening torque was not applied

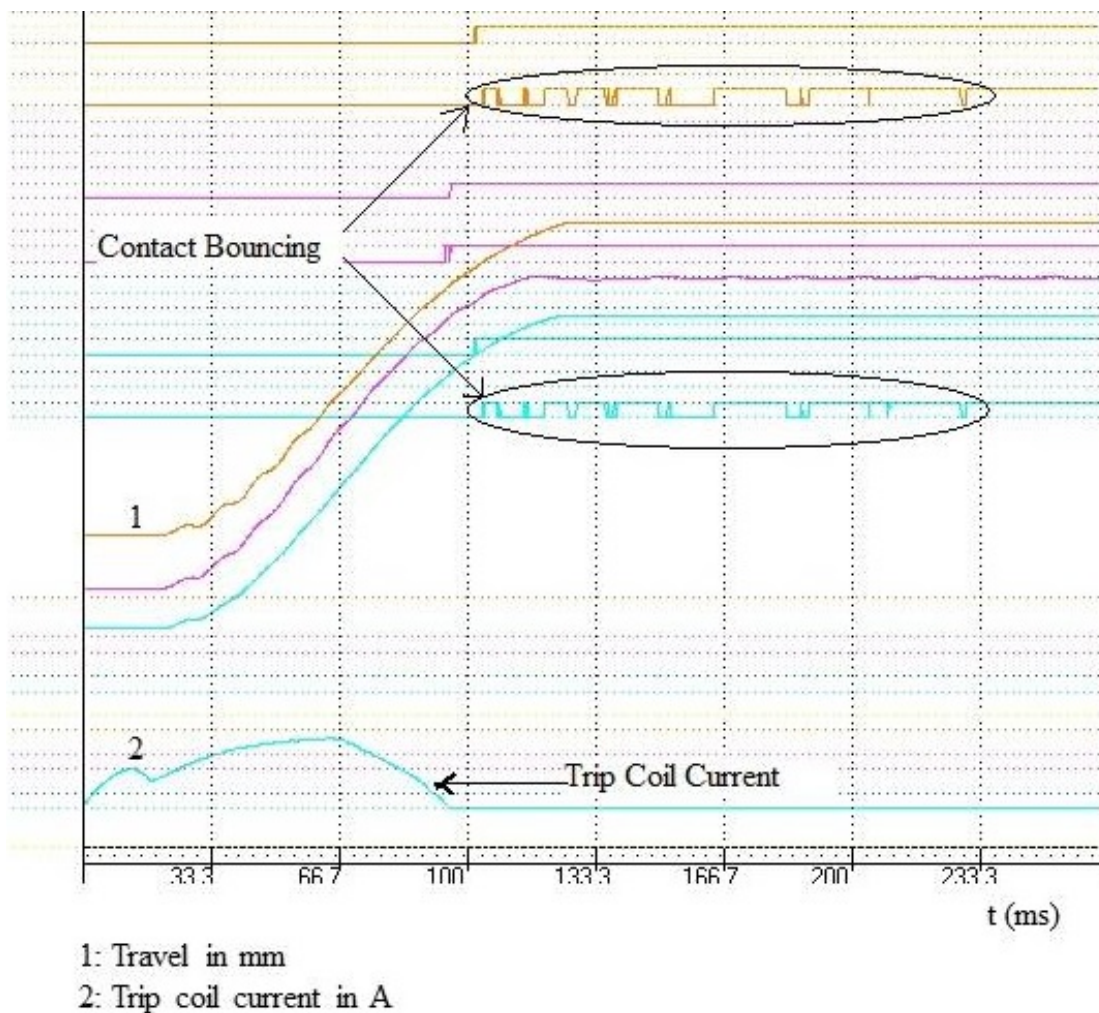


Figure 3.3.7: Contact Bouncing after Closing Cycle on 400 kV SF₆ Circuit Breaker

Case no. 2

For a 245 kV SF₆ CB, contact mismatch was observed in the opening operation. The mismatch was not getting adjusted with spring and coil adjustments. The speed time graph was analyzed and following points were noticed:

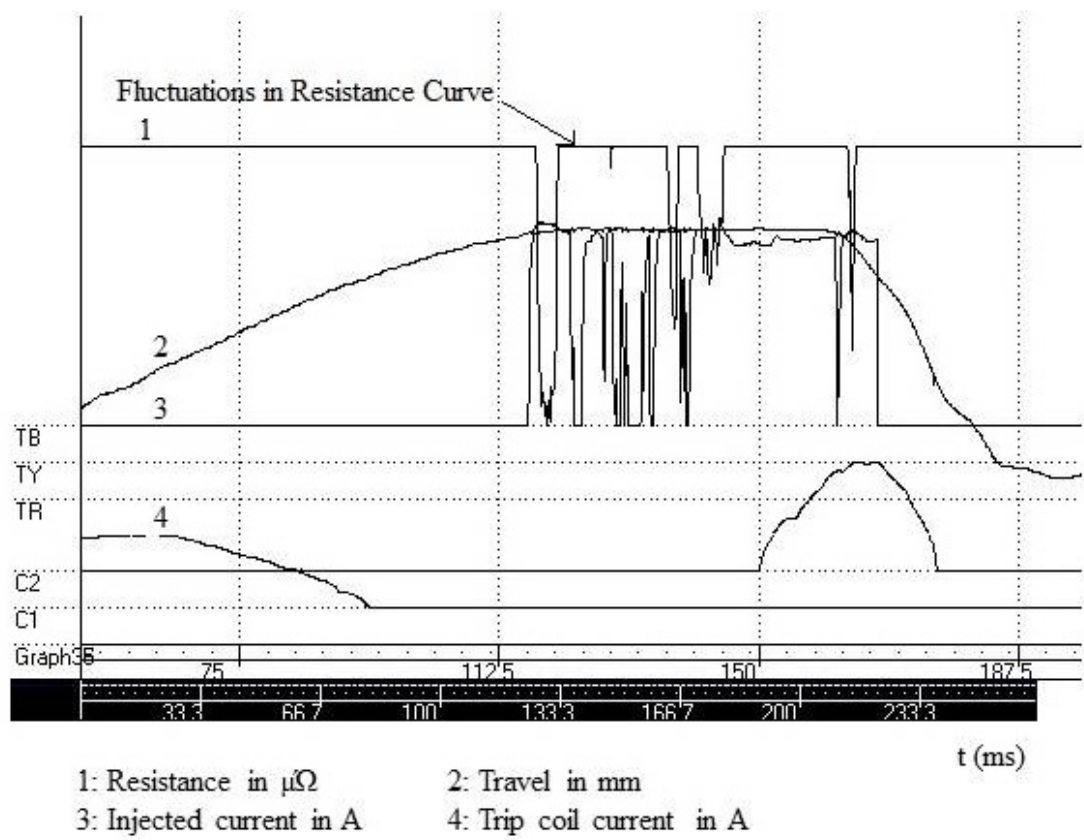


Figure 3.3.8: DCRM Signature Showing Fluctuations in Resistance Curve of B Phase Front Side Interrupter

1. For R and Y poles, abnormal contact bouncing for more than 5 milliseconds was observed in closing operation
2. As compared to B pole, the wipe was less for R and Y pole in opening operation

The DCRM signatures were obtained for all three phases. The signatures were analyzed for closing and tripping. As seen in the figures 3.3.9 and 3.3.10, abnormality in travel curve and current, as well as resistance, was observed. DCRM of R-pole during tripping can be seen in figure 3.3.11. The CB was opened. It was observed that 145 kV arcing contact was fitted instead of 245 kV arcing contact during assembly as seen in figure 3.3.12. DCRM signatures were normal after fitting proper arcing contact.

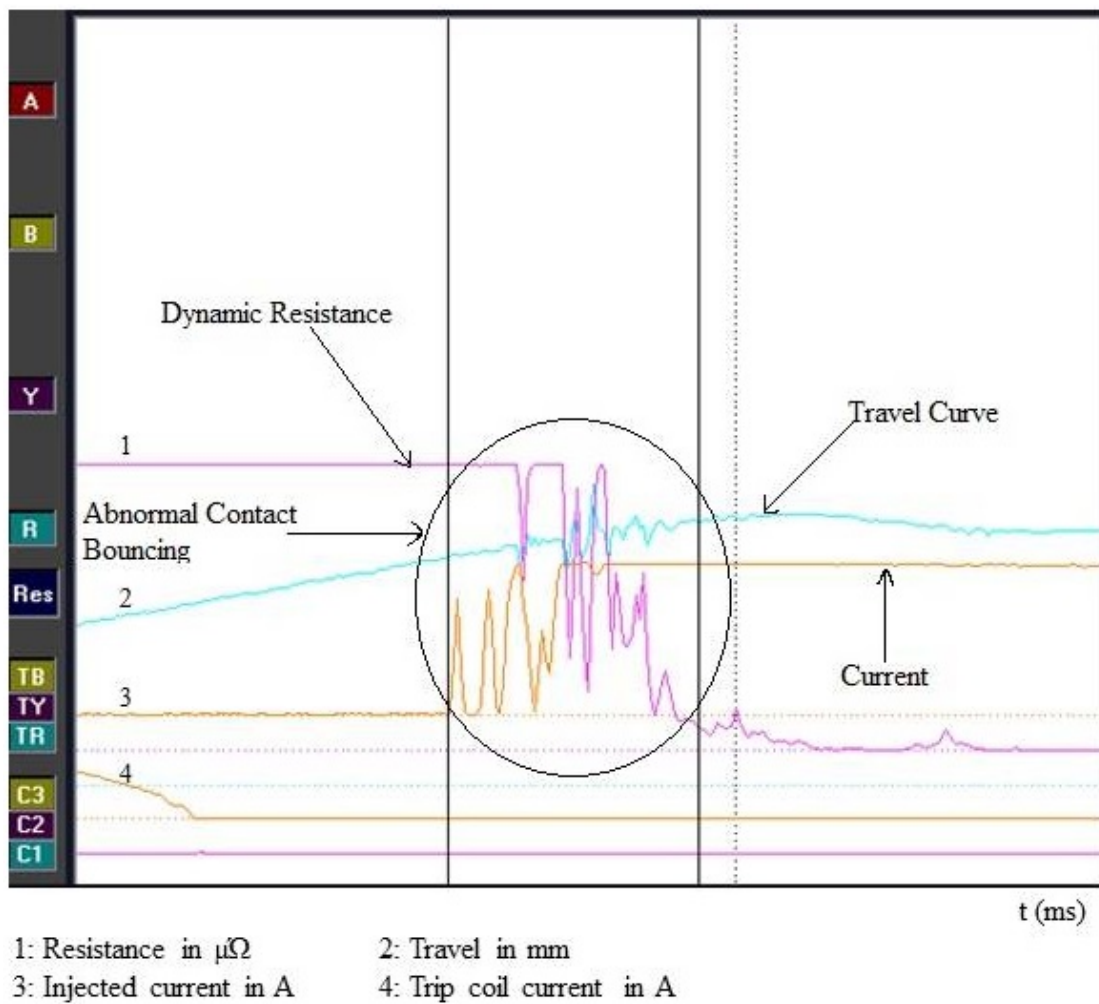
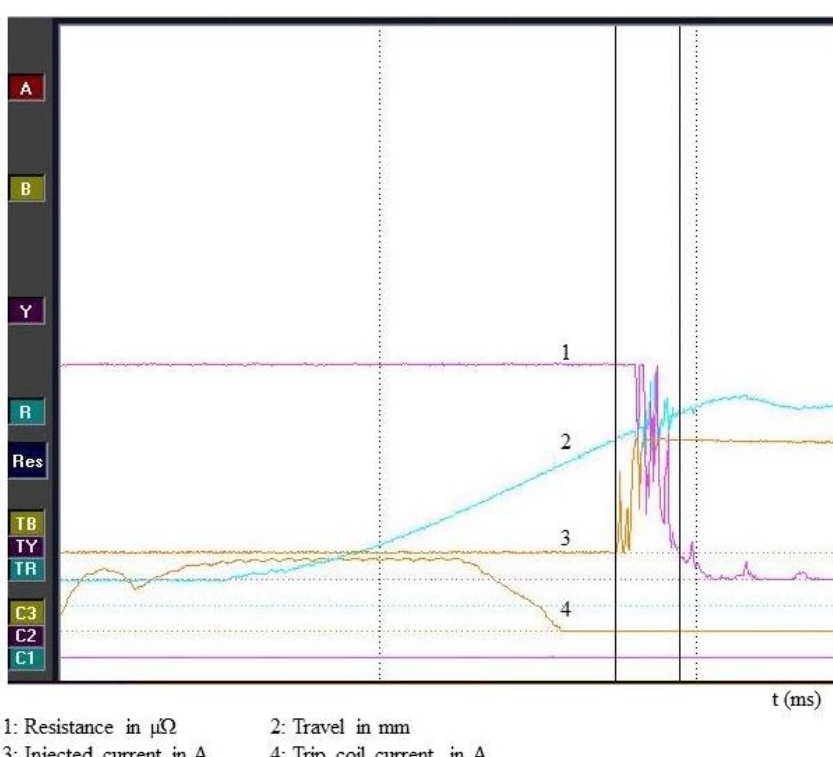
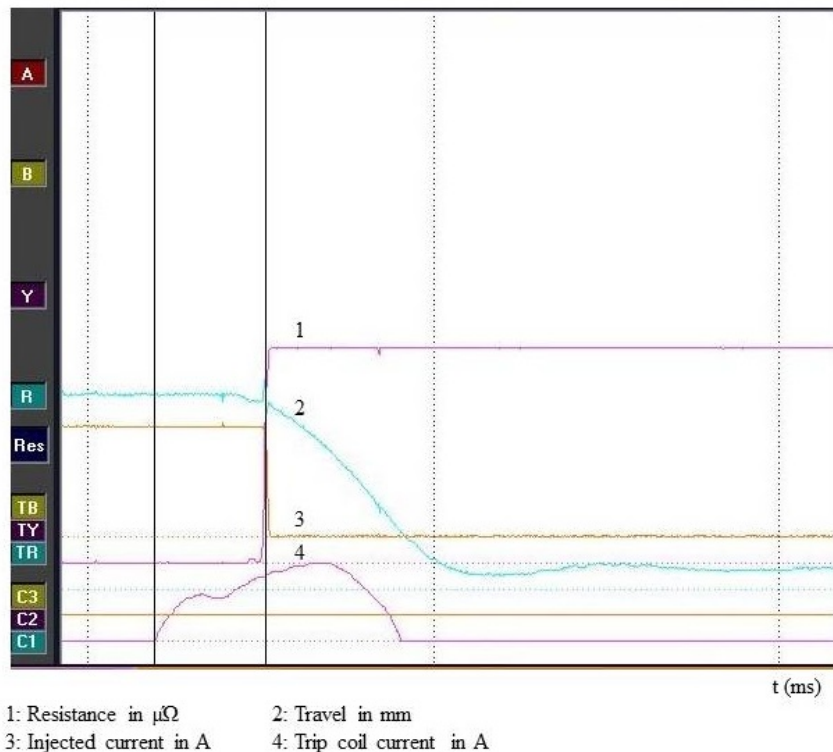


Figure 3.3.9: Enlarged View of R-Pole DCRM in Closing Part



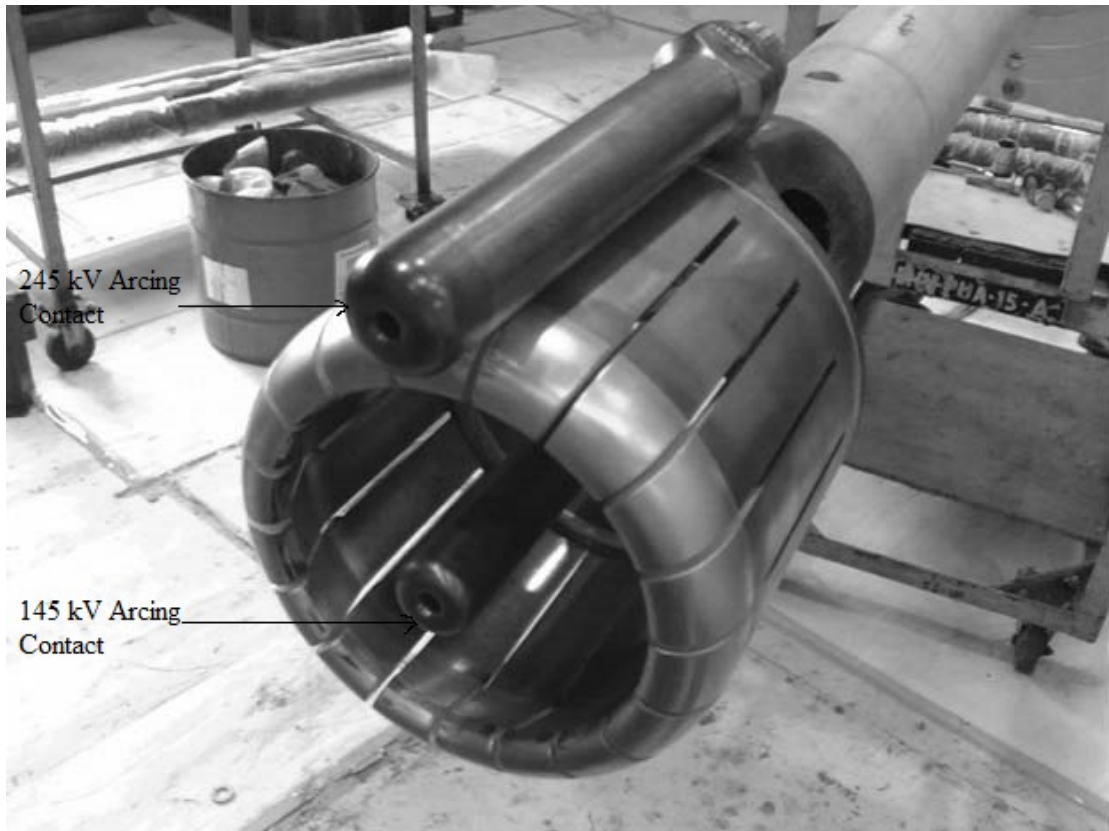
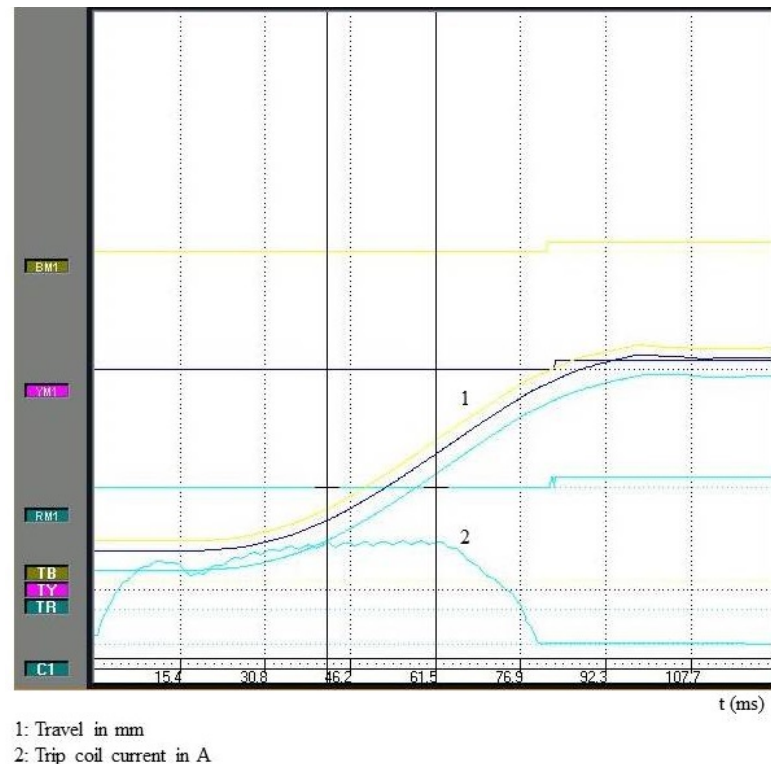
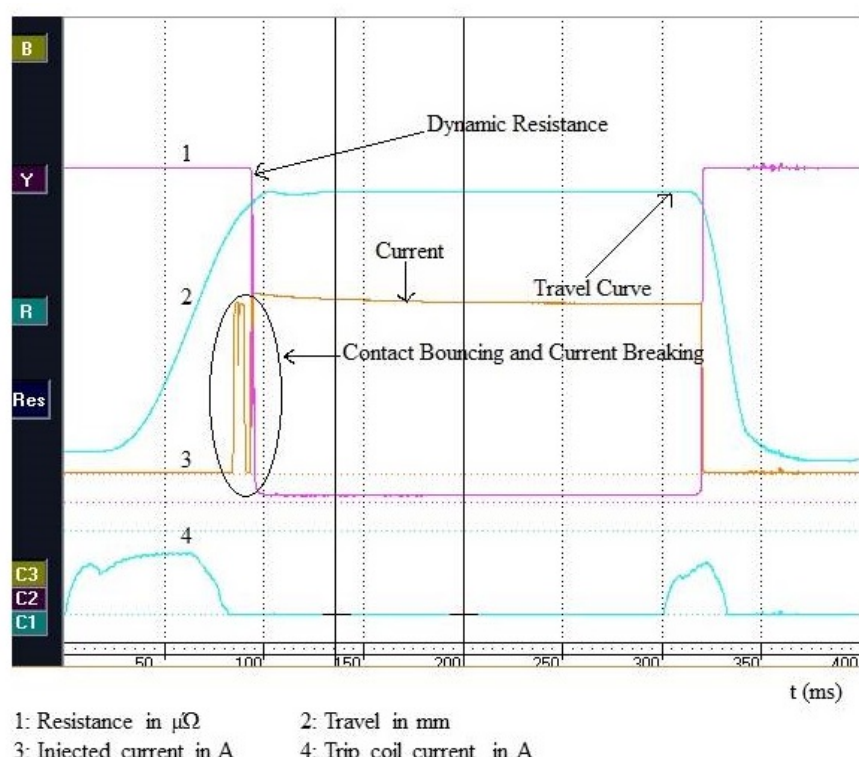


Figure 3.3.12: Wrong Assembly of Arcing Contact

Case no. 3

The no load opening graph of a 245 kV SF₆ CB during closing was normal as observed in figure 3.3.13. But contact bouncing and current breaking in the closing part of the DCRM (Figure 3.3.14) was seen. The DCRM in the tripping portion is shown in figure 3.3.15. The closing operation was repeated, and bouncing was seen in the closing graph (Figure 3.3.16). The interrupter was opened, and it was observed that moving arcing contact was become loose. The required tightening torque was not applied during assembly. In consequent mechanical operations, it started becoming more and more loose. After rectification of the problem, the normal signature was obtained.

Figure 3.3.13: Closing Graph of 245 kV SF₆ Circuit BreakerFigure 3.3.14: Complete DCRM Signature of 245 kV SF₆ Circuit Breaker

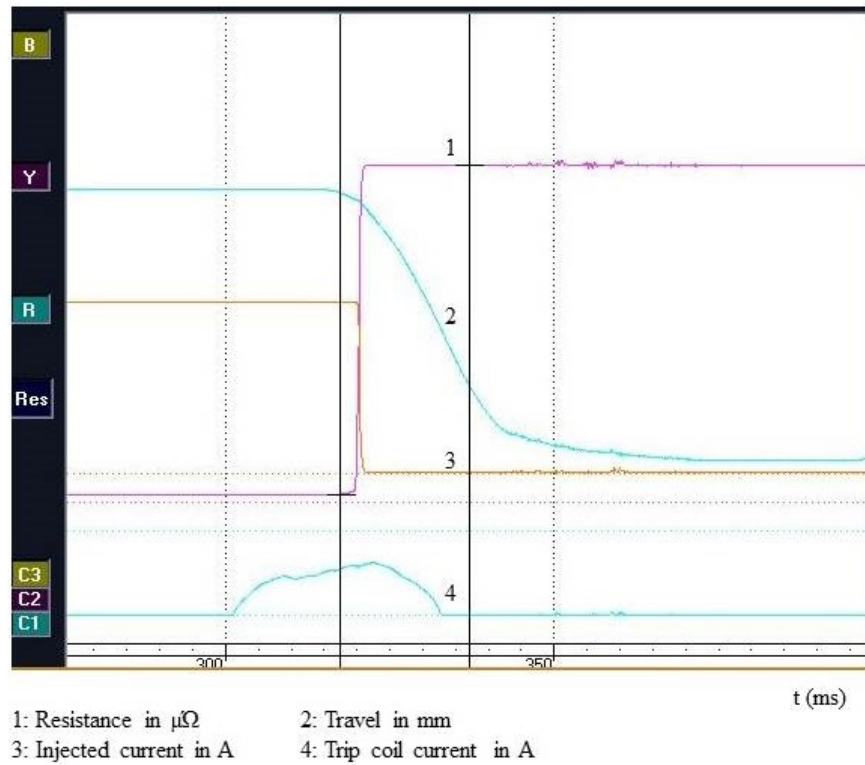


Figure 3.3.15: DCRM of 245 kV SF₆ Circuit Breaker in Tripping Zone

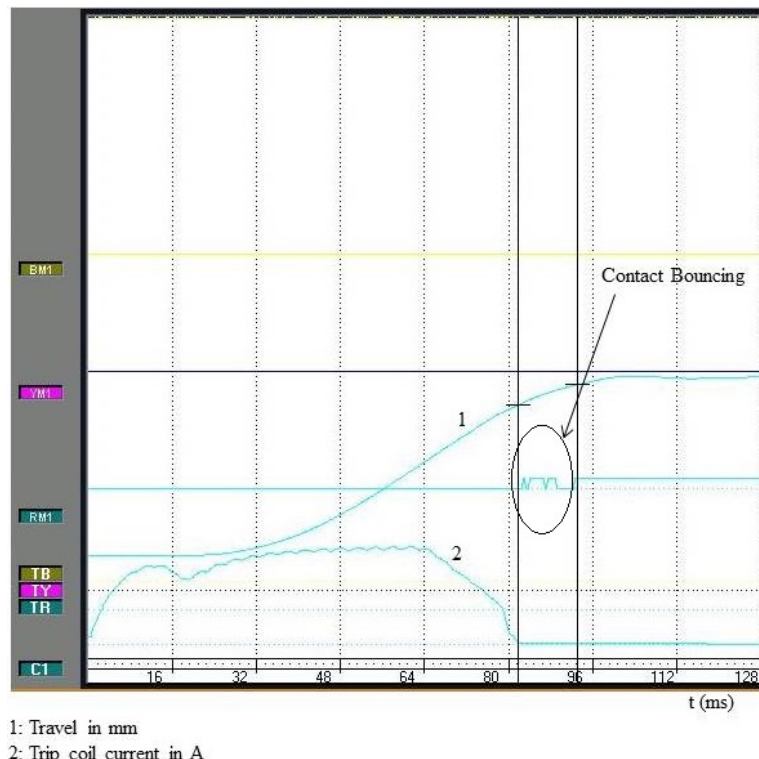


Figure 3.3.16: Contact Bouncing in Closing Graph of 245 kV SF₆ Circuit Breaker

Case no. 4

Contact resistance measurement of a 220 kV SF₆ CB used for switching 220/33 kV, 50 MVA transformer in 400 kV substation, Waluj, Aurangabad showed a high value of resistance of the order of 200 k for R-pole. The measurement test was repeated, and it was showing higher values. After repeated tests, the result was found to be higher value for resistance. DCRM test was conducted. A lot of fluctuations were observed in the resistance in no action zone of the DCRM signature as shown in figure 3.3.17. DCRM test was repeated again after confirming the connections. No change was observed in the signature. It was decided to open the R-pole. It was observed that the ring connecting the PTFE nozzle of the main contact became loose. Scratch marks were also found as seen in figure 3.3.18. The signature was normal after attending the problem.

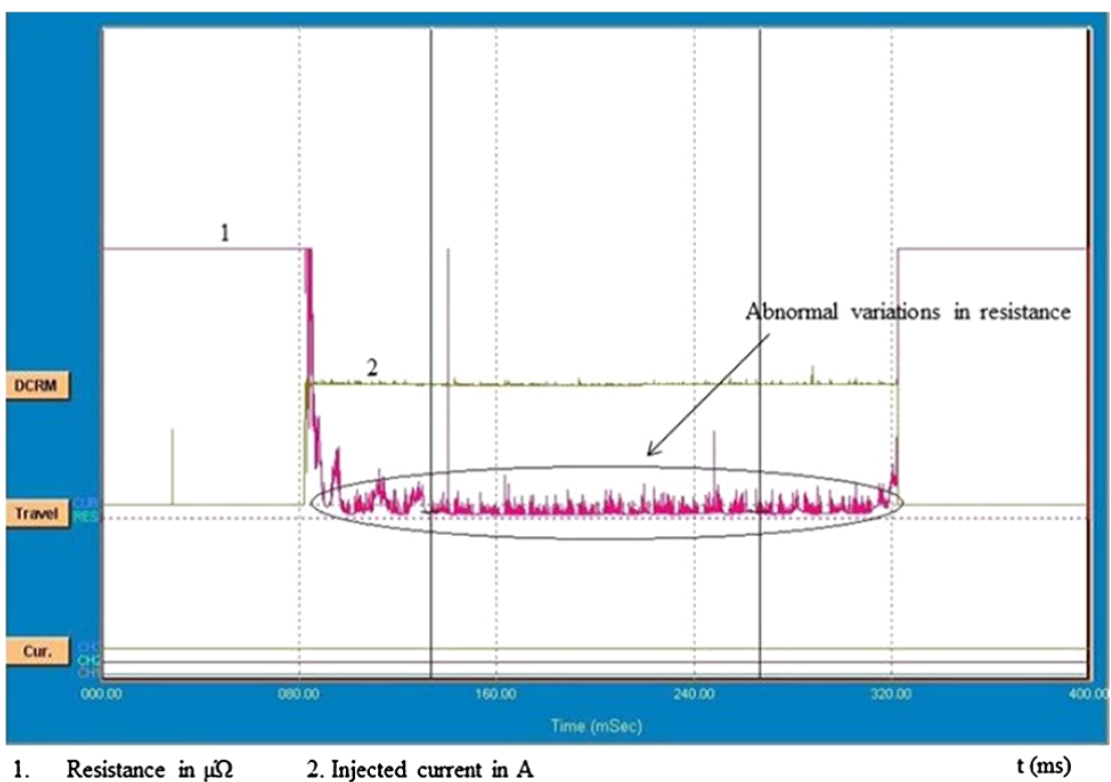


Figure 3.3.17: Abnormal Variations in Resistance in no Action Zone of DCRM Signature for 220 kV Circuit Breaker



Figure 3.3.18: Loose Ring Connecting PTFE Nozzle of Main Contact

Case no. 5

Abnormal peak in the DCRM signature in the close zone portion of a 400 kV CB was seen in after three years of installation. The static contact resistance was found be $150 \mu\Omega$. The CB was opened for contact inspection. Following observations were made.

1. This breaker has seen more fault operations and high current making and breaking operations
2. Due to arcing between contacts in SF₆ gas environment metal fluorides and metal sulfates were formed inside arcing chamber which increased the resistance to considerable value
3. Because of high temperature attained during arcing, finger contacts of moving arc contact got expanded and contact burning at both side caused abnormal DCRM
4. Because of early detection of faulty internal condition through DCRM testing, major failure is avoided

Figures 3.3.19 to 3.3.22 indicates the signature and internal contact conditions of the CB.

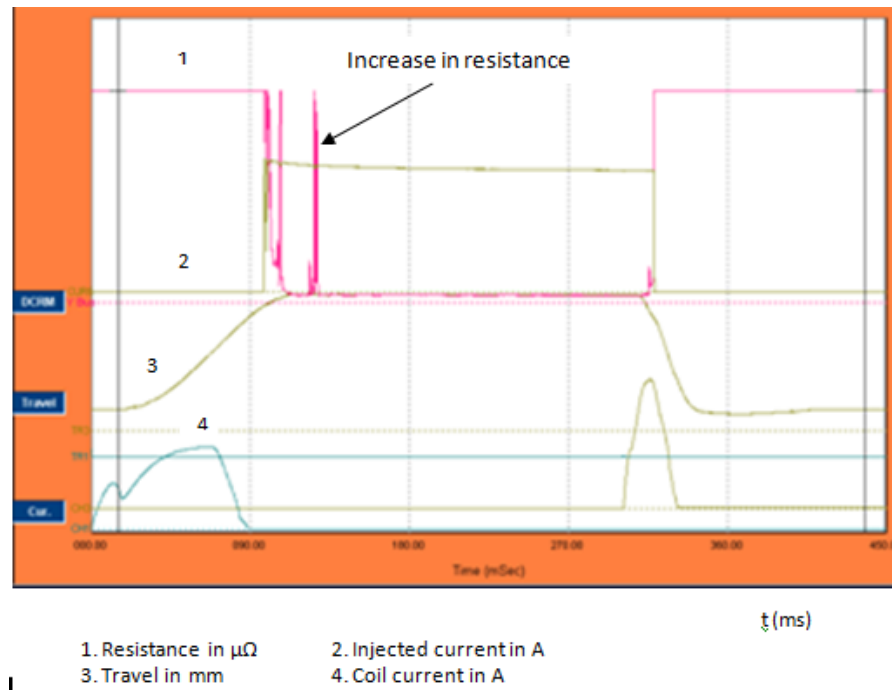


Figure 3.3.19: Problematic DCRM Signature

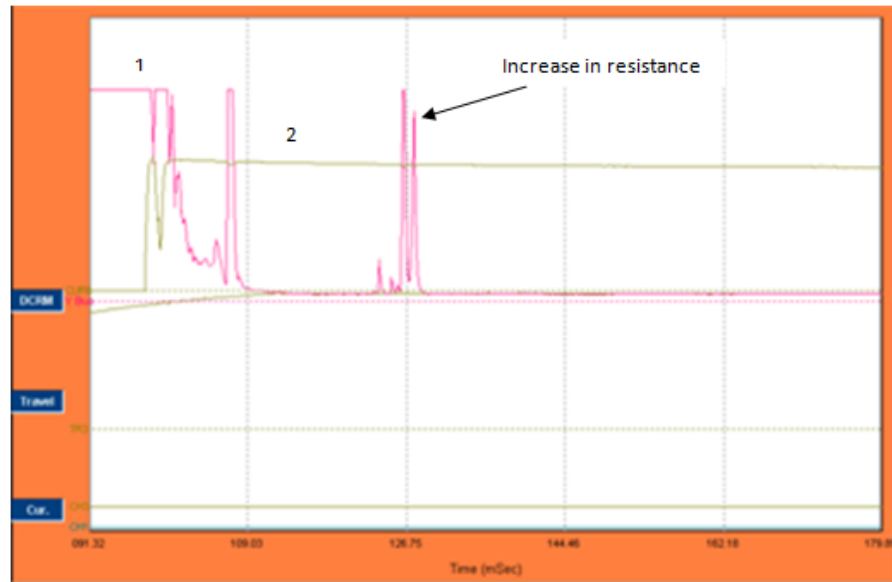


Figure 3.3.20: Increase in Resistance in Close Zone

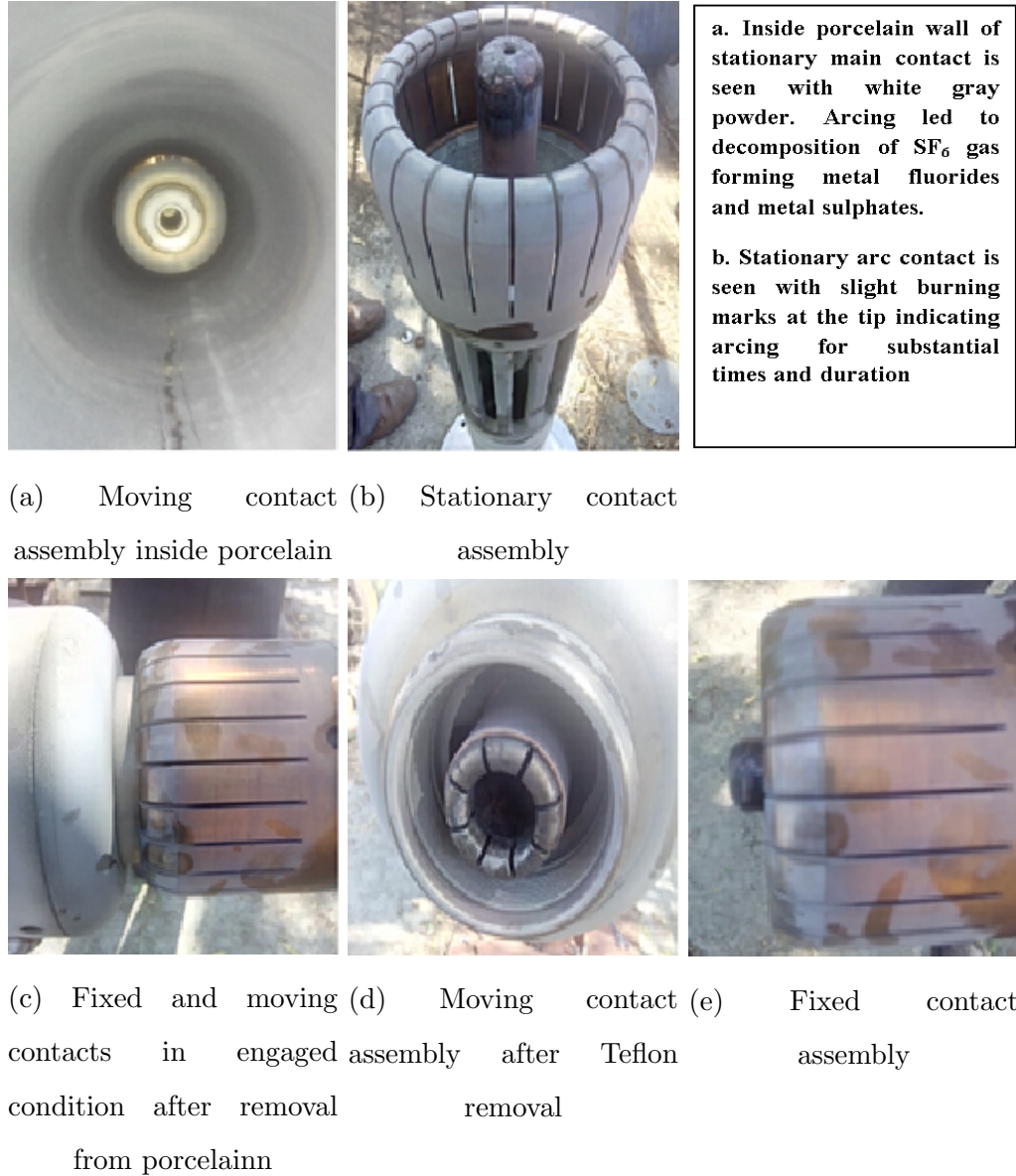


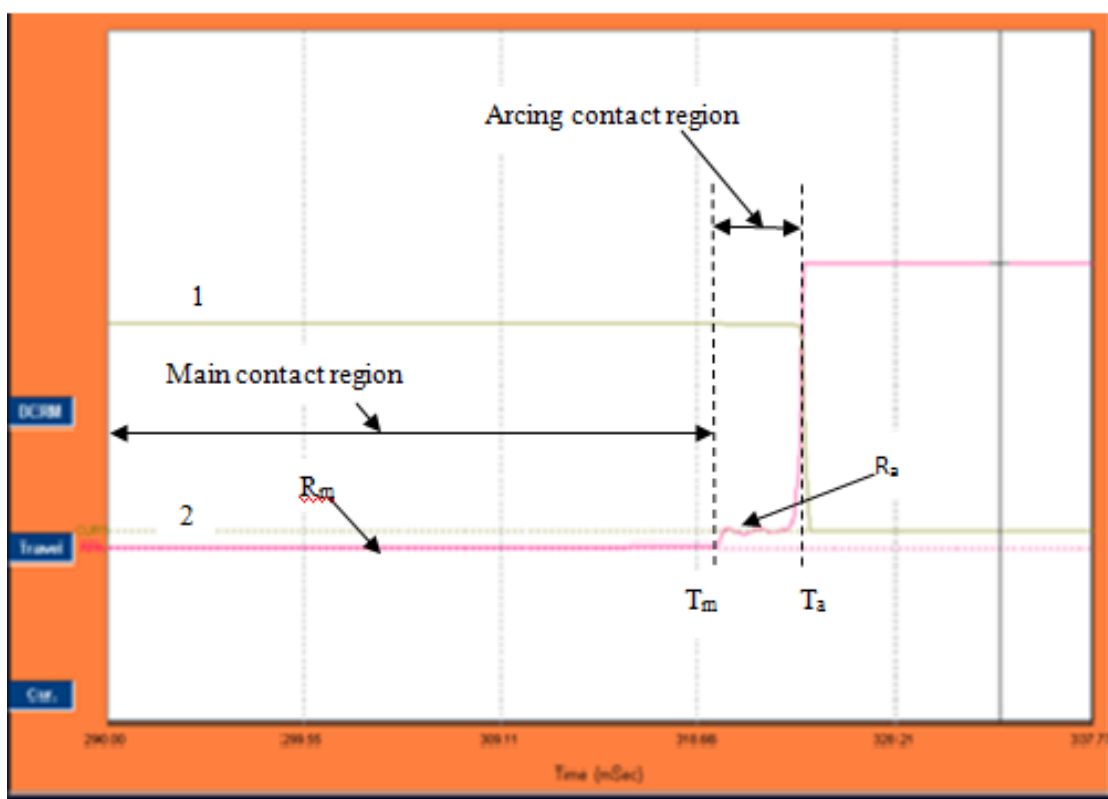
Figure 3.3.21: Fix and Moving Contact Assembly



Figure 3.3.22: Deposition of Sulfide Powder on Contact Assembly

3.4 New Algorithm for Contact Condition Detection of SF₆ CB

Tests were conducted on 400 kV and 245 kV SF₆ CBs at circuit breaker manufacturing industry, 400 kV substation Waluj, Aurangabad and 765 kV substation at Thapti Tanda Aurangabad. Timing measurement, SCRM as well as DCRM tests were conducted. Data of DCRM for healthy breakers as well as breakers with problems in condition of contact was collected from the largest utility company PGCIL as well as MSETCL. Figure 3.4.1 shows the DCRM signature in the tripping portion along with the parameters.



1: Injected current (A) 2: Resistance ($\mu\Omega$)

Figure 3.4.1: DCRM Signature Showing the Parameters used in Algorithm

Following parameters are used for developing contact wear algorithm:

T_m - time at the position when main contact disengages (ms)

T_a - time at the position when arc contact disengages (ms)

R_{aimax} - arc contact resistance at the point of main contact disengagement ($\mu\Omega$)

A_m - area below the main contact resistance zone ($\mu\Omega \times \text{ms}$)

A_a - area under the arc contact zone ($\mu\Omega \times \text{ms}$)

R_m - average contact resistance in the main contact region ($\mu\Omega$)

R_a - average contact resistance in the arc contact region ($\mu\Omega$)

Deviations in the above parameters from the healthy DCRM signature will be used for developing the contact wear algorithm. Number of DCRM signatures was analyzed and following observations are made.

Fixed arc contact tip wear

Over the times due to arcing and heat, length of fixed arc contact reduces. Shortening of fix arc contact will be reflected at the end of the resistance curve during tripping portion. Position at which the arc contact disengages finally will shift to left than normal curve. Average arc contact resistance will increase, but the area below the DCRM curve in arc contact zone will decrease due to earlier disengagement of arc contact. Since main contact condition is sound, the point at which main contact disengages will remain same so also the area below the main contact resistance zone. In this case, the motion will start earlier than in previous measurement indicating wearing of contact. $\Delta T_m = 0, \Delta T_a < 0, \Delta A_a < 0, \Delta R_{aimax} = 0$ and $\Delta A_m = 0$. Arcing contact wipe will decrease.

Wearing of moving arc contact

Excessive heat and arcing also damage the fingers of arc contact. Damage to fingers will increase the initial resistance of the arc contact at the point of disengagement of the main contact. As the fix arc contact is assumed to be sound, the position of arc contact disengagement will remain same. The area under the arc contact zone will increase. This will lead to the conditions $\Delta T_m = 0, \Delta T_a = 0, \Delta A_a > 0, \Delta R_{aimax} > 0$ and $\Delta A_m = 0$. Erosion of the moving arc contact will increase the resistance in the arc contact zone.

Main contact erosion

If the force of the fingers of the main contact is not proper or the contacts are not aligned properly, or the tightening torque is not applied then the main contact

may erode. This will not change the position of arc contact disengagement but will certainly change the point of main contact disengagement. This will slightly increase the area below the arc contact zone. Variations in the no action zone of the DCRM will be seen which will increase the average main contact resistance. Increase in resistance during static contact resistance measurement can also be observed. The condition will be $\Delta T_m < 0, \Delta A_a > 0, \Delta T_a = 0, \Delta R_{aimax} = 0, \Delta A_m > 0$.

Arc contact (fixed and moving) and main contact erosion

Erosion of fixed arc contact and main contact will change both the position of main and arc contact displacement resulting in reduction in area below the arc contact region and increasing the arc contact resistance at the disengagement of main contact resistance position at the same time variations in the close portion of the DCRM is also observed increasing the area below the main contact resistance zone. Arcing contact wipe will be reduced leading to a condition of $\Delta T_m < 0, \Delta T_a < 0, \Delta A_a < 0, \Delta R_{aimax} > 0, \Delta A_m > 0$.

Fix and Moving arc contact erosion

Excessive arcing and heating may shorten the fixed arc contact at the same time melting at the fingers of moving contact may happen over the years due to switching of short circuit currents or frequent capacitor switching. This condition can be identified as $\Delta A_a < 0, \Delta T_a < 0, \Delta T_m = 0, \Delta R_{aimax} > 0$ and $\Delta A_m = 0$.

Based on the analysis of field DCRM, an algorithm is proposed for detecting the contact wear. Deviations in the DCRM signature from normal values are the input to the algorithm. Five parameters, deviation in the main contact cut off time (ΔT_a), arcing contact cut off time (ΔT_a), area below the curve in arc contact zone (ΔA_a), arc contact resistance at the point of main contact disengagement (ΔR_{aimax}) and the area below the curve in main contact zone (ΔA_m) are used.

Following cases of contact erosion is identified:

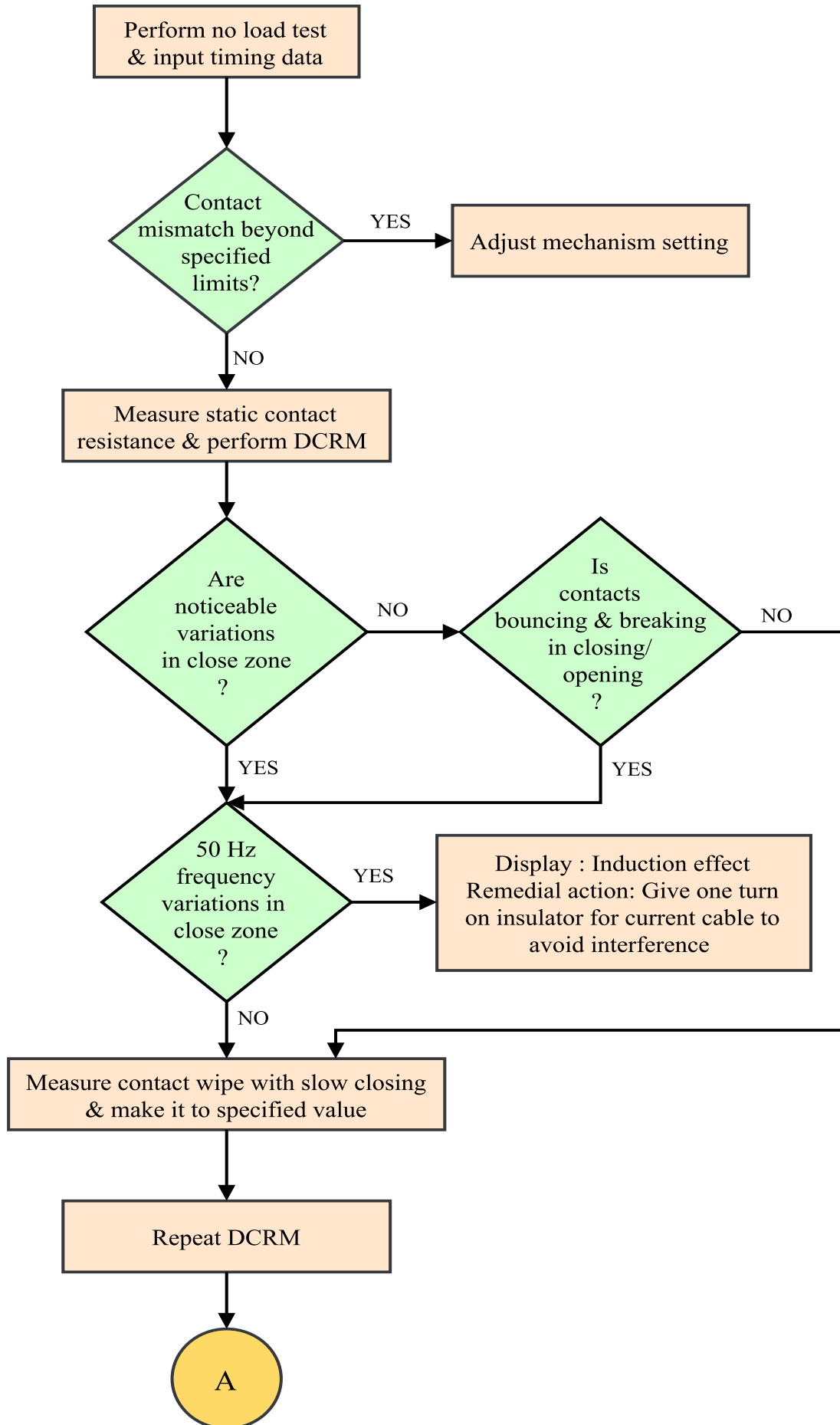
Problem 1: Main contact erosion

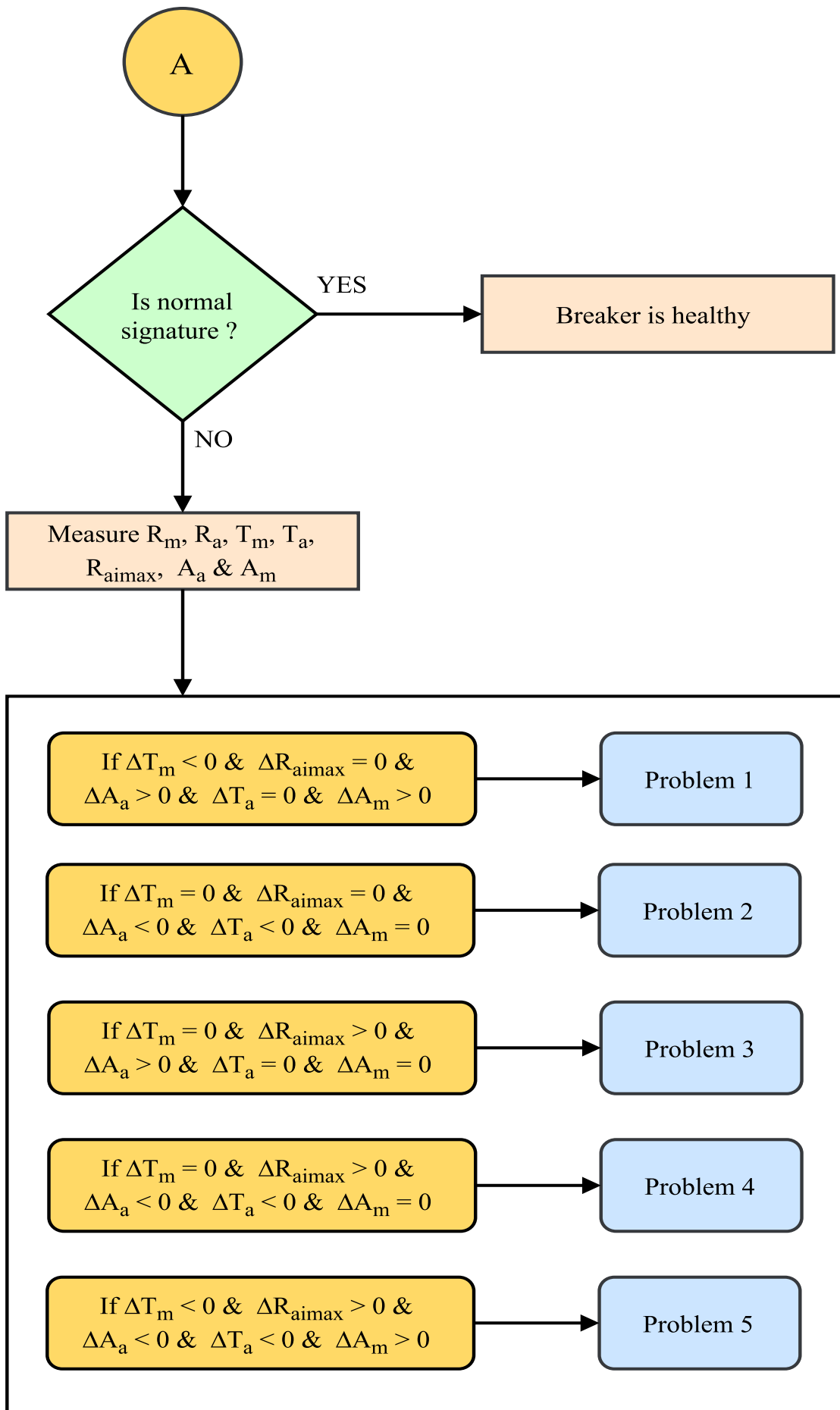
Problem 2: Fix arcing contact erosion

Problem 3: Wearing of arcing contact fingers

Problem 4: Fix and Moving arcing contact erosion

Problem 5: Arcing contact (Fix and Moving) and main contact erosion





Problem	Description
1	Main contact erosion
2	Fix arcing contact erosion
3	Wearing of arcing contact fingers
4	Fix and moving arc contact erosion
5	Arc contact (Fix and moving) and main contact erosion

Figure 3.4.2: Flow Chart of Proposed Algorithm

Figure 3.4.2 shows the flow chart for the proposed algorithm. A program is developed in Java which depicts the health of CB.

Chapter 4

PERFORMANCE ANALYSIS

Simulation of an IEEE network is carried out in EMTP-RV for determining the short circuit capability of CB under different fault conditions. The results are obtained for the following fault conditions.

1. Interruption of three phase to ground fault at the terminal of substation for switching multiple lines connected to the substation
2. Interruption of three phase to ground fault at the terminal of substation for the case of transformer switching
3. Interruption of single phase to ground short line fault and modeling the line as constant parameter and frequency dependent and comparing the results for the two
4. Interruption of three phase to ground fault at the terminal of substation with arc model

4.1 Computational Analysis

4.1.1 Simulation results for case-I

Simulation is carried out for interruption of three phase to ground fault at the terminal of the substation for switching multiple lines connected to the substation. Stray capacitance of substation equipments is considered for simulation. Current in the steady state under fault condition is measured which is 17.2 kA. For a

breaker of 30 kA short circuit interruption capabilities, the standard TRV for T60 duty is modeled by four parameter method. The rating of TRV for T60 duty is obtained from the application guide shown in the Table 4.1.1. The simulation time step of $1\mu s$ is used. The standard TRV and the TRV across the breaker is shown in the waveforms from figure 4.1.1 to figure 4.1.3. The TRV waveform is exponential as seen in figure 4.1.3. In this case when the CB is used to switch the multiple lines, CB has inductance and capacitance on source side as well as on the load side which results in double frequency recovery voltage.

4.1.2 Simulation results for case-II

Simulation is carried out for interruption of three phase to ground fault at the terminal of a substation for the case of transformer switching. The simulation time step of $1\mu s$ is used. As seen in the waveforms from figure 4.1.4 to figure 4.1.7, the TRV is oscillatory since the fault is limited by the transformer only. The electric energy is redistributed among equivalent single capacitive and single inductive elements. In this case since the CB is used for transformer switching with no transmission lines, the circuit becomes underdamped and the resulting TRV is a typical one minus cosine waveform.

4.1.3 Simulation results for case-III

Simulation is carried out for interruption of single phase to ground short line fault at various fault distance from 1.2 km to 6.2 km for a 16 km transmission line. The lines are first modeled in constant parameter mode, and TRV is recorded. Then the lines are modeled in frequency dependent mode, and TRV is recorded. TRV in both models is compared. Time step of $0.1 \mu s$ is used. Obtained waveforms are shown from figure 4.1.8 to figure 4.1.15. The reflections of the travelling waves against short circuit point and the open end at the breaker side causes a triangular shaped waveform. The increase in line length increases the line impedance and the amplitude of the triangular shaped line side oscillation which decreases the fault current; hence di/dt becomes lower. The characteristic impedance Z_{line} depends on the line parameters and remains constant. Hence the RRRV decreases with increase in line length and vice-versa.

4.1.4 Simulation results for arc interruption

Simulation is carried out for interruption of three phase to ground fault at the terminal of a substation for switching multiple lines connected to the substation as well as transformer switching. Black Box Cassie-Mayer model is used for arc interruption studies. Time step of $0.1 \mu s$ is used. The waveforms are shown in figure 4.1.16 to figure 4.1.17.

Table 4.1.1: TRV Rating for 30 kA Short Circuit Current Interruption

Rated voltage	Test duty	First pole to clear factor	Amplitude factor	First reference voltage	Time	TRV Peak value	Time	Time delay	Voltage	Time	Rate of rise
U1 kV	kpp	kaf	u1 kV	t1 μ s	uc	t2 or t3 μ s	Td	U'	t'	u_1/t_1	
									kV	μ s	u_c/t_3
											$kV/\mu s$
T100	1.3	1.40	115	58	215	232	2(16)	58	31(45)	2	
T60	1.3	1.50	11.5	38	231	228	2-12	58	21-31	3	
T30	1.3	1.54	-	-	237	47	7	79	23	5	
T10	1.5	0.9×1.7	-	-	272	39	6	91	1.9	7	
Op1-Op2	2	1.25	178	178	296	232-464	2-12	89	60-70	1.54	

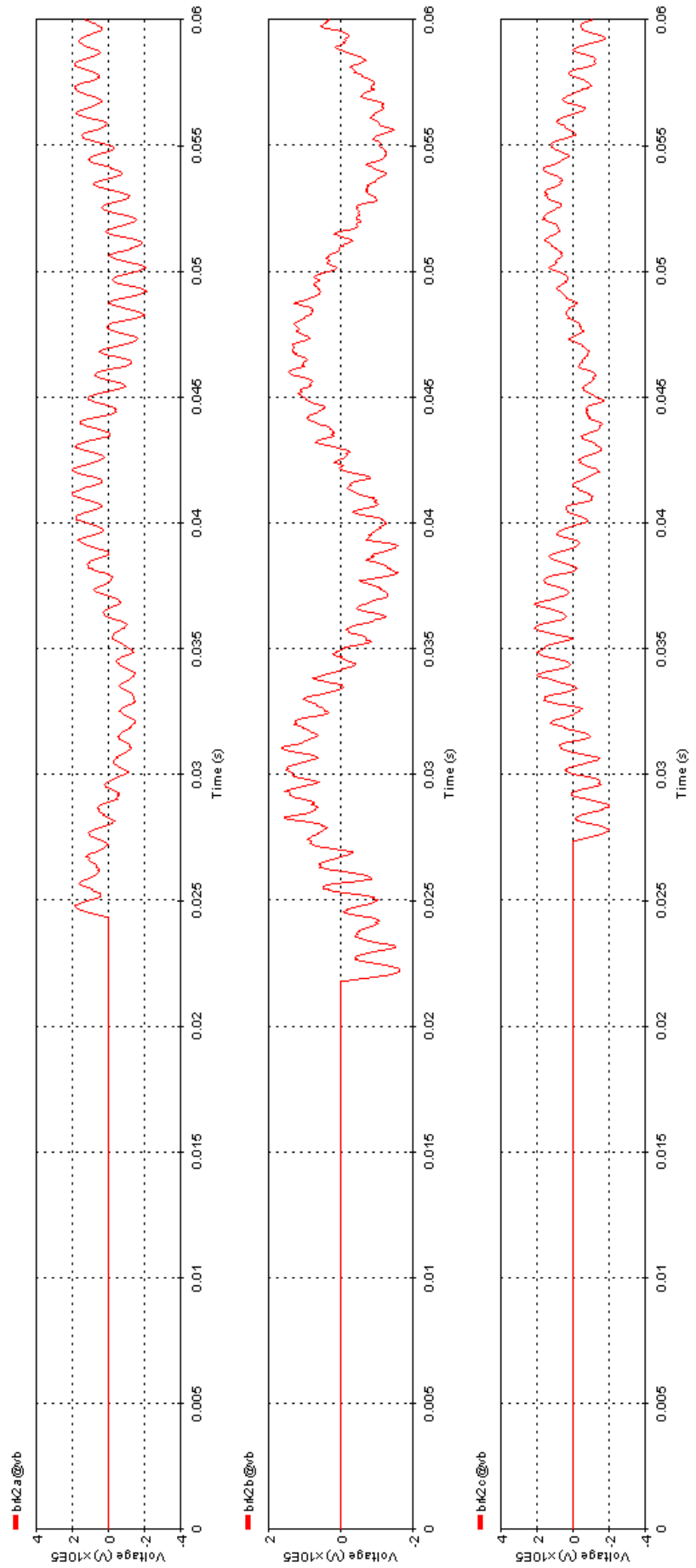


Figure 4.1.1: TRV Waveform of the Three Phases for Multiple Line Switching at Terminal of Substation for Three Phase to Ground Fault

[EMT1] terminaltrvm - Tue Apr 25 11:28:20 IST 2017 - C:\Users\sacer\Desktop\project\terminal fault\terminal trv.pj

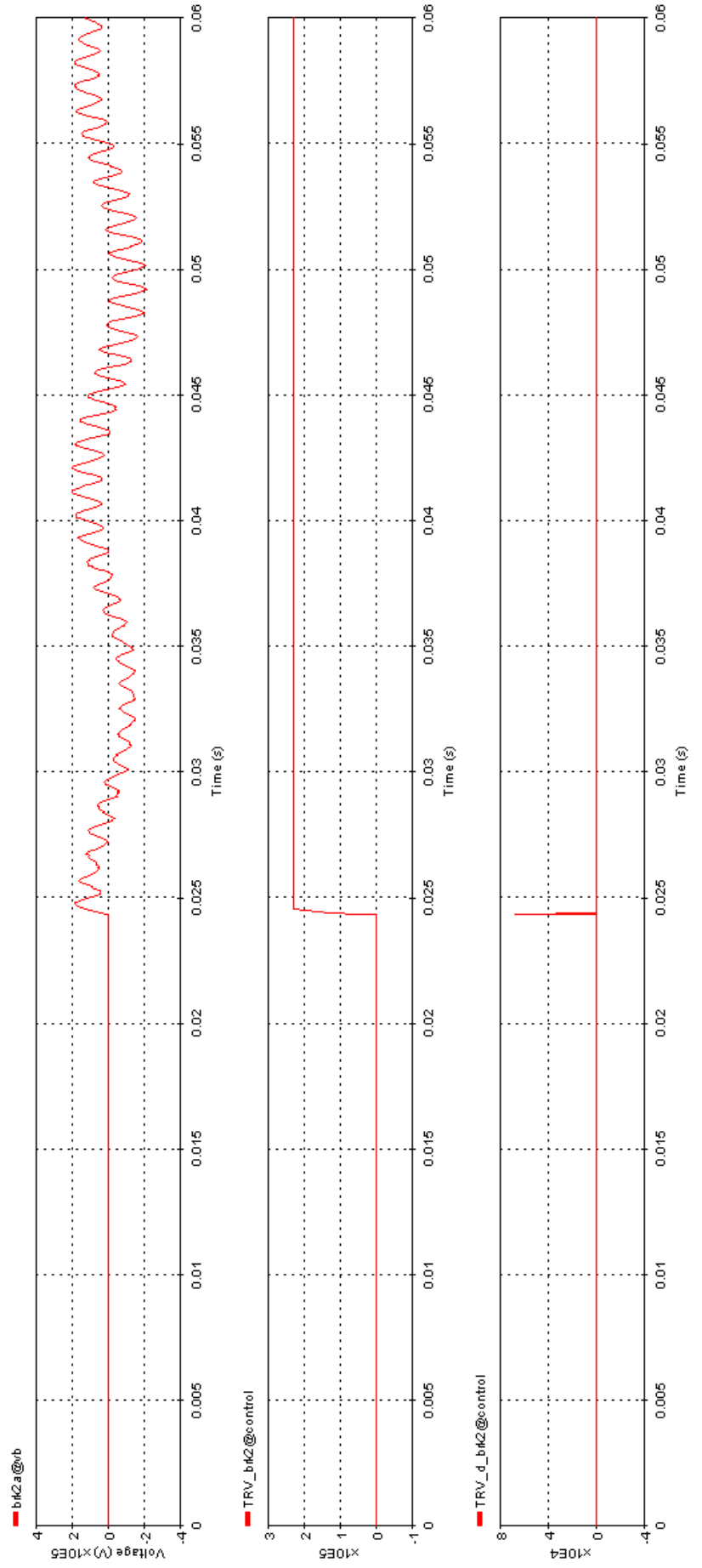


Figure 4.1.2: TRV Waveform of Phase A with Standard TRV and Delay Line for Multiple Line Switching at Terminal of Substation for Three Phase to Ground Fault

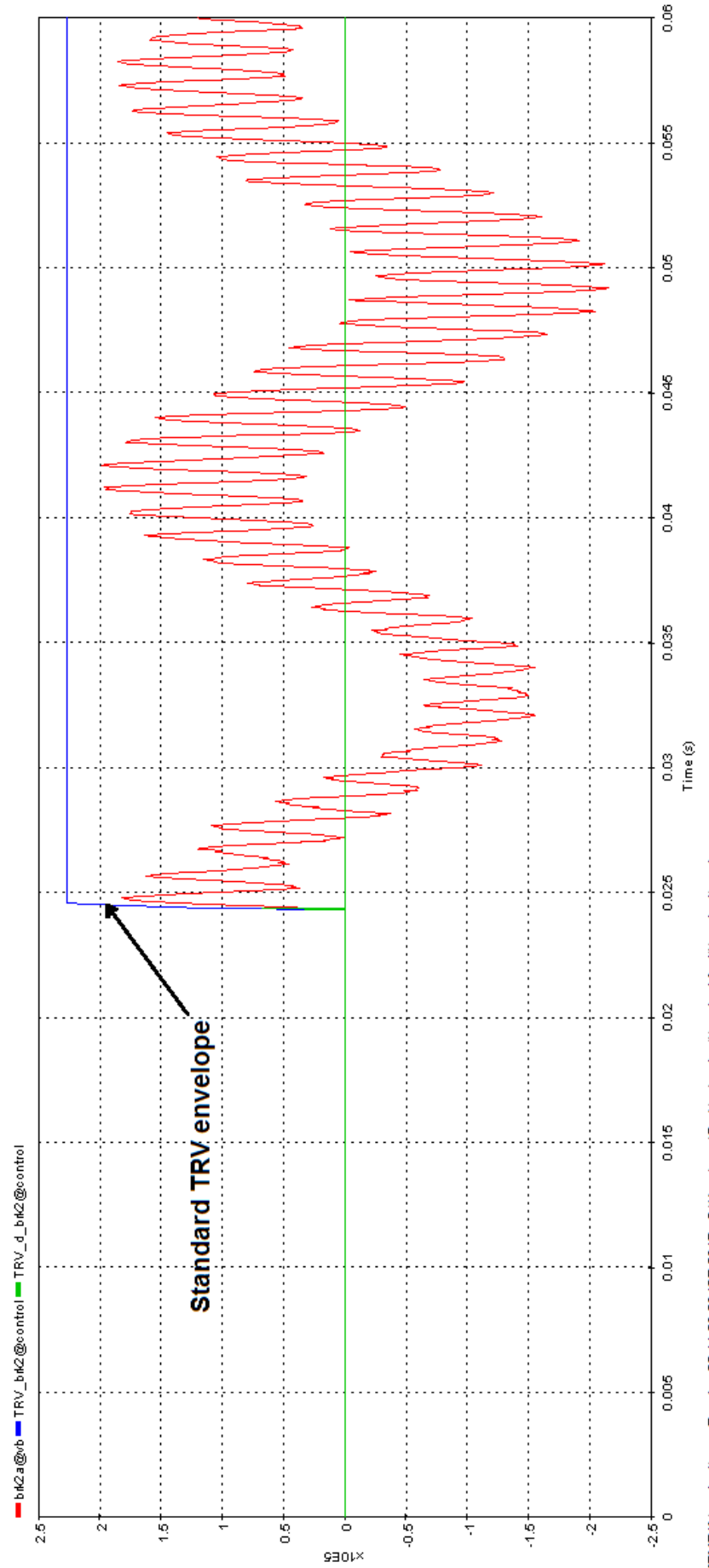


Figure 4.1.3: Standard TRV Envelope and Phase A TRV for Multiple Line Switching at Terminal of Substation for Three Phase to Ground Fault

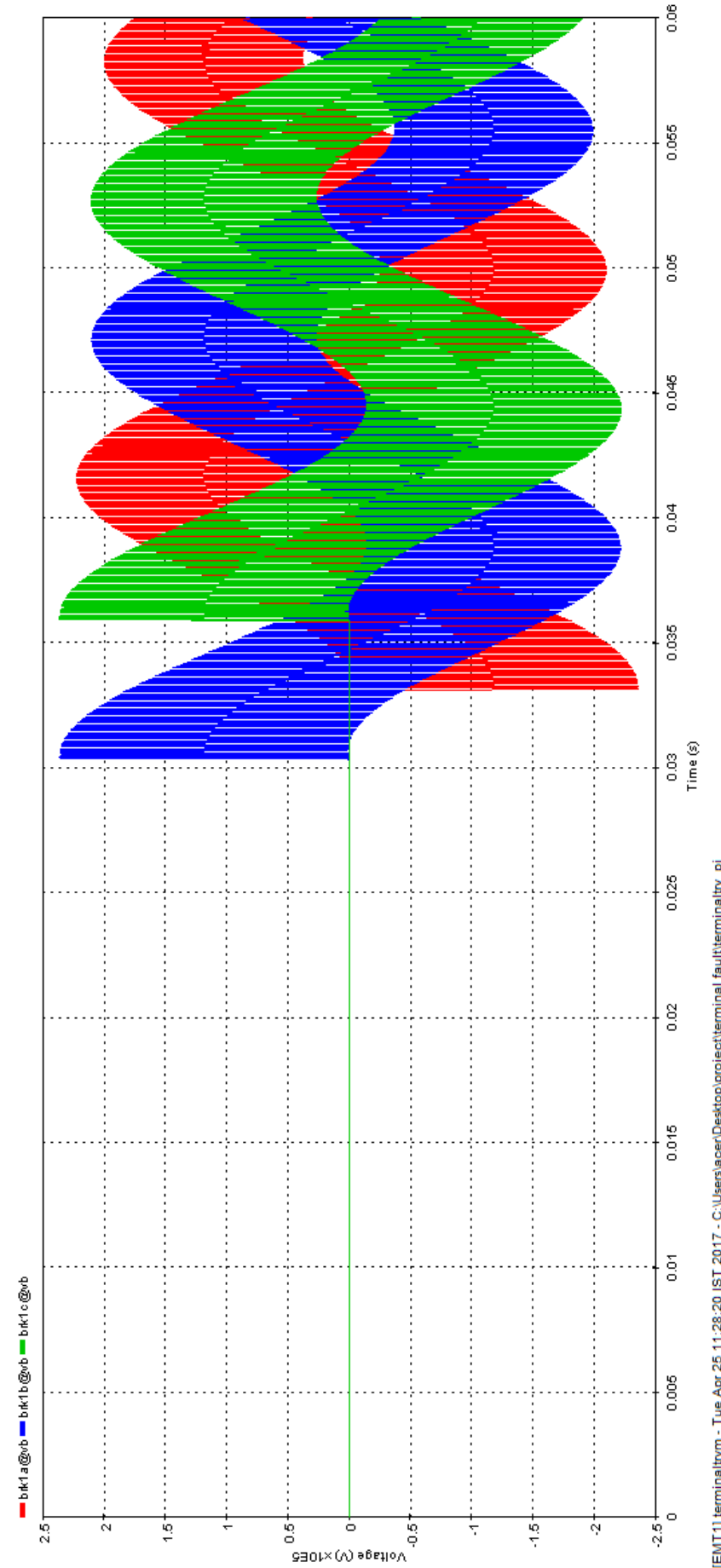


Figure 4.1.4: Oscillatory TRV for Three Phase to Ground Terminal Fault for Transformer Switching

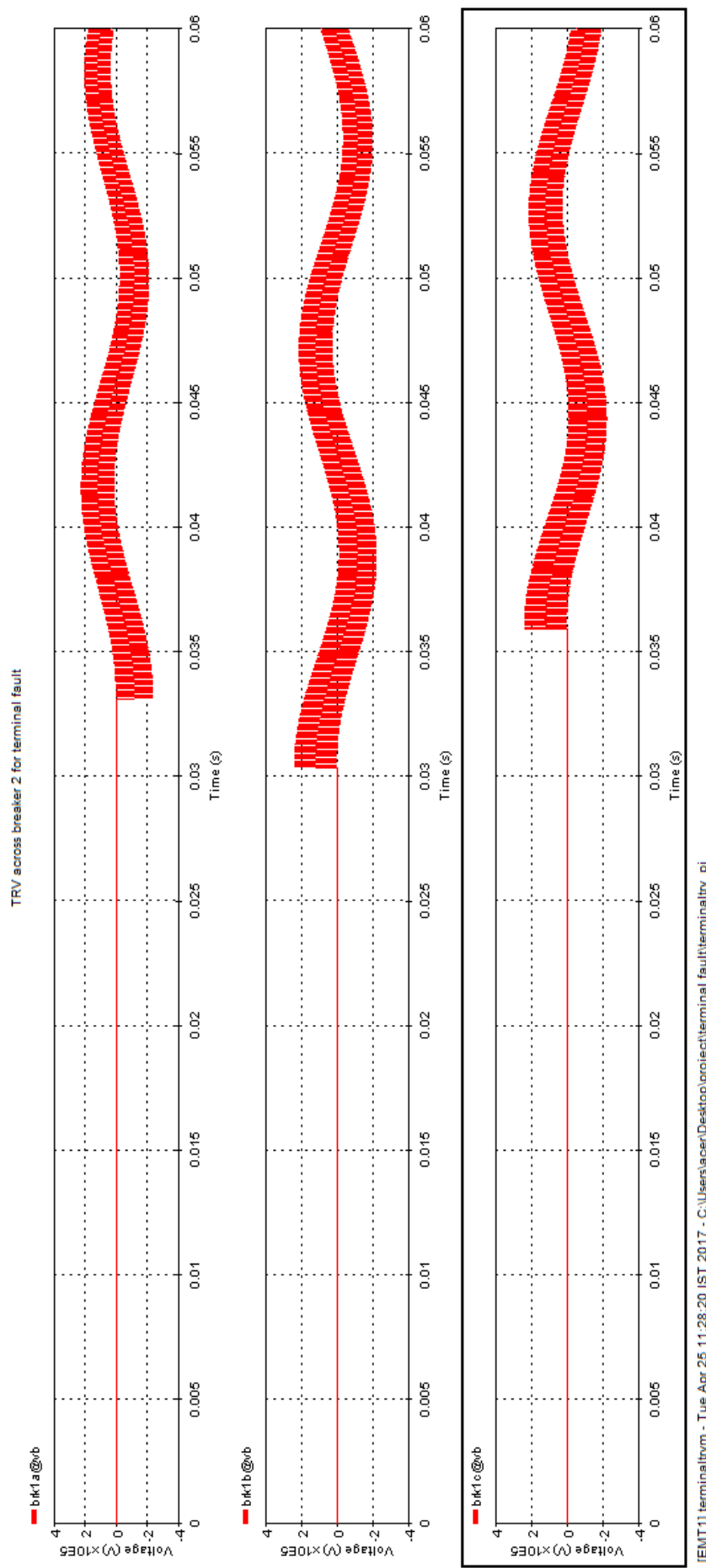


Figure 4.1.5: Three Phase Oscillatory TRV for Three Phase to Ground Terminal Fault for Transformer Switching

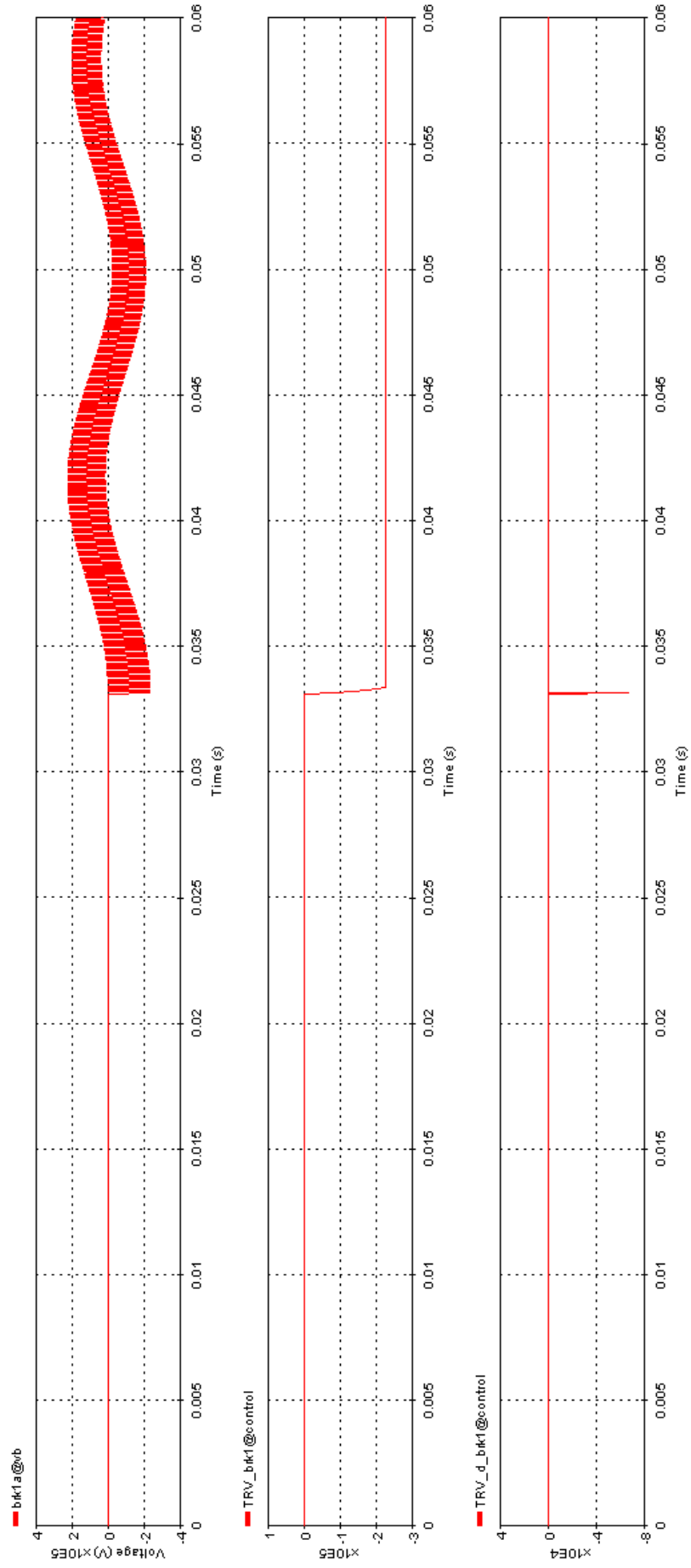


Figure 4.1.6: Phase A TRV, Standard TRV and Delay Line for Oscillatory TRV for Three Phase to Ground Terminal Fault for Transformer Switching

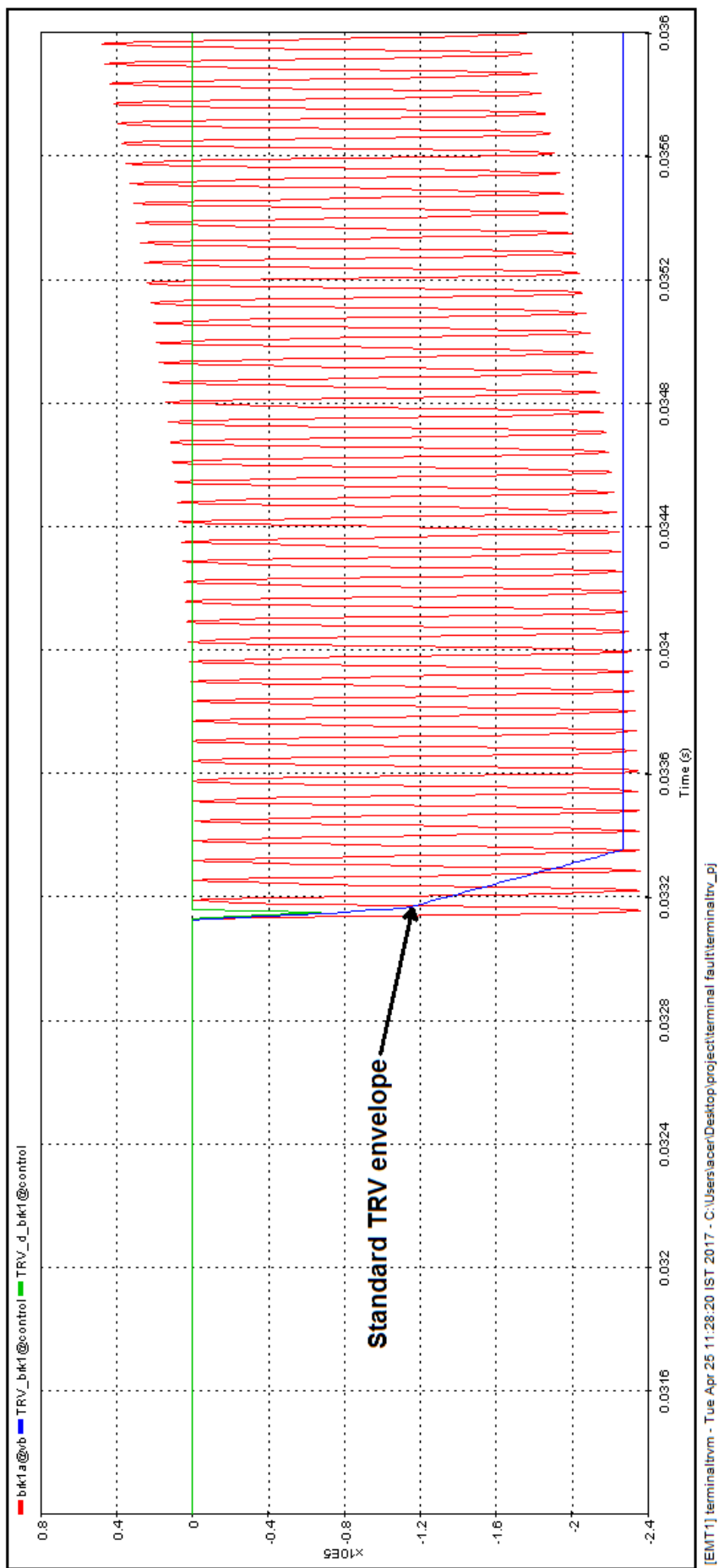


Figure 4.1.7: Enlarged View of Phase A TRV and Standard TRV Envelope for Three Phase to Ground Terminal Fault for Transformer
Switching

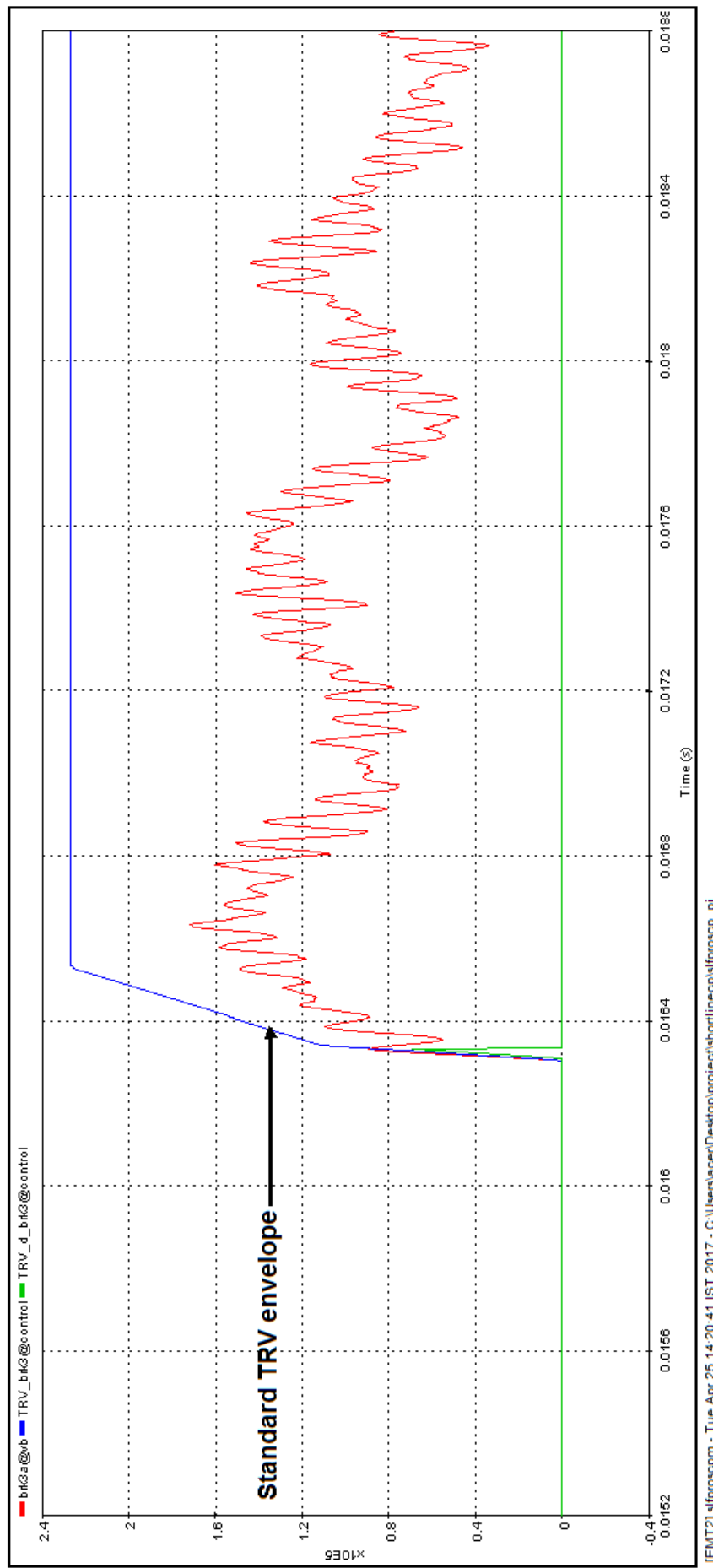


Figure 4.1.8: TRV for Short Line Single Phase to Ground Fault for Constant Parameter Model of Lines

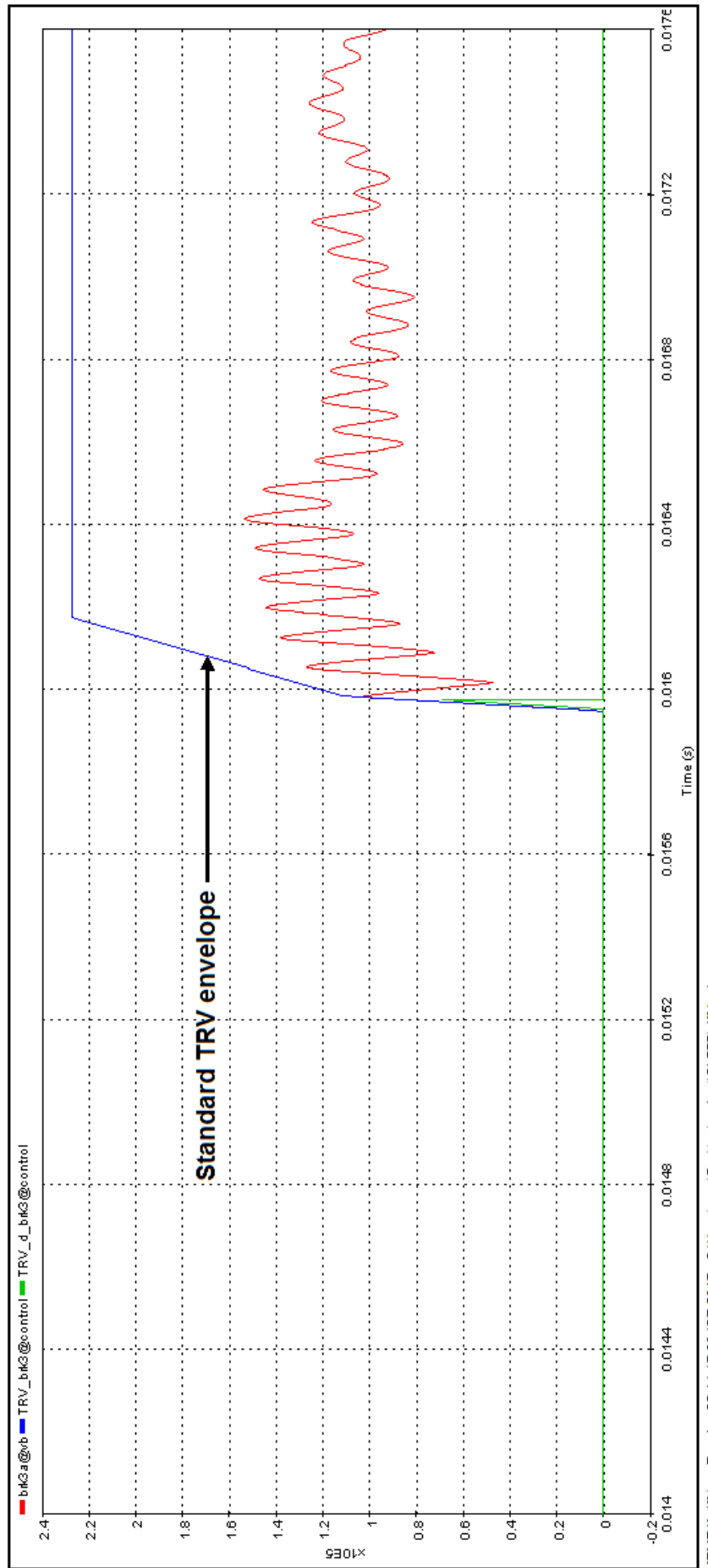


Figure 4.1.9: TRV for Short Line Single Phase to Ground Fault for Frequency Dependent Model of Lines

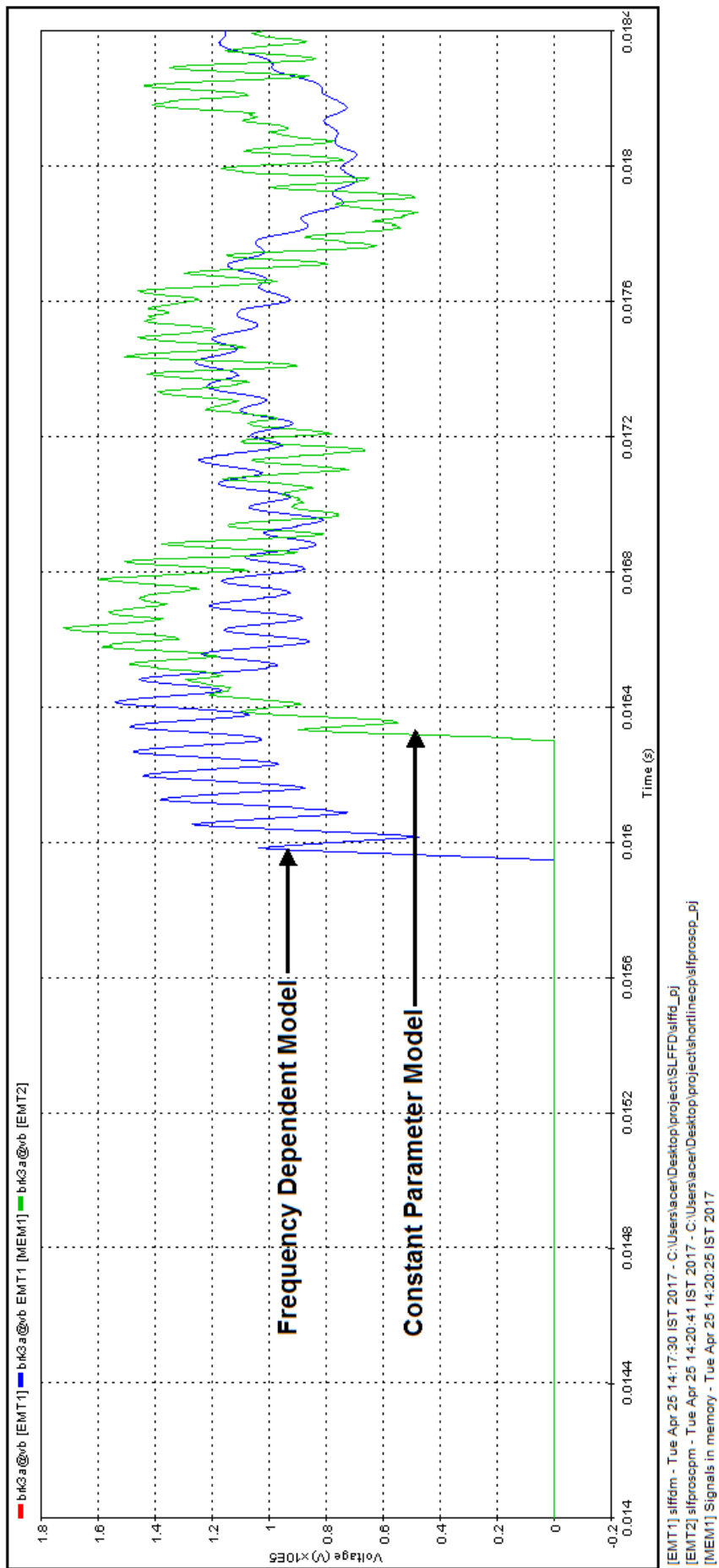


Figure 4.1.10: Comparative Waveform of TRV for Constant Parameter Model and Frequency Dependent Model of Line for Short Line Single Phase to Ground

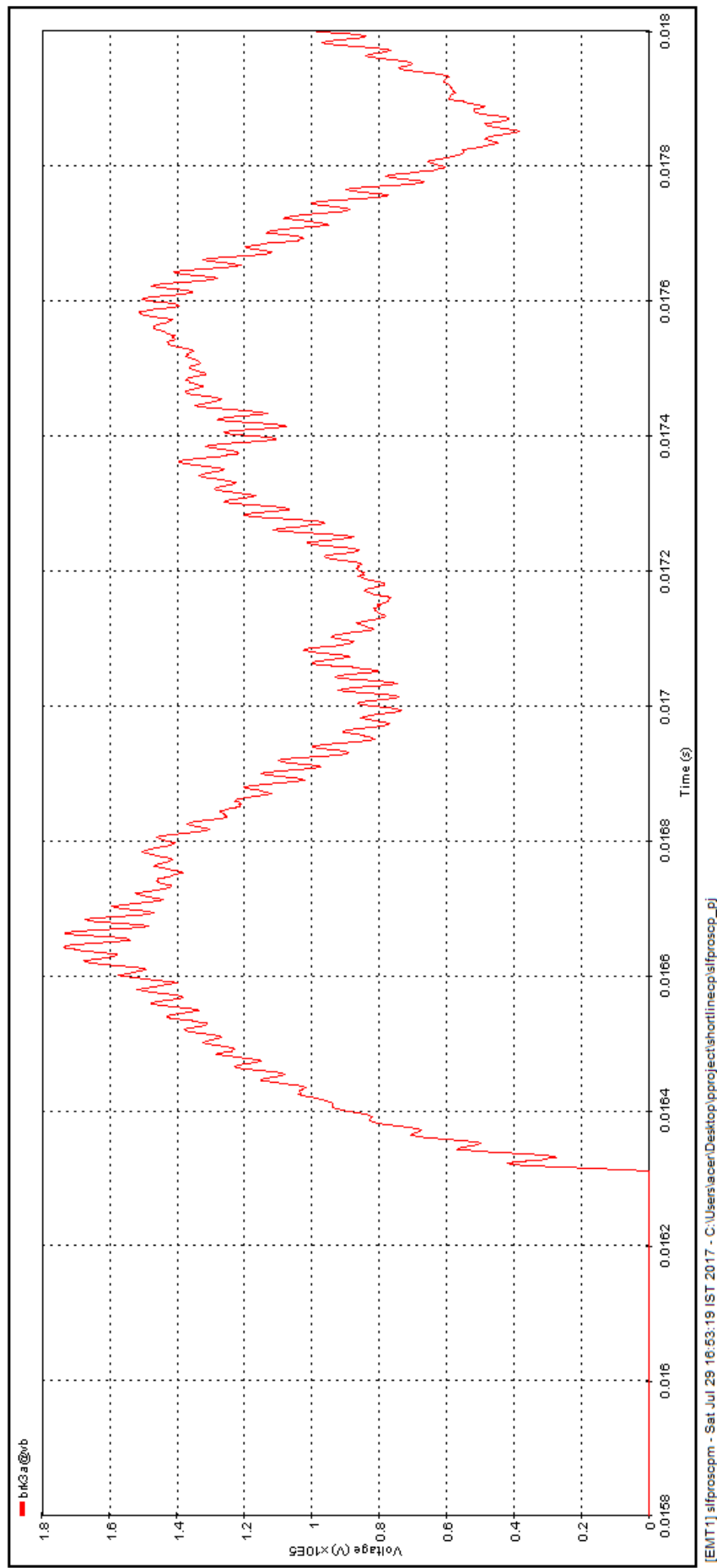


Figure 4.1.11: TRV for Short Line Single Phase to Ground Fault at 1.2 km for Constant Parameter Model of Lines

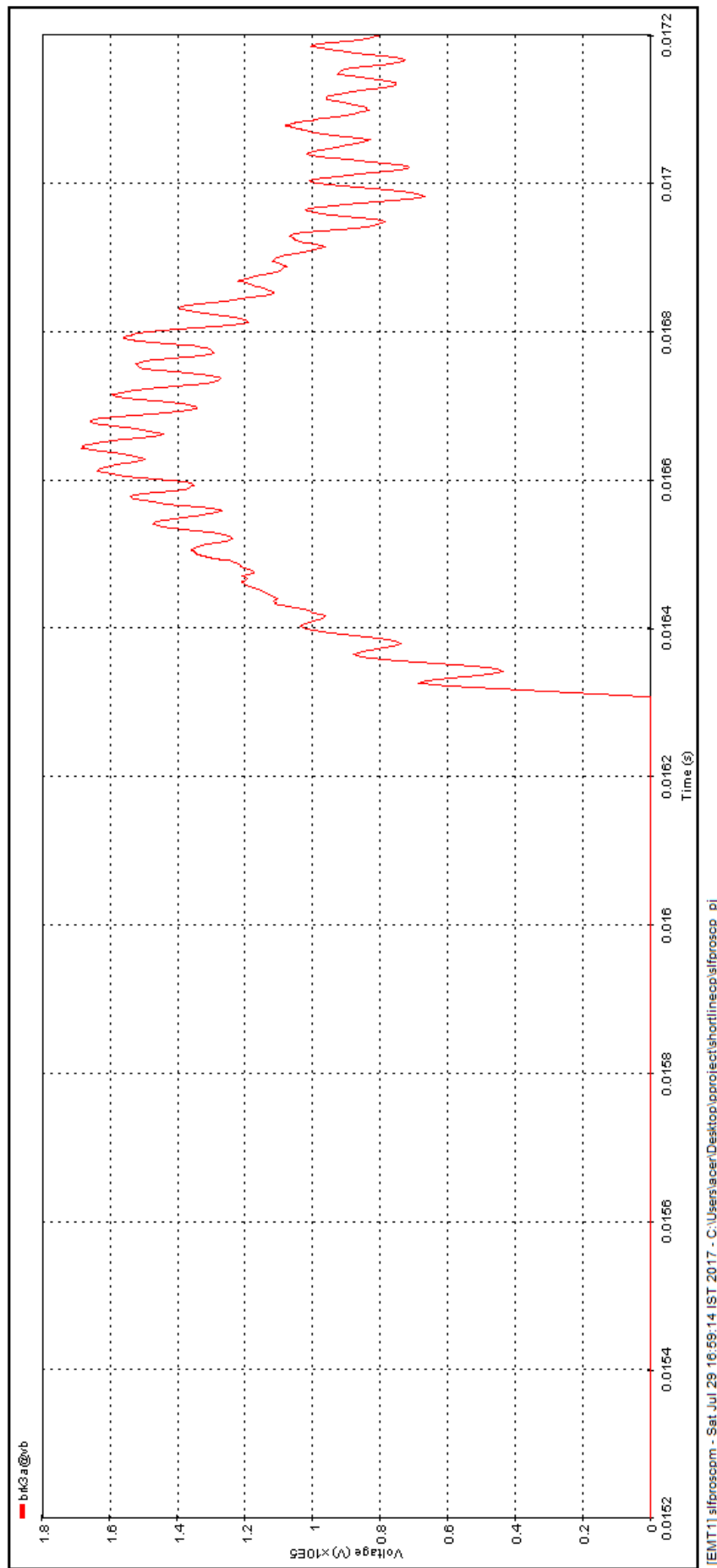


Figure 4.1.12: TRV for Short Line Single Phase to Ground Fault at 2.2 km for Constant Parameter Model of Lines

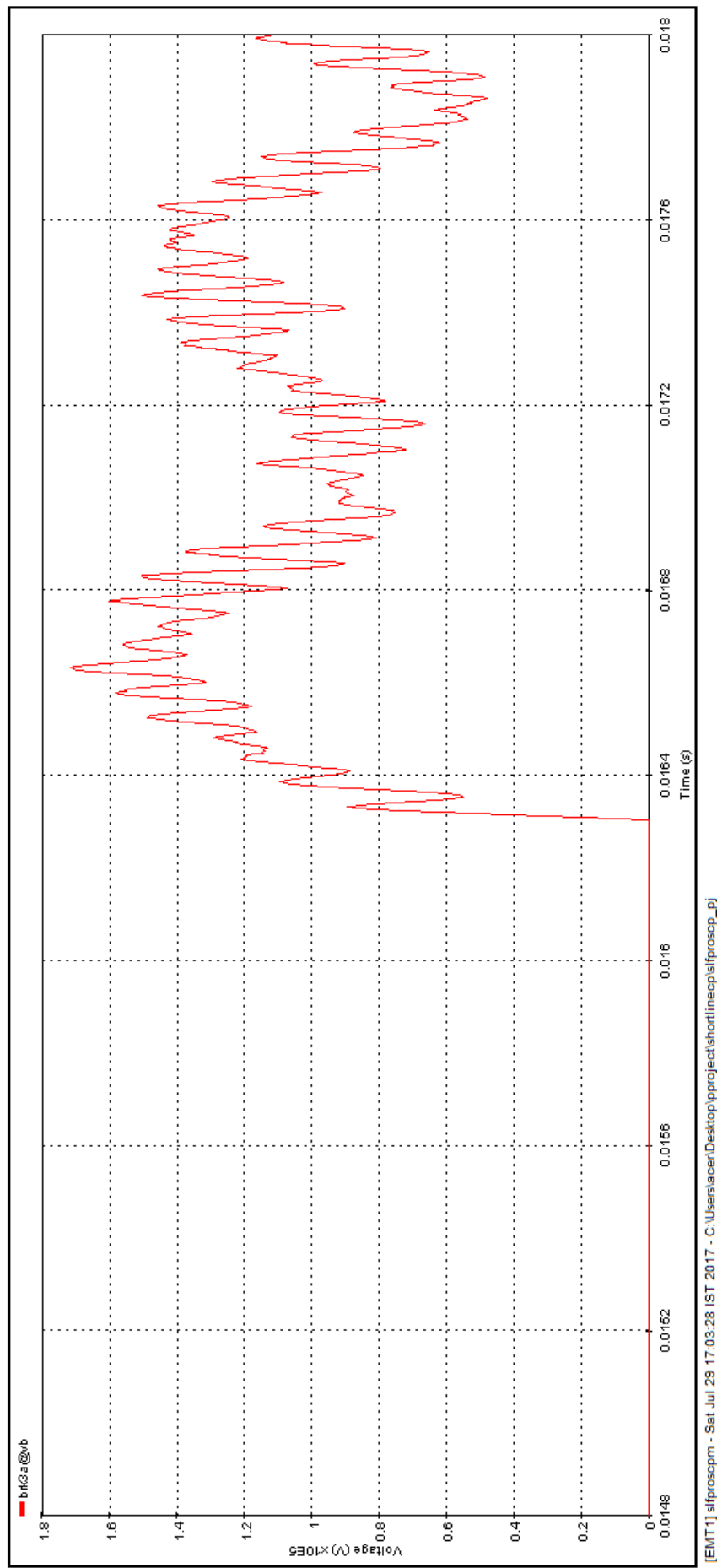


Figure 4.1.13: TRV for Short Line Single Phase to Ground Fault at 3.2 km for Constant Parameter Model of Lines

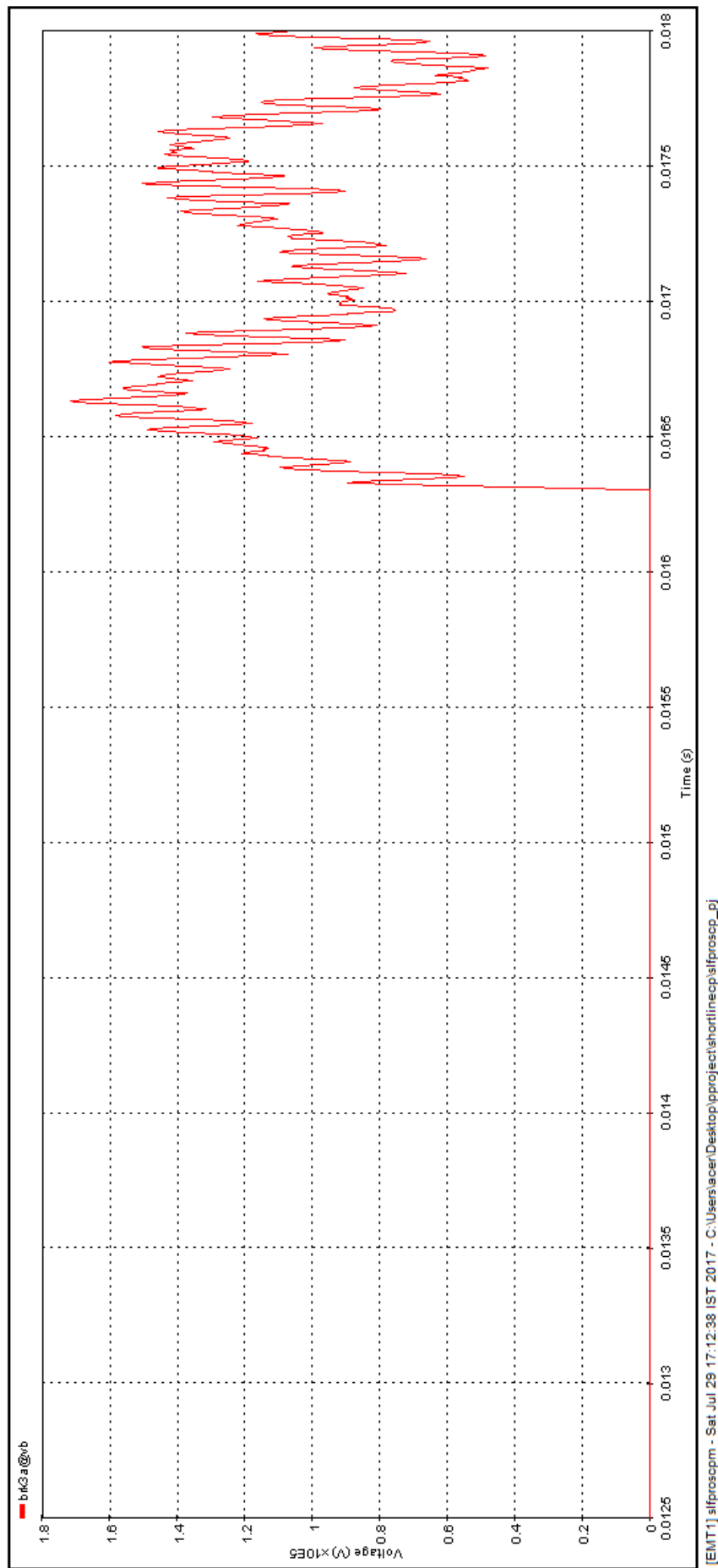


Figure 4.1.14: TRV for Short Line Single Phase to Ground Fault at 5.2 km for Constant Parameter Model of Lines

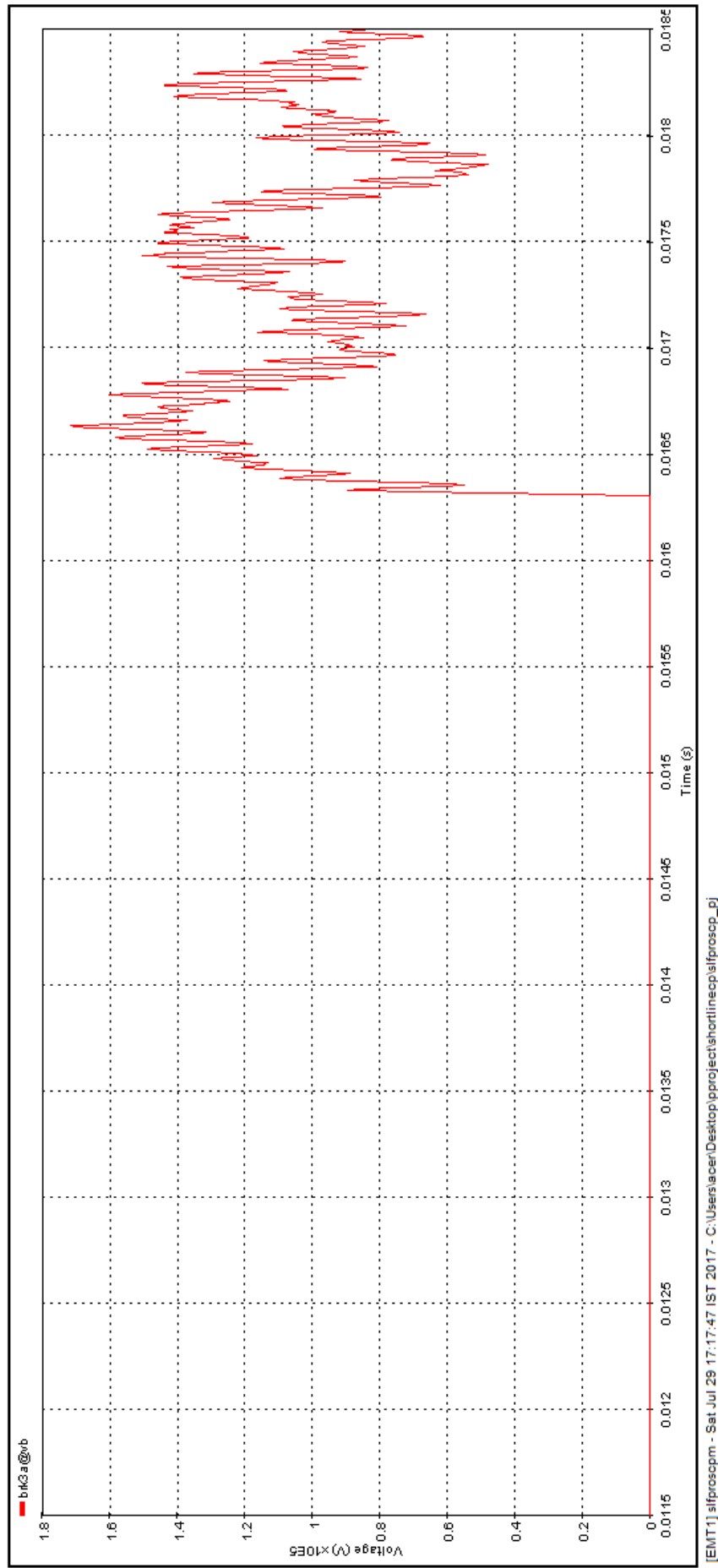


Figure 4.1.15: TRV for Short Line Single Phase to Ground Fault at 6.2 km for Constant Parameter Model of Lines

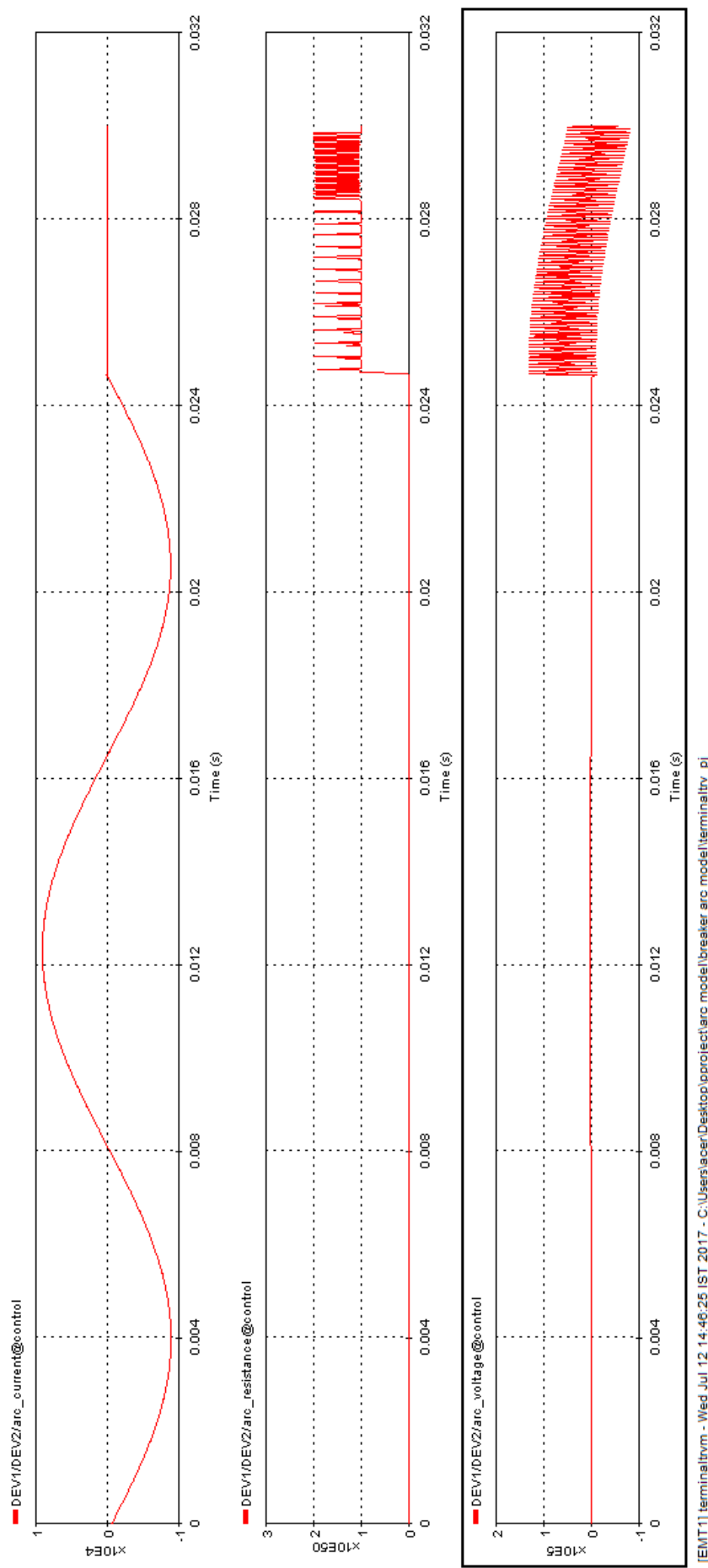


Figure 4.1.16: Arc Interruption Waveforms for Three Phase to Ground Terminal Fault for Transformer Switching

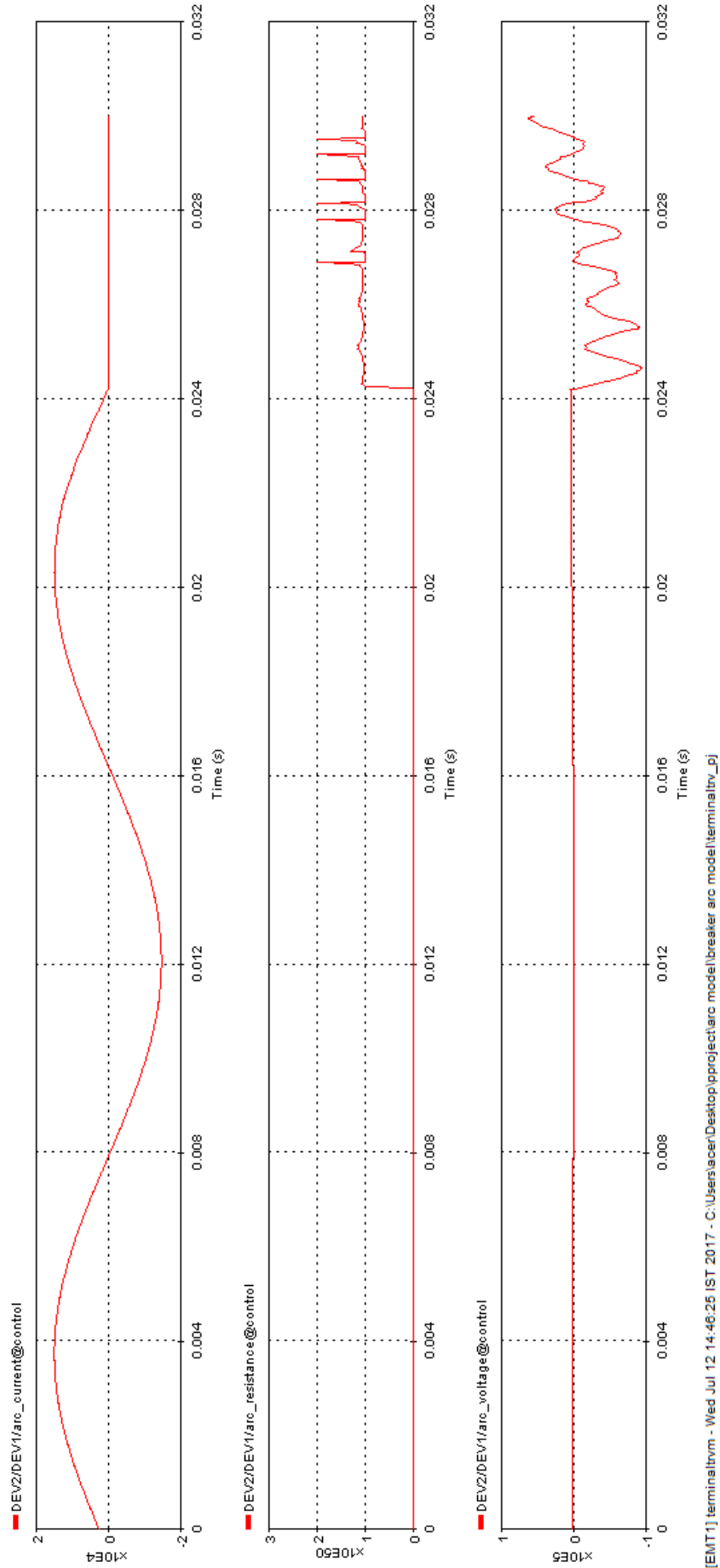


Figure 4.1.17: Arc Interruption Waveforms for Three Phase to Ground Terminal Fault for Multiple Line Switching

4.2 Analytical Analysis

Based on the developed system discussed in chapter 3, comprehensive analytical analysis is done for the following models considering and solving the mathematical equations 3.1 to 3.11.

1. The network under study is modeled for three phase to ground fault at the terminal of substation for switching multiple lines connected to the substation. Equations 3.1 to 3.5 modeling the system for this condition give the short circuit current of 17.1 kA under steady state conditions which is closed to the 17.2 kA obtained through simulation. The RRRV obtained analytically through equation 3.6 is $0.91 \text{ kV}/\mu\text{s}$ which is close to $1.2 \text{ kV}/\mu\text{s}$ obtained through simulation.
2. The network under study is modeled for three phase to ground fault at the terminal of substation for transformer switching. Equations 3.1 to 3.3 and 3.7 used to find RRRV gave the value of $6.75 \text{ kV}/\mu\text{s}$ which is in close approximation to $7.65 \text{ kV}/\mu\text{s}$ obtained through simulation.
3. The network is modeled for single phase to ground short line fault using constant parameter mode as well as frequency dependent mode of transmission line. Equations 3.8 to 3.11 give the RRRV $2.87 \text{ kV}/\mu\text{s}$ which is in good agreement with the simulated value of $2.35 \text{ kV}/\mu\text{s}$ for a fault at 4.2 km. The RRRV is plotted for different fault distance in the figure 4.2.1. It is observed that the RRRV increases with reduction in fault distance.
4. The network under study is modeled for three phase to ground fault at the terminal of substation for multiple lines switching as well as transformer switching. Black Box model using Cassie-Mayer equations is used for arc interruption studies. Successful interruption of arc is observed in both cases.

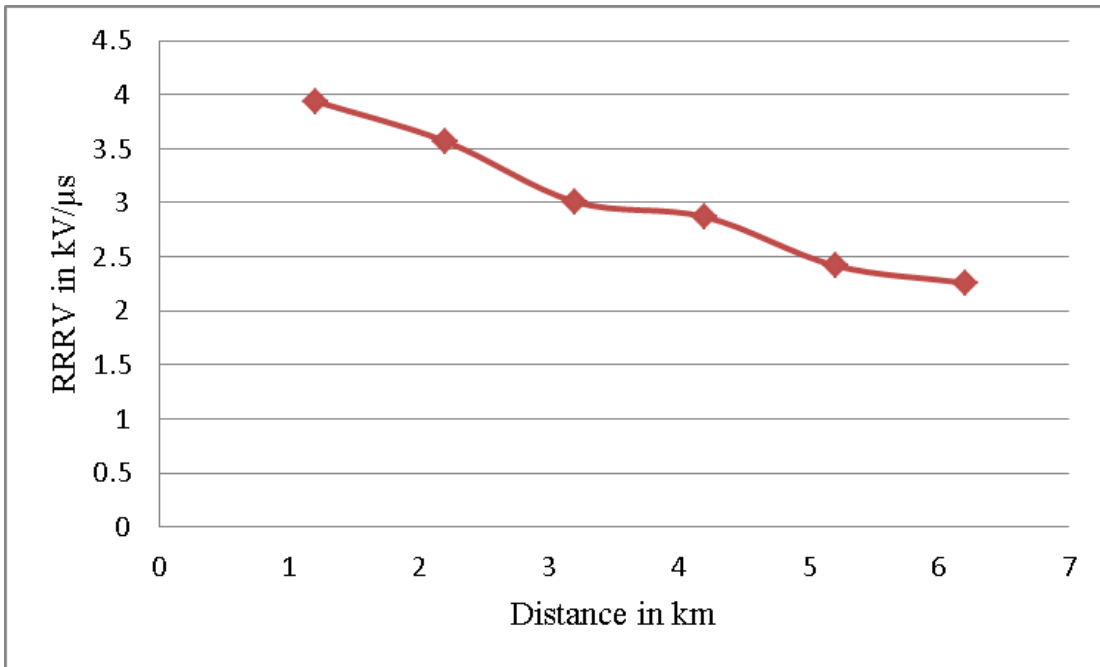


Figure 4.2.1: Variation of RRRV with Fault Distance for Single Phase to Ground Short Line Fault

4.3 Comparison between Computational and Analytical Analysis

1. Short circuit current during Three Phase to Ground fault through simulation is found to be 17.2 kA which is almost same (17.1 kA) as obtained analytically.
2. Table 4.3.1 gives the parameters of standard TRV and TRV obtained through simulation

Table 4.3.1: Comparison of Standard TRV and Simulated TRV

	u_1 kV	t_1 μs	u_c kV	t_2 μs	t_d μs	u' kV	t' μs	u_1/t_1 kV/μs
Standard	115	38	231	228	2-12	58	21-31	3
Simulated	114.8	39	230	227.4	3.2	58.2	26	2.9

3. Table 4.3.2 shows the max. Value of TRV and RRRV under different fault conditions.

Table 4.3.2: Simulation Results for TRV under Different Fault Conditions

Sr. No.	Type of fault	Max. Value of TRV (kV)	RRRV (kV/ μ s)		Nature of TRV
			Simulated	Analytical	
1	Three Phase to Ground fault at the terminal of substation	182.215	1.2	0.91	(a) Exponential as per standard (b) Oscillatory as per standard
	(a) Multiple lines connected to bus				
	(b) Transformer switching	235.855	7.65	6.75	
2	Short line fault	171.65	2.89	2.87	Saw tooth shaped as per standard
	(a) Constant parameter model				
	(b) Frequency dependent model	153.53	2.5		

4.4 Validation of Algorithm

The proposed algorithm is applied to the case study [68]. One new fixed contact (F_1) and four moving contacts, relatively new contact (M_1), slightly worn contact (M_2) a worn contact (M_3) and seriously damaged worn contact (M_4) as shown in figure 4.4.1 were considered. Figure 4.4.2 shows the DCRM of the tripping portion. The value of A_a , area below the arcing contact region is shown in table 4.4.1.

Value of ΔT_a , ΔT_m , ΔA_m and ΔR_{aimax} is not measured. But as seen from the graph in figure 4.4.2, $\Delta T_a \cong 0$, $\Delta T_m \cong 0$, $\Delta R_{aimax} > 0$ and $\Delta A_m \cong 0$ and $\Delta A_a > 0$. when this data is fed to the proposed algorithm, it detects problem no. 3 that corresponds to wearing of moving contact which is same as proposed in the algorithm.

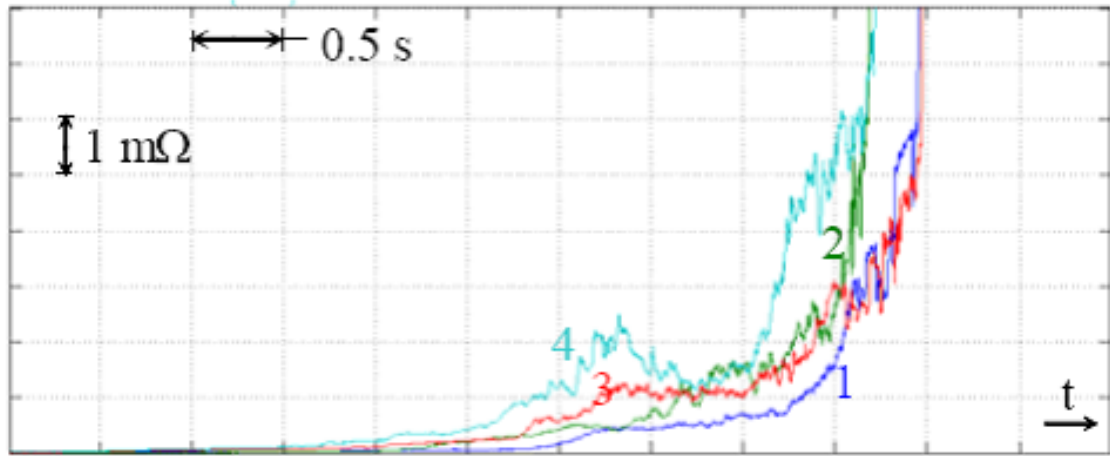


(a) Relatively New Fixed Contact (F1) (b) New Moving Contact (M1) (c) Slightly Worn Moving Contact (M2)



(d) Worn Moving Contact (M3) (e) Seriously Worn Moving Contact (M4)

Figure 4.4.1: Fix and Moving Contacts with Different Worn Conditions [68]



1: Contact set F1-M1; 2: Contact set F1-M2; 3: Contact set F1-M3; 4: Contact set F1-M4

Figure 4.4.2: DCRM Signature in the Trip Portion for Different Contact Configuration [68]

Table 4.4.1: Area below the DCRM Curve for Different Contact Configuration [68]

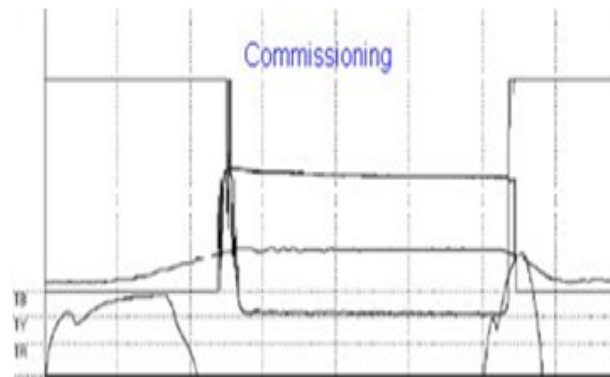
Contact set	$A_a(m\Omega.s)$
$F_1 - M_1$	2.7
$F_1 - M_2$	2.8
$F_1 - M_3$	3.9
$F_1 - M_4$	5.4

Figure 4.4.3a - d shows the DCRM signatures of R-pole of a 400 kV SF₆ circuit breaker from commissioning stage. Large variations of resistance in the no action zone are seen in the DCRM signature on 15/12/2014. Table 4.4.2 shows the CB parameters for the healthy and faulty condition from DCRM signature. When the parameters are fed, the algorithm detected problem of main contact erosion. Figure 4.4.4 shows the output of the program. It is confirmed by the static contact resistance test which gave a very high value of static contact resistance 170 $\mu\Omega$.

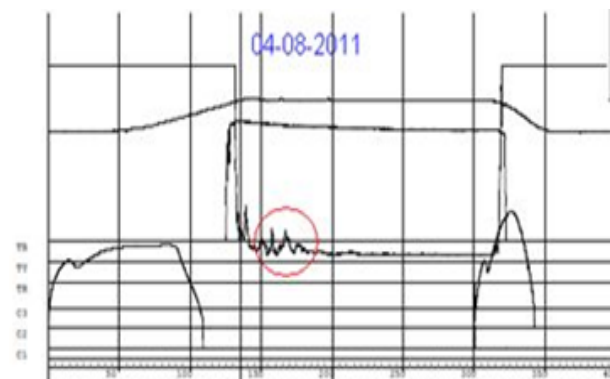
Table 4.4.2: CB Parameters for the Healthy and Faulty Condition from DCRM Signature

Description	T_m (ms)	T_a (ms)	R_{iam} ($\mu\Omega$)	A_m ($\mu\Omega \times \text{ms}$)	A_a ($\mu\Omega \times \text{ms}$)
Current Value	315.6	318.9	860	30430	1665
Base Value	316.8	318.9	860	6120	886.2
Difference Δ	-1.2	0	0	24310	778.8

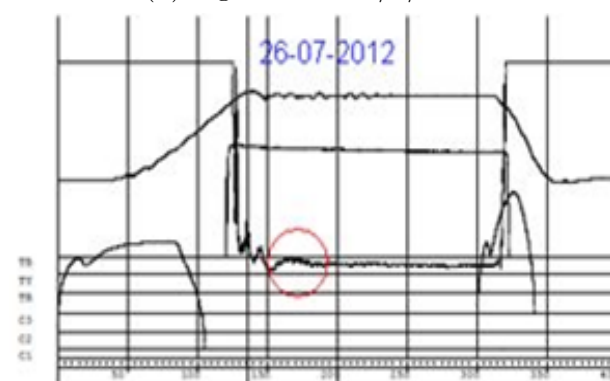
Figure 4.4.5a - d shows the DCRM signatures of Y-pole of the same circuit breaker from commissioning stage. Spike is seen in close zone portion of the signature. When algorithm is applied step by step, the problem of contact wipe is detected. The contact wipe was found to be 16 mm. When contact wipe is adjusted to specified limit, normal DCRM signature is obtained as shown in figure 4.4.5d.



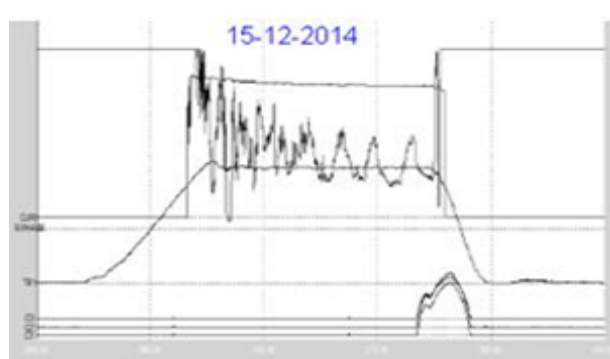
(a) Signature at Commissioning



(b) Signature on 4/8/2011

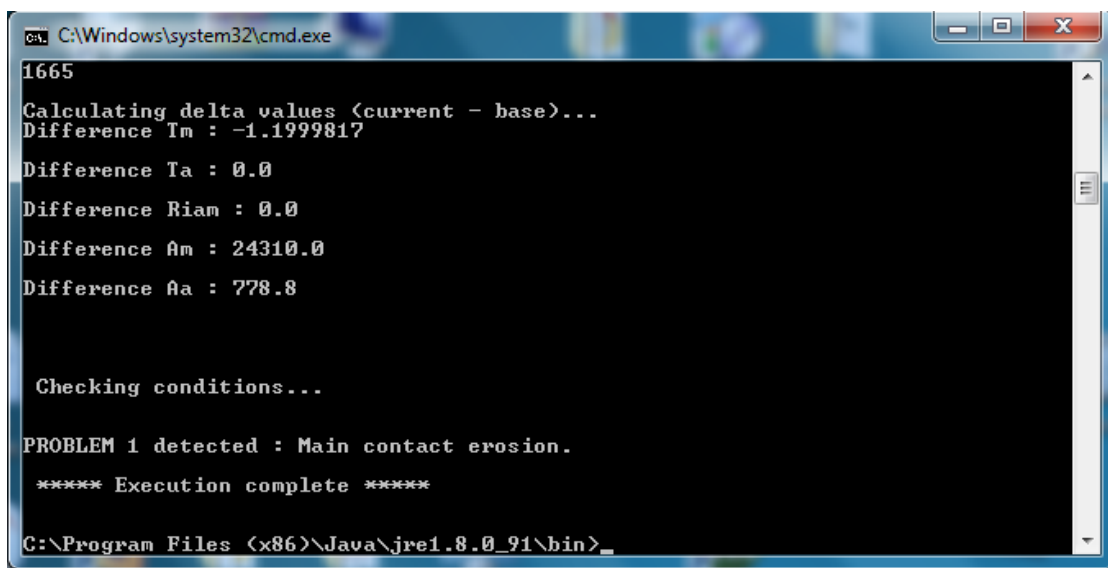


(c) Signature on 26/7/2012



(d) Signature on 15/12/2014

Figure 4.4.3: Signatures of R-pole from Commissioning



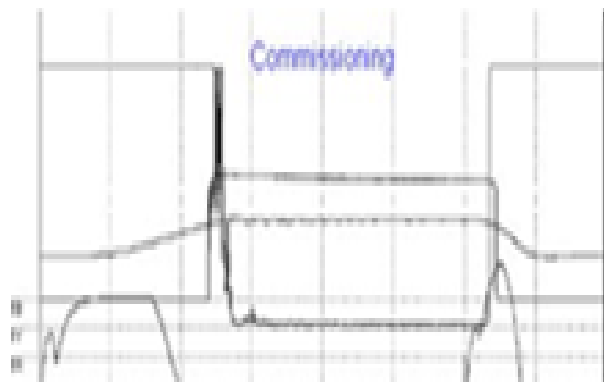
The screenshot shows a Windows Command Prompt window titled 'C:\Windows\system32\cmd.exe'. The window contains the following text output:

```
1665
Calculating delta values (current - base)...
Difference Tm : -1.1999817
Difference Ta : 0.0
Difference Riam : 0.0
Difference Am : 24310.0
Difference Aa : 778.8

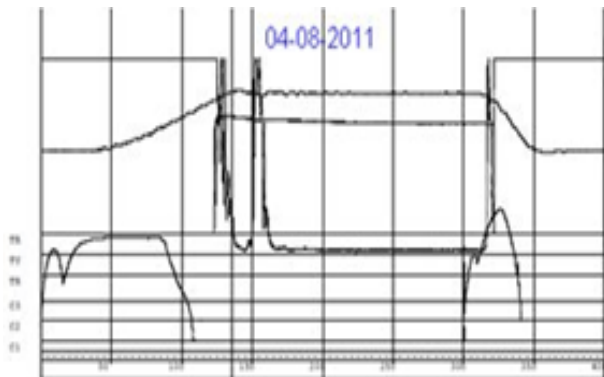
Checking conditions...
PROBLEM 1 detected : Main contact erosion.
***** Execution complete *****

C:\Program Files (x86)\Java\jre1.8.0_91\bin>
```

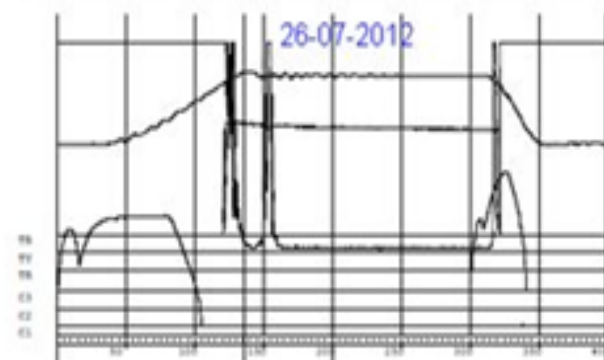
Figure 4.4.4: Output of the Program



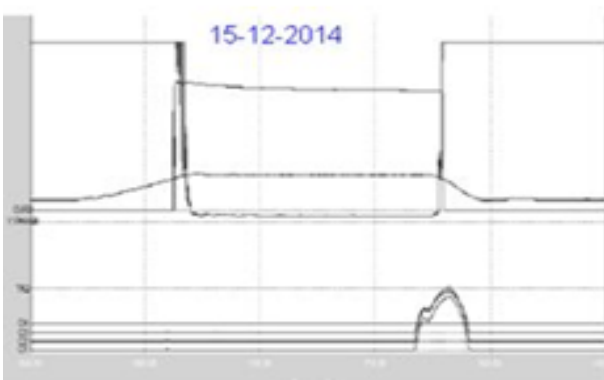
(a) Signature at Commissioning



(b) Signature on 4/8/2011



(c) Signature on 26/7/2012



(d) Signature on 15/12/2014 After Wipe Adjustment

Figure 4.4.5: Signatures of Y-pole from Commissioning

4.5 Justification for Difference

The difference in the results obtained is because of the round off of the parameters in decimals. The nature of TRV obtained for different fault conditions is in good agreement with the standard waveforms available in the literature. Improper placement of the travel transducer or linkage ratio results in error in the DCRM signature. Induction effect in the substation switching yard also affects the measurement. DCRM must be taken with the same sampling frequency, resistance range and plot length so as to compare for variation. Change in any of the setting details for data acquisition will lead to variation in the signature which makes it difficult for comparison.

Chapter 5

CONCLUSIONS

5.1 Conclusions

From the study, simulation results, field measurements and case studies following conclusions are drawn:

- The TRV across breaker which is used for switching a transformer under three phase to ground terminal fault is much higher than the standard TRV. Higher RRRV may lead to restrike and reignition. Hence either the breaker of higher short circuit interruption capability is to be used, or capacitance should be added to CBs terminals to reduce the RRRV of TRV
- The TRV across breaker used for multiple line switching is within the standard TRV capability curve. Hence the existing CB can be used for switching
- For short line fault the magnitude of TRV is quite less but the RRRV is high leading to restrike. Hence either the breaker of higher short circuit interruption capability is to be used or capacitance should be added to CBs terminals to reduce the RRRV of TRV. Constant parameter model of transmission line gives 10.6% higher magnitude of TRV and 13.49% higher RRRV compared to frequency dependent model of line
- Arc interruption studies for a given model show the successful arc interruption for the terminal fault case
- It is observed from the fault interruption studies that short circuit capability

of CB depends upon the type of fault and TRV seen by the breaker

- Contact travel of CB must be optimally designed. Smaller contact travel will lead to restrike whereas higher value will increase the size of interrupter
- The trip velocity of CB should be such that assumed arcing time is always less than the total travel time of the interrupter. Low trip velocity will lead to restrike whereas CB with high value of trip velocity would not be able to interrupt the short circuit current
- Increase in CB main and arcing contact resistance results in increase in TRV reducing the short circuit interruption capability
- Bouncing in no load curve, current breaking and variations in resistance at the corresponding points in DCRM signature indicates the mechanical problem like lack of tightening torque and wrong assembly of contacts
- Variations in resistance during the close portion zone of the DCRM signature should be carefully observed
- Over travel at the end indicates defective damping system
- DCRM must be recorded with travel transducer and the signature during each maintenance schedule is to be properly recorded for study in the change in signature. Analysis of DCRM signature needs the knowledge of anatomy of CB. That is CB design, operating mechanism to conclude the case
- DCRM is very useful to the manufacturers as the human error or manufacturing error such as wipe adjustment, lack of tightening torque, wrong assembly of contacts, mechanism problem can be detected before despatch
- Utility maintenance crew can avoid CB failure and improve the reliability of power system through DCRM

5.2 Future Scope

This thesis deals with the study of dynamic properties of CB on short circuit capacity. The main focus is on the determination of contact condition of CB which is stressed more during the fault current interruption. The algorithm is proposed for 400 kV and 245 kV SF₆ CB of one make. To conclude the case design details of CB are required. The study can be extended for other make of CBs. The DCRM is included as one of the condition maintenance techniques in PGCIL and few state utility companies. Proper record of DCRM signatures from the time of commissioning can be kept. Post mortem report in case of CB failure will give a strong base for the studies to effectively use the technique of DCRM in future which may give a better understanding of the design of CBs.

5.3 Applications

In the deregulated environment of the fast growing power systems, the reliability of the CB in switching and interrupting the fault current is important. CBs are like insurances for every utility company. If something mishap takes place, then they are there to take care. Hence the condition based maintenance of the CB is of prime importance. Manufacturers can detect any manufacturing error such as wipe requirement, wrong assembly of contacts, lack of tightening torque, mechanism problem which is not detected during the set procedure of testing. Utility engineers can detect the contact anomaly and avoid the major failure of the system. The proposed algorithm is useful to manufacturers as well as utility engineers to detect the problem at an early stage and avoid the major accident and failure of the system.

Contributions

1. Number of DCRM signatures from the field are analyzed and conclusions are drawn which will be useful in reading the DCRM signature
2. Developed an algorithm to determine the contact condition from DCRM signature that suggests the availability of CB for future switching operation
3. Identified a program to determine the health of CB during performance
4. Short circuit capability of CB under different fault conditions and its suitability for particular switching operation is determined
5. EMTP-RV model for Trnsient Recovery Voltage under faulty condition is suggested

References

- [1] *Definition for Power Switchgear.* ANSI/IEEE C37.100-1981.
- [2] L. Van Der Sluis, “Transients in Power Systems,” Ch. 3,4,5,6. New York: John Wiley and Sons Ltd, 2001.
- [3] CIRGE Working Group 13.09, “User guide for the application of monitoring and diagnostic techniques for switching equipment for rated voltages of 72.5 kV and above,” *CIGRE Techn Broch*, Vol. 167, Aug 2000, pp. 2–5.
- [4] K. W. Hedman *et al.*, “Optimal transmission switching with contingency analysis,” *IEEE Transactions on Power Systems*, Vol. 24, No. 3, 2009, pp. 1577–1586.
- [5] M. Kezunovic *et al.*, “Reliable implementation of robust adaptive topology control,” in *47th Hawaii International Conference on System Sciences (HICSS)*. IEEE, 2014, pp. 2493–2502.
- [6] Y. Gu and L. Xie, “Fast sensitivity analysis approach to assessing congestion induced wind curtailment,” *IEEE Transactions on Power Systems*, Vol. 29, No. 1, 2014, pp. 101–110.
- [7] M. Hinow and M. Mevissen, “Substation maintenance strategy adaptation for life-cycle cost reduction using genetic algorithm,” *IEEE Transactions on Power Delivery*, Vol. 26, No. 1, 2011, pp. 197–204.
- [8] F. Li and R. E. Brown, “A cost-effective approach of prioritizing distribution maintenance based on system reliability,” *IEEE Transactions on Power Delivery*, Vol. 19, No. 1, 2004, pp. 439–441.

- [9] A. A. Razi-Kazemi *et al.*, “Priority assessment of online monitoring investment for power system circuit breakers—Part I: Qualitative-quantitative approach,” *IEEE Transactions on Power Delivery*, Vol. 28, No. 2, 2013, pp. 928–938.
- [10] Y. Liu and H.-Z. Huang, “Optimal selective maintenance strategy for multi-state systems under imperfect maintenance,” *IEEE Transactions on Reliability*, Vol. 59, No. 2, 2010, pp. 356–367.
- [11] A. A. Razi-Kazemi *et al.*, “Priority assessment of online monitoring investment for power system circuit breakers—Part II: Determination of optimum number,” *IEEE Transactions on Power Delivery*, Vol. 28, No. 3, 2013, pp. 1440–1446.
- [12] N. Sodha *et al.*, “Condition assessment of EHV class circuit breakers using dynamic contact resistance measurement technique,” in *Proc. CIGRE Session*, 2012, pp. 1–11.
- [13] X. Long *et al.*, “Online monitoring of substation grounding grid conditions using touch and step voltage sensors,” *IEEE Transactions on Smart Grid*, Vol. 3, No. 2, 2012, pp. 761–769.
- [14] V. C. Gungor and D. Sahin, “Cognitive radio networks for smart grid applications: A promising technology to overcome spectrum inefficiency,” *IEEE Vehicular Technology Magazine*, Vol. 7, No. 2, 2012, pp. 41–46.
- [15] R. Moghe, F. C. Lambert, and D. Divan, “Smart stick-on sensors for the smart grid,” *IEEE Transactions on Smart Grid*, Vol. 3, No. 1, 2012, pp. 241–252.
- [16] A. A. Razi-Kazemi *et al.*, “Circuit-breaker automated failure tracking based on coil current signature,” *IEEE Transactions on Power Delivery*, Vol. 29, No. 1, 2014, pp. 283–290.
- [17] G. Qiang *et al.*, “High voltage equipment online monitoring system of smart substation,” in *Innovative Smart Grid Technologies-Asia (ISGT Asia)*. IEEE, 2012, pp. 1–5.

- [18] A. Janssen, D. Makareinis, and C.-E. Solver, “International surveys on circuit-breaker reliability data for substation and system studies,” *IEEE Transactions on Power Delivery*, Vol. 29, No. 2, 2014, pp. 808–814.
- [19] G. Mazza and R. Michaca, “The first international enquiry on circuit-breaker failures and defects in service,” *Electra*, Vol. 79, 1981, pp. 21–91.
- [20] CIGRE Working Group 13.06, “Final report of the second international enquiry on high voltage circuit breaker failures and defects in service,” *CIGRE Tech. Brochure 83*, June 1994.
- [21] CIGRE Working Group A3.06, “Final report of 2004-2007 international enquiries on reliability of high voltage equipment, part 2- reliability of high voltage SF₆ circuit breakers,” *CIGRE Tech. Brochure 510*, Octombor 2012.
- [22] E. Nasrallah, F. Brikci, and S. Perron, “Electrical contacts in MV and HV power circuit breakers,” *Electric Energy T and D Magazine*, 2007, pp. 50–55.
- [23] R. D. Garzon, “High voltage circuit breakers: Design and applications,” Ch. 3,5,6. CRC Press, 2002.
- [24] T. E. Browne, “Circuit Interruption: Theory and Techniques,” 1984.
- [25] Live tank circuit breaker application guide. [Online]. Available: <http://www.abb.com/>
- [26] EPRI Report EL-4651. EMTP Workbook II, 1987.
- [27] CIGRE Working Group 33.02, “Guidelines for representation of network elements when calculating transients,” *CIGRE Technical Brochure*, Vol. 39, 1990.
- [28] E. Anke *et al.*, “Practical applications of arc physics in circuit breakers. Survey of calculation methods and application guide,” *CIGRE, Electra*, Vol. 118, 1988, pp. 63–79.
- [29] CIGRE Working Group 13.01, “Applications of black box modelling to circuit breakers,” *Electra*, Vol. 149, 1993, pp. 40–71.

- [30] L. Van der Sluis, W. Rutgers, and C. Koreman, “A physical arc model for the simulation of current zero behavior of high-voltage circuit breakers,” *IEEE Transactions on Power Delivery*, Vol. 7, No. 2, 1992, pp. 1016–1022.
- [31] L. Van der Sluis and W. R. Rutgers, “Comparison of test circuits for high-voltage circuit breakers by numerical calculations with arc models,” *IEEE Transactions on Power Delivery*, Vol. 7, No. 4, 1992, pp. 2037–2045.
- [32] J. Martinez, J. Mahseredjian, and B. Khodabakhchian, “Parameter determination for modeling system transients-Part VI: Circuit breakers,” *IEEE Transactions on Power Delivery*, Vol. 20, No. 3, 2005, pp. 2079–2085.
- [33] A. Avdonin *et al.*, “Some problems of EHV and UHV air-blast circuit breakers,” in *CIGRE meeting August 27 to September 4*, 1980.
- [34] S. Maximov, V. Venegas, and J. L. Guardado, “A method of obtaining of electric arc model parameters for SF₆ power circuit breakers,” in *EUROCON 2009, EUROCON'09*. IEEE, 2009, pp. 458–463.
- [35] G. St-Jean *et al.*, “A new concept in post-arc analysis applied to power circuit-breakers,” *IEEE Transactions on Power Delivery*, Vol. 3, No. 3, 1988, pp. 1036–1044.
- [36] P. H. Schavemaker and L. Van der Slui, “An improved mayr-type arc model based on current-zero measurements [circuit breakers],” *IEEE Transactions on Power Delivery*, Vol. 15, No. 2, 2000, pp. 580–584.
- [37] S. Nitu *et al.*, “Comparison between model and experiment in studying the electric arc,” *Journal of Optoelectronics and Advanced Materials*, Vol. 10, No. 5, 2008, pp. 1192–1196.
- [38] H. Knobloch and U. Habedank, “Behaviour of SF₆ high-voltage circuit breakers with different arc-extinguishing systems at short-line fault switching,” *IEE Proceedings-Science, Measurement and Technology*, Vol. 148, No. 6, 2001, pp. 273–279.
- [39] R. P. P. Smeets *et al.*, “Performance evaluation of high-voltage circuit breakers by means of current zero analysis,” in *Transmission and Distribution*

Conference and Exhibition 2002: Asia Pacific. IEEE/PES, Vol. 1. IEEE, 2002, pp. 424–429.

- [40] D. Thomas *et al.*, “The simulation of circuit breaker switching using a composite cassie-modified mayr model,” *IEEE Transactions on Power Delivery*, Vol. 10, No. 4, 1995, pp. 1829–1835.
- [41] P. Schavemaker, A. De Lange, and L. Van der Sluis, “A comparison between three tools for electrical transient computations,” in *International Conference on Power System Transients, Budapest, Hungary, IPST’99*, 1999, pp. 13–18.
- [42] A. Iturregi *et al.*, “Considerations for simulation of the switching arc,” *Electrical Review, ISSN 0033-2097*, Vol. 88, No. 1a, 2012, pp. 104–107.
- [43] F. Karetta and M. Lindmayer, “Simulation of the gasdynamic and electromagnetic processes in low voltage switching arcs,” *IEEE Transactions on Components, Packaging, and Manufacturing Technology: Part A*, Vol. 21, No. 1, 1998, pp. 96–103.
- [44] Q. Bui-Van *et al.*, “Performance of series-compensated line circuit breakers under delayed current-zero conditions,” *IEEE Transactions on Power Delivery*, Vol. 12, No. 1, 1997, pp. 227–233.
- [45] M. Liao *et al.*, “Study on dynamic arc model for high voltage hybrid circuit breaker using vacuum interrupter and SF₆ interrupter in series,” in *24th International Symposium on Discharges and Electrical Insulation in Vacuum (ISDEIV)*. IEEE, 2010, pp. 174–178.
- [46] J. Zhang *et al.*, “Modelling of the interruption process in SF₆ high voltage circuit breaker and preliminary study of the arc characteristics for different gases,” in *Proceedings of the 55th IEEE Holm Conference on Electrical Contacts*. IEEE, 2009, pp. 240–245.
- [47] A. Ziani and H. Moulai, “Application of artificial neural networks for electric arc extinction modeling in high voltage circuit breakers,” in *15th IEEE Mediterranean Electrotechnical Conference MELECON*. IEEE, 2010, pp. 248–252.

- [48] J. A. Martinez-Velasco, *Power System Transients: Parameter Determination*. CRC press, 2009.
- [49] J. A. Martinez-Velasco, “Digital computation of electromagnetic transients in power systems: current status,” *Chapter 1 of Modeling and Analysis of System Transients Using Digital Systems*, 1998.
- [50] O. Svensen, “The influence of prestrike on the peak values of energisation transients,” *IEEE Transactions on Power Apparatus and Systems*, Vol. 95, No. 2, 1976, pp. 711–720.
- [51] S. Theoleyre, “MV breaking techniques,” *Cahiers Techniques (Schneider Electric Technical Documents), Cahier*, Vol. 193, 1999.
- [52] IEC 6227–100 High Voltage Switchgear and Controlgear-Part 100, *Alternating - Current Circuit Breakers*. IEC.
- [53] IEEE Standard C37.011, *IEEE Guide for the Application of Transient Recovery Voltage for AC High Voltage Circuit Breakers*. IEEE, 2011.
- [54] IEEE Standard C37.015, *IEEE Application Guide for Shunt Reactor Switching*. IEEE, 1993.
- [55] ANSI/IEEE Standard C37.012, *IEEE Application Guide for Capacitance Current Switching for AC High Voltage Circuit Breakers Rated on a Symmetrical Current Basis*. IEEE, 2005.
- [56] J. Bachiller *et al.*, “The operation of shunt reactors in the spanish 400 kV network-study of the suitability of different circuit breakers and possible solutions to observed problems,” in *International Conference on Large High Voltage Electric Systems*, Vol. 1, 1994, pp. 23–106.
- [57] W. Z. Gandhare, “Impulse and Switching Surge Studies on High Voltage Motors.” Ph. D. Thesis, Indian Institute of Technology, Bombay, 1998, pp. 29–30.

- [58] G. W. Chang, H. M. Huang, and J.-H. Lai, “Modeling SF₆ circuit breaker for characterizing shunt reactor switching transients,” *IEEE Transactions on Power Delivery*, Vol. 22, No. 3, 2007, pp. 1533–1540.
- [59] J. Lopez-Roldan *et al.*, “Analysis of modern high voltage circuit breaker failure during shunt reactor switching operations and corrective measures,” in *Proceedings of MATPOST European Conference on HV and MV substation equipment, Lyon, France*, 2007.
- [60] P. Dehghanian, T. Popovic, and M. Kezunovic, “Circuit breaker operational health assessment via condition monitoring data,” in *North American Power Symposium (NAPS)*. IEEE, 2014, pp. 1–6.
- [61] H. Johal and M. Mousavi, “Coil current analysis method for predictive maintenance of circuit breakers,” in *Transmission and Distribution Conference and Exposition, T and D. IEEE/PES*. IEEE, 2008, pp. 1–7.
- [62] S. Natti and M. Kezunovic, “Assessing circuit breaker performance using condition-based data and bayesian approach,” *Electric Power Systems Research*, Vol. 81, No. 9, 2011, pp. 1796–1804.
- [63] Y. Guan *et al.*, “Assessing circuit breaker life cycle using condition-based data,” in *Power and Energy Society General Meeting (PES)*. IEEE, 2013, pp. 1–5.
- [64] S. S. Biswas, A. K. Srivastava, and D. Whitehead, “A real-time data-driven algorithm for health diagnosis and prognosis of a circuit breaker trip assembly,” *IEEE Transactions on Industrial Electronics*, Vol. 62, No. 6, 2015, pp. 3822–3831.
- [65] A. A. Razi-Kazemi *et al.*, “Data mining of online diagnosed waveforms for probabilistic condition assessment of SF₆ circuit breakers,” *IEEE Transactions on Power Delivery*, Vol. 30, No. 3, 2015, pp. 1354–1362.
- [66] M. Landry *et al.*, “A new measurement method of the dynamic contact resistance of HV circuit breakers,” in *Transmission and Distribution Conference and Exposition, T and D. IEEE/PES*. IEEE, 2008, pp. 1–6.

Conference and Exposition: Latin America, TDC'06. IEEE/PES. IEEE, 2006, pp. 1–8.

- [67] M. Landry, O. Turcotte, and F. Brikci, “A complete strategy for conducting dynamic contact resistance measurements on HV circuit breakers,” *IEEE Transactions on Power Delivery*, Vol. 23, No. 2, 2008, pp. 710–716.
- [68] F. Salamanca *et al.*, “Preventive diagnosis on high-voltage circuit breakers,” in *Proc. CIGRE Symp.*, 1993, pp. 120–02.
- [69] R. K. Tyagi and N. S. Sodha, “Condition-based maintenance techniques for EHV-class circuit breakers,” in *Doble Client Conf., Boston, MA*, 2001.
- [70] M. Ohlen, B. Dueck, and H. Wernli, “Dynamic resistance measurements-A tool for circuit breaker diagnostics,” in *Stockholm Power Tech International Symposium on Electric Power Engineering*, Vol. 6, 1995, pp. 108–113.
- [71] Z. Stanisic and R. Neimanis, “A new ultra lightweight method for static and dynamic resistance measurements,” in *IEEE International Symposium on Electrical Insulation (ISEI)*. IEEE, 2010, pp. 1–4.
- [72] R. De Souza *et al.*, “Characterization of contacts degradation in circuit breakers through the dynamic contact resistance,” in *Transmission and Distribution Conference and Exposition-Latin America (PES T and D-LA)*. IEEE, 2014, pp. 1–6.
- [73] Dynamic Resistance Measurement: Part of the Analysis Inspection Service. [Online]. Available: <http://www.abb.com/>
- [74] S. Fujie, W. Zhangqi, and Q. Hongsan, “Diagnosis techniques on contact electrical endurance of high voltage circuit breakers,” in *Proceedings of International Conference on Power System Technology, POWERCON'98*, Vol. 1. IEEE, 1998, pp. 105–109.
- [75] Engineer, B. Milovic - Application and Power-Sweden, DV. Dynamic resistance measurement method applying high dc current. [Online]. Available: <http://www.amforum.org/site/journal/breakers%20drm.pdf>

- [76] M. Khoddam, J. Sadeh, and P. Pourmohamadiyan, “Electrical contact failure detection based on dynamic resistance principle component analysis and RBF neural network,” in *International Conference on Condition Monitoring and Diagnosis (CMD)*. IEEE, 2016, pp. 380–383.
- [77] M. Khoddam, J. Sadeh, and P. Pourmohamadiyan, “Performance evaluation of circuit breaker electrical contact based on dynamic resistance signature and using health index,” *IEEE Transactions on Components, Packaging and Manufacturing Technology*, Vol. 6, No. 10, 2016, pp. 1505–1512.
- [78] K. Obarčanin, A. Šečić, and N. Hadžimejlić, “Design and development of the software solution for analysis and acquisition of the high voltage circuit breakers dynamic resistance measurement results,” in *38th International Convention on Information and Communication Technology, Electronics and Microelectronics (MIPRO)*. IEEE, 2015, pp. 1032–1036.
- [79] R. T. de Souza *et al.*, “A system for dynamic contact resistance with arduino platform on MV and HV circuit breaker,” in *Proceedings of International Instrumentation and Measurement Technology Conference (I2MTC)*. IEEE, 2014, pp. 369–373.
- [80] E. Alibašić, S. Nikolovski, and B. Planojević, “A new measurement method for testing a 400 kV circuit breaker,” in *International Conference on Smart Systems and Technologies (SST)*. IEEE, 2016, pp. 149–154.

Publications

1. “An Overview of Dynamic Contact Resistance Measurement of HV Circuit Breakers”, J. Inst. Eng. (India) B, Vol. 97, No. 2, Jan. 2015, pp. 219-226.
2. “Dynamic Contact Resistance Measurement on High Voltage Circuit Breaker”, International Journal of Engineering Research and Technology (IJERT), Vol. 3, Issue 1, January 2014, pp. 1292-1296.
3. “Black Box Arc Modeling of High Voltage Circuit Breaker Using Matlab / Simulink”, International Journal of Electrical Engineering and Technology (IJEET), Vol. 3, Issue 1, January- June 2012, pp. 69-78.

Annexure A

```
1 import java.util.Scanner;
2
3 public class EEPProgram {
4
5     static float baseTa, baseTm, baseRiam, baseAm, baseAa;
6     static float curTa, curTm, curRiam, curAm, curAa;
7     static float deltaTa, deltaTm, deltaRiam, deltaAm, deltaAa;
8
9
10    public static void main(String[] args) {
11        Scanner scanner = new Scanner(System.in);
12
13        System.out.println("Step 1 : Perform no load test & input
14            Timing data \n");
15
16        System.out.println ("Decision 1 : Is Contact mismatch
17            beyond specified limits? (y/n) : ");
18        String contactMismatch = scanner.next();
19
20
21        if (contactMismatch.equalsIgnoreCase("n")) {
22            System.out.println("Step 2 : Measure static contact
23                resistance & perform DCRM \n");
24            System.out.println ("Decision 2 : Are noticeable
25                variations in close zone? (y/n) : ");
26            String notVariations = scanner.next();
27
28
29        if (notVariations.equalsIgnoreCase("y")) {
30            System.out.println ("Decision 3 : 50 Hz frequency
31                variations in close zone? (y/n) : ");
32            String freqVar = scanner.next();
33
34            if (freqVar.equalsIgnoreCase("y")) {
35                System.out.println("Action required :
36                    Induction effect Remedial action: Give one
37                    turn on insulator for current cable to
38                    avoid interference.\n\n");
39                System.exit(0);
40            } else if (freqVar.equalsIgnoreCase("n")) {
41                //do nothing
42            } else {
43                System.out.println("Incorrect value entered.
44                    Please enter 'y' or 'n'. \n\n");
45                System.exit(0);
46            }
47        }
48    }
49}
```

```

42 } else if (notVariations.equalsIgnoreCase("n")) {
43     System.out.println ("Decision 3 : Is contacts
44         bouncing & breaking in closing/opening? (y/n) :
45         ");
46     String contBounce = scanner.next();
47
48     if (contBounce.equalsIgnoreCase("y")) {
49         System.out.println ("Decision 3 : 50 Hz
50             frequency variations in close zone? (y/n)
51             ");
52         String freqVar1 = scanner.next();
53
54         if (freqVar1.equalsIgnoreCase("y")) {
55             System.out.println("Action required :
56                 Induction effect Remedial action: Give
57                     one turn on insulator for current
58                     cable to avoid interference.\n\n");
59             System.exit(0);
60         } else if (freqVar1.equalsIgnoreCase("n"))
61             {
62                 //do nothing
63             } else {
64                 System.out.println("Incorrect value
65                     entered. Please enter 'y' or 'n'. \n\n
66                     ");
67                 System.exit(0);
68             }
69
70     } else if (contBounce.equalsIgnoreCase("n")) {
71         //do nothing
72     } else {
73         System.out.println("Incorrect value entered.
74             Please enter 'y' or 'n'. \n\n");
75         System.exit(0);
76     }
77
78     System.out.println("Step 3 : Measure contact wipe
79         with slow closing & make it to specified value \n"
80         );
81     System.out.println("Step 4 : Repeat DCRM \n");
82     System.out.println ("Decision 4 : Is Normal
83         Signature? (y/n) : ");
84     String normSig = scanner.next();
85
86     if (normSig.equalsIgnoreCase("y")) {
87         System.out.println("Output : Breaker is healthy.\n
88             n\n");
89         System.exit(0);
90     } else if (normSig.equalsIgnoreCase("n")) {
91
92         //TODO calculate deltas
93         System.out.println("\n\n Please enter the BASE
94             values below:\n Enter base Tm : ");
95         baseTm = Float.parseFloat(scanner.next());
96
97         System.out.println("Enter base Ta : ");
98

```

```

89         baseTa = Float.parseFloat(scanner.next());
90
91         System.out.println("Enter base Riam : ");
92         baseRiam = Float.parseFloat(scanner.next());
93
94         System.out.println("Enter base Am : ");
95         baseAm = Float.parseFloat(scanner.next());
96
97         System.out.println("Enter base Aa : ");
98         baseAa = Float.parseFloat(scanner.next());
99
100        System.out.println("\n\n Please enter the CURRENT
101           values below:\n Enter current Tm : ");
102        curTm = Float.parseFloat(scanner.next());
103
104        System.out.println("Enter current Ta : ");
105        curTa = Float.parseFloat(scanner.next());
106
107        System.out.println("Enter current Riam : ");
108        curRiam = Float.parseFloat(scanner.next());
109
110        System.out.println("Enter current Am : ");
111        curAm = Float.parseFloat(scanner.next());
112
113        System.out.println("Enter current Aa : ");
114        curAa = Float.parseFloat(scanner.next());
115
116        System.out.println("\nCalculating delta values (
117           current - base)...");
118
119        deltaTm = curTm - baseTm;
120        deltaTa = curTa - baseTa;
121        deltaRiam = curRiam - baseRiam;
122        deltaAm = curAm - baseAm;
123        deltaAa = curAa - baseAa;
124
125        System.out.println("Difference Tm : " + deltaTm +
126           "\n");
127        System.out.println("Difference Ta : " + deltaTa +
128           "\n");
129        System.out.println("Difference Riam : " +
130           deltaRiam + "\n");
131        System.out.println("Difference Am : " + deltaAm +
132           "\n");
133        System.out.println("Difference Aa : " + deltaAa +
134           "\n\n");
135
136        System.out.println("\n\n Checking conditions...\n
137           ");
138
139        if ((deltaTm < 0) && (deltaRiam == 0) && (
140           deltaAa > 0) && (deltaTa==0) && (deltaAm>0) )
141        {
142            System.out.println("PROBLEM 1 detected : Main
143               contact erosion. ");
144        }
145
146        if ((deltaTm==0) && (deltaRiam ==0) && (deltaAa
147           <0) && (deltaTa<0) && deltaAm==0) {
148            System.out.println("PROBLEM 2 detected : Fix
149               arcing contact erosion. ");
150        }

```

```

140     if ((deltaTm==0) && (deltaRiam>0) && (deltaAa>0)
141         && (deltaTa==0) && (deltaAm==0)) {
142         System.out.println("PROBLEM 3 detected :
143             Wearing of arcing contact fingers. ");
144     }
145
146     if ((deltaTm==0) && (deltaRiam>0) && (deltaAa<0)
147         && (deltaTa<0) && (deltaAm==0)) {
148         System.out.println("PROBLEM 4 detected : Fix
149             and moving arc contact erosion. ");
150     }
151
152     if ((deltaTm<0)&&(deltaRiam>0) &&(deltaAa<0) &&
153         (deltaTa<0) && (deltaAm>0)) {
154         System.out.println("PROBLEM 5 detected : Arc
155             contact -Fix and moving- and main contact
156             erosion. ");
157     }
158
159
160
161
162 } else if (contactMismatch.equalsIgnoreCase("y")) {
163     System.out.println("Action required : Adjust
164         mechanism setting.\n\n");
165     System.exit(0);
166 } else {
167     System.out.println("Incorrect value entered. Please
168         enter 'y' or 'n'. \n\n");
169     System.exit(0);
170 }
171
172
173 }
174
175 }
```

ACKNOWLEDGEMENT

I take this opportunity to thank my guide Dr. W. Z. Gandhare, Director, G.S.Moze College of Engineering, Pune for his valuable guidance and constant motivation during the research work. I wish to thank Internal Monitoring Committee Members Dr. A. S. Bhalchandra, Dr. M. G. Shaikh and Dr. A. G. Thosar, Head of Electrical Engineering Department, Government College of Engineering, Aurangabad for their valuable support, suggestions and extending all the facilities for completion of this research work. I am thankful to Dr. P.B. Murnal for permitting to carry out the research work. Many thanks to my colleagues at the institute for their help and support.

I owe special thanks to the authority of Crompton Greaves, Nashik for permitting to conduct the experimentation and measurements. Also I greatly acknowledge the authorities of PGCIL and MSETCL for the technical support and permission to visit the substation and carry out the testing.

Last but not least, I express my deepest love to my family with all my heart for patience and unfailing support through the research work.

Anita Arun Bhole